UB
NASA TM X-1421

NASA TECHNICAL MEMORANDUM

UB
NASA TM X-1421

(NASA-TM-X-1421)   FEASIBILITY STUDY OF A
TUNGSTEN WATER-MODERATED NUCLEAR ROCKET.
2:   FUELED MATERIALS   N.T. Saunders, et al
(NASA)   Mar. 1968   97 p

N72-74698

00/99

Unclas
40222

C 00431
(ACCESSION NUMBER)   (THRU)

97
(PAGES)   (CODE)

(NASA CR OR TMX OR AD NUMBER)   (CATEGORY)

FF No. 602(D)

FEASIBILITY STUDY OF A TUNGSTEN WATER-

MODERATED NUCLEAR ROCKET

II. FUELED MATERIALS

By Neal T. Saunders, Richard E. Gluyas, and Gordon K. Watson

Lewis Research Center
Cleveland, Ohio

~~RESTRICTED DATA~~ ████████████

~~ATOMIC ENERGY ACT OF 1954~~ ████████████

████████████

████████████

NATIONAL AERONAUTICS AND SPACE ADMINISTRATION
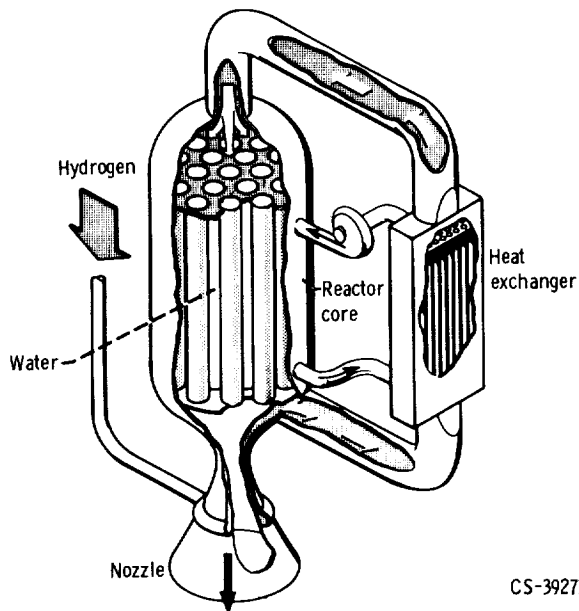
PREFACE

The concept of a nuclear rocket system based on the use of a tungsten water-moderated reactor (TWMR) was originated at the Lewis Research Center. The TWMR is a thermal reactor that uses water as the moderator, uranium dioxide as the fuel, and tungsten enriched in tungsten 184 as the fuel element structural material. As is common to all nuclear rocket systems, hydrogen is used as the propellant to maximize specific impulse. The reactor (see illustration) consists of a tank containing a number of pressure tubes that are attached to tube sheets at the inlet and outlet ends of the reactor. The pressure tubes contain the fuel elements. The space inside the tank between the tubes is filled with water, which serves both as the neutron moderator and as a coolant for the structure. Heat is generated in the water by neutrons and gamma rays and is also transferred to the water by heat leakage from the hot fuel elements, each of which is located in a pressure tube. The removal of heat is provided by pumping the water through the core and a heat exchanger in a closed loop. The water is regeneratively cooled in the heat exchanger by the hydrogen propellant, which flows from a supply tank through the nozzle and heat exchanger into the core. As the hydrogen flows through the core pressure tubes and through the fuel elements, it is heated to a high temperature and is expanded out the nozzle to produce thrust.

The potential advantages of the concept lie in the following areas: The use of tungsten provides a high-temperature material with good thermal shock resistance, tensile and compressive strength, thermal conductivity, and resistance to corrosion by the hydrogen propellant. The properties of tungsten also permit the fabrication of fuel elements with very thin cross sections for good heat transfer. The use of water as the moderator provides a good coolant for the pressure vessel and structural members and reduces core size and weight over that obtained for most moderator materials. In this concept, the fuel element assemblies are structurally independent of each other and thus permit individual development of these assemblies.

A program was undertaken at Lewis to investigate the engineering feasibility and performance of the TWMR nuclear rocket system. The results of these investigations, which are summarized in part I (NASA Technical Memorandum X-1420) of this series of reports, are presented in detail in the other six parts of the series as follows: II. Fueled Materials (NASA Technical Memorandum X-1421); III. Fuel Elements (NASA Technical Memorandum X-1422); IV. Neutronics (NASA Technical Memorandum X-1423); V. Engine System (NASA Technical Memorandum X-1424); VI. Feed System and Rotating Machinery (NASA Technical Memorandum X-1425); VII. System Dynamics (NASA Technical Memorandum X-1426).

CONTENTS

PRECEDING PAGE BLANK NOT FILMED.

FEASIBILITY STUDY OF A TUNGSTEN WATER-MODERATED NUCLEAR ROCKET

II. FUELED MATERIALS (U)

by Neal T. Saunders, Richard E. Gluyas, and Gordon K. Watson

Lewis Research Center

SUMMARY

Studies were conducted on tungsten-uranium dioxide ($W-UO_2$), dispersion-type composites that could be used in fuel elements of a nuclear rocket concept. These studies included development of fuel element fabrication processes, study of methods to improve the fuel retention capability of these composites, and evaluation of the properties of $W-UO_2$ composites. The results indicate that $W-UO_2$ fuel element stages of complex configurations can be fabricated, that high-temperature fuel losses can be controlled to tolerable levels, and that the properties of these composites are adequate for reactor design requirements.

The most promising of several particle consolidation processes studied for producing complex configurations are hot isostatic compaction or hot pneumatic impaction of W-coated UO_2 particles. The best current method of cladding the surfaces of $W-UO_2$ composites with unfueled tungsten involves vapor deposition techniques utilizing hydrogen reduction of tungsten halides. Methods for welding and nondestructively testing $W-UO_2$ composites also were developed and evaluated. Further development of these fabrication processes is necessary, however, before reactor fuel elements can be manufactured.

Fuel loss at high temperatures, particularly under conditions of thermal cycling was a major problem encountered in this study. The problem of surface vaporization of UO_2 can best be solved by preparing the composites from W-coated UO_2 particles and then cladding the surfaces of these composites with thin layers of tungsten. The most promising solution to the problem of fuel decomposition and migration under thermal cycling conditions is the use of small amounts of metal oxide additions in solid solution with the fuel. In particular, cerium oxide and yttrium oxide appear attractive as fuel stabilizers.

Data on the high-temperature tensile, creep-rupture, modulus of elasticity, thermal conduction, and thermal expansion properties of $W-UO_2$ composites were determined at temperatures to 2760° C. The results of these tests are reported and discussed in this report.

INTRODUCTION

The TWMR concept utilizes fuel elements consisting of uranium dioxide (UO_2) fuel particles dispersed in a continuous tungsten (W) matrix. Because of the difficulties involved in fabricating composites of these materials plus the initial lack of information about the properties and behavior of such composites at reactor operating temperatures, an extensive investigation of these potential fuel element materials was conducted as part of the feasibility study. This report summarizes the significant aspects of this materials program.

The primary requirements, from a nonnuclear materials viewpoint, for these $W-UO_2$ fuel elements are listed as follows:

(1) The fuel elements must be capable of operating at extremely high temperatures for several hours with intermittent thermal cycling to ambient temperatures: current minimum goals require operating capability at 2500° C (about 4500° F) for 10 hours with at least 25 thermal cycles between ambient and maximum operating temperatures.

(2) The fuel elements must effectively retain their fuel during their entire lifetime (less than 1 percent fuel loss is desired).

(3) The individual segments (stages) of the fuel elements must be capable of structural self-support under the high aerodynamic loads imposed by the rapidly flowing hydrogen propellant.

(4) The fuel elements must effectively transmit the fission-generated heat to the hydrogen propellant.

Dispersion-type composites of W and UO_2 (10 to 40 volume percent) were selected at the outset of this program as having the best potential of meeting these requirements. These materials were selected primarily because they both have melting points above the expected maximum reactor operating temperature and, for the most part, are chemically compatible with each other and with the hydrogen propellant. In addition, use of a continuous tungsten matrix utilizes the relatively good high-temperature strength of tungsten and its excellent thermal conductivity. On the other hand, selection of these materials also requires acceptance of some associated problems. For example, tungsten is brittle at low temperatures and is extremely difficult to fabricate by conventional metalworking processes. In addition, UO_2 has the disadvantage that its high vapor pressure at nuclear rocket operating temperatures makes retention of fuel a difficult problem.

Based on this selection of fuel element materials, a research program was undertaken to seek solutions to some of the anticipated problems, to determine if any unexpected problems existed, and to establish the potential of $W-UO_2$ composites for use under nuclear rocket operating conditions (nonnuclear). This program, which utilized a combination of in-house and contracted studies, was divided into the following three major areas of effort:

  (1) Development and evaluation of various methods of fabricating potential fuel element configurations

  (2) Study of methods to prevent loss of fuel at operating temperatures

  (3) Determination of mechanical and physical properties of W-UO_2 composites for design use

Each of these major areas is reviewed in separate sections of this report.

Although actual reactor fuel elements will require UO_2 fully enriched in the U^{235} isotope and tungsten enriched in the W^{184} isotope, all studies conducted under this program employed composites containing 10- to 40-volume-percent UO_2 with uranium in either the natural isotopic composition or depleted of U^{235} and tungsten in its natural isotopic composition. The latter materials were used because of ready availability and ease of handling. And they are expected to behave, from a nonnuclear standpoint, identically to the ultimately required enriched materials.

The significant results and conclusions attained during the course of this program are summarized in this report. Because of the extent of the program, experimental procedures used in the various studies are not described in detail. However, more detailed discussions of each of the studies covered in this report are included in the referenced publications cited for each study.

The following Lewis personnel contributed to the work described in this report: Charles P. Blankenship, Robert J. Buzzard, Robert M. Caves, Arthur S. Doan, Marvin Garfinkle, Michael A. Gedwill, William A. Gordon, Salvatore J. Grisaffe, Charles A. Gyorgak, Robert W. Hall, Thomas J. Moore, Paul F. Sikora, and Philip D. Takkunen.

FABRICATION DEVELOPMENT

Configurations

The fabrication development studies were directed toward the following three W-UO_2 configurations: (1) flat plates, (2) concentric cylinders, and (3) honeycomb grids. These three configurations are described in the following paragraphs.

Flat plates. - The flat-plate configuration consisted of thin (less than 1/32-in. (0.8 mm) thick) plates containing a uniform fuel loading in the range of 10- to 40-volume-percent UO_2 uniformly distributed in a continuous tungsten matrix. The length and width of numerous plates used in this program varied, but most plates produced were 3 to 8 inches (7.6 to 20.3 cm) long and 1 to 2 inches (2.5 to 5.1 cm) wide. Test specimens of this configuration were used for mechanical and physical property evaluations, as specimens for fuel retention studies, and as a starting point in the forming of more complex fuel element geometries.

Cylinders. - The concentric cylinder fuel stage considered for the TWMR consists of 10 concentric W-UO$_2$ cylinders, as shown in figure 1(a). Each cylinder has a 0.020-inch (0.051 mm) wall thickness and is about 1.5 inches (3.8 cm) long. The smallest cylinder is 0.5 inch (1.3 cm) in diameter and the largest is approximately 2 inches (5.1 cm) in diameter. Although the required fuel loading is uniform within each cylinder, it must be varied from cylinder to cylinder for uniform heat generation. In this configuration, the fuel loading must vary from about 10- to 32-volume-percent UO$_2$, and the smallest cylinder has the highest fuel loading. One advantage of this configuration is that each cylinder can be made separately and then assembled into the desired configuration. Two unfueled tungsten pins, which are located 90° apart to position the cylinders, are used to support these stages in the fuel element assembly. This configuration also has the advantage that each cylinder is free to expand both axially and radially, and thus stresses due to thermal gradients are minimized.

Honeycomb grid. - The honeycomb-grid fuel element stage, shown in figure 1(b), is inherently more rigid than the concentric cylinder configuration, but this increased rigidity may cause an increase in thermal stresses within the webs as a result of temperature gradients arising under normal reactor operation. The hexagonal flow channels of this honeycomb grid are 0.125 inch (3.2 mm) across the flats and are separated by 0.020-inch-thick (0.51 mm) webs of W-UO$_2$. The external dimensions of this configuration are similar to those of the concentric cylinder configuration, as indicated in figure 1(b). For uniform heat generation, the composition of the honeycomb webs must be varied radially from about 32-volume-percent UO$_2$ in the center of the honeycomb to about 10 volume percent at the edges. This fuel loading variation could be either linear or incremental; however, the majority of the grids produced in this study were loaded in 4-volume-percent-UO$_2$ increments.

Consolidation Techniques

Various methods were studied for the consolidation of W-UO$_2$ fuel elements. Early work was devoted primarily to the development of roll compaction as a consolidation process for flat plates. As it became evident that more complex fuel element geometries were required, several other consolidation methods were investigated, primarily under contracted programs. Although some of these consolidation processes were used only to produce certain configurations, development of all these processes was directed toward the following general goals:

(1) Consolidation of the powder constituents into crack-free composites with a uniform dispersion and minimum distortion of the initially spherical UO$_2$ particles

(2) Attainment of high density (i.e., greater than 98 percent of theoretical density)

(3) Good control of dimensions, particular on the 0.020-inch (0.51 mm) thickness

(±0.001-in. (±0.03 mm) tolerance desired)

(4) Prevention of contamination by foreign materials during processing

The consolidation methods studied in this program are described in the following sections. Descriptions of the materials used in these studies and methods for their chemical analysis are presented in the appendixes.

Roll compaction. - Roll compaction was used extensively to produce flat plates both by the densification of sintered $W-UO_2$ composites prepared by powder-metallurgy techniques and by direct consolidation of W-coated UO_2 particles.

The powder-metallurgy technique developed at Lewis is described in detail in reference 1. This technique, which was used as a reference fabrication process for $W-UO_2$ plates, consists of blending, cold pressing, sintering, and hot rolling mixtures of W and UO_2 powders, as shown schematically in figure 2. Weighed amounts of tungsten powder (approximately 1 micron (μm)) and UO_2 powder (-270/400 mesh) were dry blended in a twin-shell blender for 4 hours. The tungsten powder was selected on the basis of its sintering characteristics, and the selection of the UO_2 size range was based on experimental results, which indicated that plates fabricated from this size range of fuel particles had the highest strength and best fuel-retention characteristic of any of those tested (ref. 2). Stearic acid was added to the mixture as both a binder and die lubricant, and the mixture was cold compacted into a flat-plate configuration at a pressure of 20 000 pounds per square inch (140 MN/m^2). Sintering of the pressed plates was accomplished by heating at 1750° C for 15 hours in a flowing hydrogen atmosphere. This process yielded a sintered density in excess of 90 percent of theoretical. Final densification to at least 98 percent of theoretical was achieved by hot rolling at 1950° C until a total reduction in thickness of 40 to 50 percent was obtained. Typical microstructures of finished plates containing 10- to 40-volume-percent UO_2 are shown in figure 3.

This process was used extensively at Lewis to produce plate-type specimens for the fuel retention and property studies discussed in subsequent sections of this report. In addition, this method was used with minor modifications by other organizations under NASA contracts (refs. 3 and 4) to produce plates for use in various NASA studies.

The UO_2 dispersion shown in the microstructures of figure 3 is relatively nonuniform due to the poor blending characteristics and widely different sizes of the W and UO_2 powders. Since this type of dispersion could lead to nonuniform properties, more uniform fuel dispersions are desired. One method of attaining a uniform dispersion is through the use of W-coated fuel particles in which all the tungsten matrix is present (before consolidation) as a coating on the UO_2 particles (as discussed in ref. 5). Particles of this type are shown in figure 4(a), and methods of producing them are described in appendix A.

Attempts to consolidate these coated particles by the pressing, sintering, and rolling techniques used for powder mixtures were unsuccessful because of the poor sintering

characteristics of the relatively large particles. This consolidation process restricted the use of coated particles to thinly coated ($<$5-μm coating thickness) particles because additions of fine ($\sim$1 μm) tungsten powder were needed to aid sintering of these composites. Unfortunately, the addition of tungsten powder to the coated particles also resulted in a nonuniform fuel dispersion. However, a hot-rolling consolidation technique was developed (ref. 6) for thickly coated UO_2 particles (with all the required matrix tungsten in the coating).

In this process, which does not involve pressing and sintering, coated particles of the desired fuel loading were loaded into a molybdenum can, furnace cleaned at 1100° C for 2 hours in a hydrogen atmosphere, and then compacted by hot rolling at 1700° C until a total reduction in thickness of 60 percent was obtained. After the particles were consolidated, the molybdenum was removed by dissolution in a 1 to 1 nitric acid solution. The W-UO_2 plates then were rerolled a small amount (usually about 5-percent reduction in thickness) at 1950° C to improve the surface finish. This process was successfully used to consolidate fully dense plates containing up to 70-volume-percent UO_2 and as thin as 0.008 inch (0.2 mm). Figure 4(b) shows a photomicrograph of a W - 20-volume-percent-UO_2 plate fabricated in this manner. This photomicrograph illustrates the improved uniformity of the UO_2 fuel dispersion and the increased elongation of the UO_2 particles in the rolling direction.

Although flat plates were used in this program primarily as test specimens, these plates could be considered for use in constructing more complex fuel-element configurations. To demonstrate this potential, the finished flat plates produced by either sintering and hot rolling of W and UO_2 powder mixtures or hot roll compaction of coated particles were hot formed at about 900° C into a variety of shapes such as those shown in figure 5. The smallest cylinder shown is about 1/2 inch (1.3 cm) in diameter. Each corrugation of the corrugated shape is about 1/4 inch (0.6 cm) on a side and has a bend radius of less than 1/32 inch (0.8 mm) at all bends. The joining processes described later in this report could be used to construct more complex configurations from shapes such as these.

In summary of this section, the significant results of this roll-compaction study are listed as follows:

(1) The roll-compaction technique was used to consolidate W-UO_2 plates either by densification of sintered powder mixtures or by direct consolidation of coated particles.

(2) Composite densities in excess of 98 percent of theoretical with some elongation of the UO_2 particles were obtained with either process.

(3) Improved fuel distribution in the plates was obtained by the use of W-coated UO_2 particles.

(4) The W-UO_2 plates were hot formed into a variety of shapes.

Hot isostatic compaction. - Since the use of roll compaction is limited to the fabrication of flat plates (that require further processing to produce more complex shapes), the use of hot isostatic compaction (gas-pressure bonding) was evaluated in a contracted study (ref. 7) to consolidate the potential fuel element configuration directly. This study primarily involved development of techniques to produce honeycomb grids; however, methods of fabricating flat plates by this process also were investigated.

This consolidation process (shown schematically in fig. 6 along with the hot-pneumatic-impaction process described in the next section) uses a combination of high pressure (10 000 to 32 000 psi ($\sim$70 to 220 MN/m^2)) inert gas and high temperatures (1600° to 1700° C) to effect the consolidation of W-UO$_2$ powders encapsulated in sealed and evacuated, deformable containers. A high-pressure cold-wall autoclave is employed to obtain the temperature and pressure. After cooling, the composite-container assembly is removed from the autoclave, and the container is stripped from the composite by chemical dissolution (leaching).

In order to fabricate honeycombs by isostatic compaction, the container assembly shown in figure 7 was required. Photoetched molybdenum templates, such as those shown in the figure, were used to position hexagonal molybdenum mandrels in the desired configuration. The mandrel assembly was encased in an unfueled, sintered (partially dense) tungsten sleeve, which served as the outer wrap of the fuel element. This assembly, in turn, was placed in a molybdenum container (not shown in the figure). The container assembly then was loaded with W-coated UO$_2$ particles and vibratory compacted to about 65 percent density. Partially dense molybdenum end plugs were used to minimize "dumbbelling" during compaction. Prior to evacuation and electron-beam welding of the container, the assembly was thoroughly outgassed at 1400° C in vacuum to eliminate any volatile impurities present. This assembly then was isostatically compacted at 1700° C and 30 000 pounds per square inch ($\sim$210 MN/m^2) for 1 to 2 hours. A typical microstructure of a W-UO$_2$ composite produced by this method is shown in figure 8. As can be seen, nearly full density (>99 percent of theoretical) was attained, and the fuel-particle distortion was not as severe as that resulting from roll compaction (fig. 4(b)).

Twenty full-size honeycomb grids were successfully fabricated by the hot-isostatic-compaction technique and were supplied to Lewis for evaluation. Approximately 70 percent of the web and channel dimensions of those grids were within specifications ($\pm$0.001 in. ($\pm$0.025 mm) of the desired web dimensions and $\pm$0.005 in. (0.127 mm) of the desired channel dimensions), and the densities of all the grids exceeded 99 percent of theoretical. Ten of the grids supplied had a uniform fuel loading of 20 volume percent, while the fuel loading in the other grids varied from 30 volume percent in the center to 10 volume percent at the periphery in 4-volume-percent incremental changes at each radial ring (zone) of the hexagonal channels.

The radial variations in the fuel loading of the honeycomb grids were accomplished

by the use of a removable-dam technique. This method utilized removable metal foil or mylar partitions which were placed between the mandrels so that each fuel loading zone was separated from the adjacent zone. (Examples of the mylar sleeves are shown in fig. 7.) After loading of the zones with W-coated UO_2 particles containing the desired fuel loadings, the dams were removed, and the grids were consolidated. As many as six different fueled zones were incorporated into one honeycomb grid.

Fabrication of plates by hot isostatic compaction also utilized a molybdenum container that was removed chemically after compaction. The container design used for plates allowed compaction of two plates per assembly. In this design, the composites were separated by a thick molybdenum plate which did not deform appreciably and thereby prevented buckling of the thin assembly during compaction. Loading, pretreatment, evacuation, sealing, compaction, and post-treatment techniques used for the plates were similar to those previously described for the honeycomb grids.

During the latter stages of this research program, numerous W-UO_2 plates were produced from W-coated UO_2 particles by this process. These particles were used in tests to determine the mechanical properties and fuel-retention characteristics of composites produced from coated particles. The compacted plates usually were fully dense and well bonded and had microstructures similar to that shown for a honeycomb web (fig. 8); however, the generally good quality of the plates was not consistently reproducible. Difficulties encountered included local areas of low density, surface irregularities, and matrix porosity formation during high-temperature tests. To overcome these problems, optimization of the compaction parameters and better control of the starting materials and processing steps are required.

Although it was evident that additional development work is required to optimize process parameters further, the feasibility of using hot isostatic compaction to fabricate W-UO_2 composites was clearly demonstrated.

The results of this investigation show that

(1) It is feasible to consolidate honeycomb grids and flat plates from W-coated UO_2 particles by hot isostatic compaction.

(2) Integrally sound honeycomb grids with densities in excess of 99 percent of theoretical can be obtained, but improvement of the dimensional control is needed.

(3) Radial fuel-loading variations in the honeycomb grid can be achieved by a removable-dam technique.

Hot pneumatic impaction. - Hot pneumatic impaction was investigated under a contracted study as an alternate method of fabricating W-UO_2 honeycomb grids and plates (refs. 8 and 4, respectively). The primary objective of this study was to develop a high-energy-rate, pneumatic-mechanical process, for the fabrication of W-UO_2 composites conforming to the specifications listed previously.

Assembly of honeycomb-grid structures for hot pneumatic impaction is similar to

that used for hot isostatic compaction (as shown in fig. 7). Preparation for hot pneumatic impaction consists of assembling sacrificial molybdenum mandrels in the configuration of the honeycomb channels; placing the mandrel assembly in a cylindrical, molybdenum impaction can; and filling the voids in this assembly with the W-coated UO_2 particles by vibratory compaction. Consolidation of these assemblies was accomplished by heating the billets while evacuating, sealing the evacuation port, and impacting them in the cylindrical closed die of a hot pneumatic impaction machine. After impaction, the assemblies were furnace-cooled and then annealed at 1750° C for 3 hours. The can and mandrel assemblies then were removed from the densified grid by leaching in nitric acid.

Although the process parameters were not fully optimized, integrally sound grids with densities greater than 99 percent of theoretical were consistently fabricated at a temperature of 1600° C and at impaction pressures near 300 000 pounds per square inch ($\sim$2100 MN/m^2). Representative microstructures of a highly dense, impacted and annealed grid are shown in figure 9. These microstructures, which are similar to those of isostatically compacted grids, indicate that good densification and particle bonding was attained. The fine grains in the tungsten matrix surrounding some UO_2 particles are thought to be the result of contaminants in the coated particles.

Both machine loading and removable-dam techniques were employed in this study to provide a variable fuel loading in the honeycomb grids. The machine-loading process was developed to obtain a linear variation in radial loading. A cam-controlled, mechanical feeding system was utilized to load the grids with W-coated UO_2 particles containing the desired minimum or maximum amounts of fuel. Mechanical mixing of the two types of particles provided variation in fuel loading. Linear fuel loading variations were achieved in some of the grids loaded by this method; however, the variations were generally within the range of 12- to 24-volume-percent UO_2 rather than the variations of 10- to 30-volume-percent UO_2 desired. Much of this problem stemmed from inadequate control of the UO_2 content in the coated particles used, but some of the variation was attributed to nonoptimization of the feed system, particularly the cams controlling the feed rate. Thus, improvement of the machine-loading technique is required before it can be used to achieve the desired fuel loadings.

A removable-dam fuel loading technique, similar to that used with hot isostatic compaction, also was used to achieve radial fuel loading variations in hot pneumatically impacted grids. Considerable difficulties were encountered with this technique because the dam-removal procedures used often caused movement and misalinement of the mandrels. However, relatively good results were achieved in one grid in that fuel loading variations of 10- to 30-volume-percent UO_2 were achieved in 4-volume-percent-UO_2 increments with a maximum fuel loading variation of $\pm$2 percent.

Either method of producing fuel loading variations in the honeycomb grids appears attractive for use in producing fuel elements. The best grids produced by each process

exhibited localized variations within ±2 percent, and a tolerance of ±1 percent appears to be attainable with either process with better control of the fuel loading in the coated particles and improvement of the loading techniques. The removable-dam technique appears to be easier to control, but the machine-loading technique produces a linear, rather then incremental, loading variation. Thus both techniques warrant further development.

Fifteen honeycomb grids were fabricated for evaluation at Lewis. Five of these variably loaded grids were cracked as a result of either mandrel misalinement or poor quality fuel particles which in some instances did not exhibit a high degree of bonding. In addition, only about 65 percent of the webs of the best grids were within ±0.001 inch (0.025 mm) of the desired thickness. Impacted densities, however, were greater than 99 percent of theoretical. Further development work is required to refine the hot pneumatic impaction process, but this process is considered to have excellent potential for providing the high quality fuel elements required in the TWMR concept.

Flat plates of $W-UO_2$ also were fabricated by hot pneumatic impaction. The container design used to produce these plates utilized a cylindrical outer can to encase several composite plates that were separated by thick molybdenum spacers. Although the plates were positioned parallel to the axis of the outer can and the main impaction pressure, upset of the container assembly during impaction transmitted forces perpendicular to the plates. Processing conditions used for these plates were similar to those used for producing the honeycomb grids.

The resultant impacted plates were nearly fully dense, and the W-coated UO_2 particles were well bonded. However, the general quality of plates produced by this process was not as good as that of impacted honeycomb grids or as that of plates produced by the previously described methods of consolidation. Many of the impacted plates were extremely fragile and/or had numerous microcracks. In addition, the maximum length of the plates was restricted, at the current state of development, to about 4 inches (~10 cm), and the plate surfaces after leaching were very rough. The rough surfaces apparently resulted from the relatively long time required to dissolve the large mass of molybdenum required in the container. Methods of overcoming these problem areas must be developed before pneumatically impacted $W-UO_2$ plates can be evaluated in comparison with plates produced by other methods.

The results of this study of the hot-pneumatic-impaction process for fabricating $W-UO_2$ composites are summarized as follows:

(1) The feasibility of consolidating honeycomb grids and plates from W-coated UO_2 particles by hot pneumatic impaction was demonstrated.

(2) Honeycomb grids were produced that were integrally sound and had densities approaching theoretical, but improvements in dimensional control are needed.

(3) Both the machine-loading and removable-dam techniques demonstrated the capability of achieving a radial fuel-loading variation in the honeycomb grids.

(4) The quality of hot pneumatically impacted plates generally was not as good as that of impacted honeycomb grids.

Green state forming and sintering. - Two contracted studies were conducted to investigate honeycomb-grid fabrication by powder metallurgy techniques that utilize organic binders to aid forming powder compacts in the green state. Both studies were similar in that $W-UO_2$ composites were formed in the green state and then sintered to final density and dimensions. No additional working after sintering was employed in either case.

The green-rolling method (described in ref. 9 and shown schematically in fig. 10) utilized a mixture of a binder, plasticizer, and solvent with fine tungsten powder (required to improve sinterability) and W-coated UO_2 particles. In this process, the mixture was blended until the desired consistency was obtained and then it was passed through a rubber-type rolling mill to form a green, pliable sheet. This composite sheet was clad with unfueled tungsten by laminating thin, green, unfueled tungsten sheet to the fueled sheet. The green sheet then was corrugated and dried. After the nodes of the corrugated sheet were ground to half their thickness, the ground surfaces were joined (by use of the solvent) to other ground, corrugated sheets to form the hexagonal flow channels. After a presintering treatment to volatilize the binder, plasticizer, and solvent, the grids were densified by a high-temperature sintering operation (1800° C for at least 12 hr in hydrogen).

This consolidation method was used successfully to produce $W-UO_2$ honeycombs with either uniform or radially varying fuel loadings. Wedge-shaped segments (as illustrated in fig. 10) were fabricated from corrugated green plates with each corrugated plate of a different fuel loading. These wedge-shaped sections then were joined together to form the full-size grid. The assembled grids subsequently were densified by sintering.

Four of the honeycombs with radial fuel-loading variations were supplied to Lewis for evaluation. Typical microstructures of this material are shown in figure 11. Because mechanical working was not used in this process, the fuel particles were not distorted like those in the previously described fabrication processes. However, the fuel distribution is not as uniform as that attained with the other processes because fine tungsten powder had to be blended with the W-coated UO_2 particles to aid sintering. Also shown in figure 11 is the tungsten cladding on the surfaces of the $W-UO_2$ composites. This represents an advantage for this consolidation process, since cladding was easily applied to the surfaces of all channels in the honeycomb grids.

Although the grids evaluated were generally of good quality, problems were noted in the control of dimensional tolerances due to differential shrinkages during sintering: only about 50 percent of the webs were within ±0.001 inch (±0.025 mm) of the desired thickness. In addition, cracking and separation of the web joints were frequently observed. Although these problems could be overcome with additional development, work was terminated on this method since the previously described consolidation methods

looked more promising.

Flat plates were also fabricated by the green-state forming and sintering process by using forming techniques identical to the initial steps (up to the clad-bonding step in fig. 10) used in producing the honeycomb grids. The quality of these face-clad plates was generally good, and the microstructures were similar to those shown in figure 11 for the honeycombs webs.

A variation of the green-forming process was investigated in a parallel contracted study (ref. 10). In this process, a binder-solvent-plasticizer $W-UO_2$ mixture was cold-extruded into hexagonal tubes, and the tubes were glued together to form a green honey-comb grid. After sintering, the grids showed irregularities in shape and were poorly bonded. Therefore, this process was abandoned in favor of an alternate process in which the mixture was extruded into a full honeycomb-grid configuration in a single step before sintering. Problems were encountered in achieving adequate sintered densities: the poor sinterability caused nonuniform web thickness and occasional cracking. Because success of this process did not appear imminent and since considerable additional development work was required, this program also was terminated.

The results of these investigations showed that

(1) The feasibility of using the green-state rolling and sintering process to fabricate $W-UO_2$ grids and plates was demonstrated.

(2) High-density honeycomb grids were produced by this process, but further development of this process is needed to improve dimensional control and to eliminate web cracking and joint separation.

(3) Radial fuel loading variations were achieved in honeycomb grids, and tungsten cladding was applied to the flow channels with this process.

(4) The green-state extrusion and sintering process, at the current state of development, cannot produce high-quality $W-UO_2$ honeycomb grids.

Hot extrusion. - The feasibility of fabricating concentric cylinder and honeycomb-grid fuel elements by hot extrusion was investigated in two separate studies. In each study, efforts were directed toward the development of techniques for extruding fueled tungsten in the desired geometric shapes. In addition, coextrusion techniques were employed for integrally cladding the major surfaces of both fuel element configurations with unfueled tungsten.

Initial in-house studies on the extrusion of $W-UO_2$ tubing demonstrated process feasibility (ref. 11). In these studies, 5/8-inch-diameter (1.6 cm) tubing (both clad and un-clad) having a wall thickness of 0.030 inch (0.76 mm), was successfully extruded at temperatures of 2000° and 2200° C using molybdenum-canned billets and a floating-mandrel technique. A representative sample and a microstructure of extruded tubing are shown in figure 12. Note the extreme elongation (stringering) of the fuel in this section. Although this fuel elongation resulted in increased composite strength in the direction paral-

lel with the stringers (as described in the section PROPERTY EVALUATION), this excessive elongation of UO_2 in the tungsten matrix is expected to be detrimental to the transverse strength of the tubing. In addition, it has been shown, from theoretical considerations, that elongated UO_2 reduces the transverse thermal conductivity of the composite (ref. 12). In view of these factors, further development of this process was not undertaken.

Development of a hot-extrusion process for the honeycomb-grid configuration was attempted in a contracted study (ref. 13). The process used in this study consisted of fabricating an extrusion billet with a $W-UO_2$ hexagonal array with sacrificial molybdenum mandrels. After extruding the molybdenum-canned billet through a round die to obtain the desired cross-sectional area, the molybdenum can and mandrels were removed by chemical dissolution.

Initial studies were conducted to determine the extrusion characteristics of tungsten and molybdenum in simple rod or plate configurations. The molybdenum-tungsten interfaces in these extrusions were severely distorted because of the asymmetric flow of materials of different grain sizes (caused by use of different types of starting materials and by thermal gradients in the extrusion billets). Fine grained sintered materials yielded the least interface distortion. Subsequent attempts to extrude unfueled tungsten honeycombs resulted in distortion and wrinkling of the honeycomb webs. Wrinkling of the tungsten web and associated channel distortion are considered the major problem areas in development of the hot-extrusion process for producing honeycomb grids. Further study of these problem areas is necessary if this consolidation process is to be considered for use in manufacturing fuel elements.

Only one attempt was made in this study to extrude a $W-UO_2$ composite. A rod containing W - 10-volume-percent-submicron-UO_2 particles was extruded (at 1875° C) to determine if the smaller particle size fuel would not elongate as readily as the 30- to 60-micron UO_2 contained in the extruded tubing described previously. However, fuel stringers with major- to minor-axis ratios of about 9 resulted. Since other fabrication techniques showed more promise of success without the problem of fuel elongation, this program also was terminated.

The results obtained in the investigations of hot-extrusion of fueled composites are summarized as follows:

(1) Process feasibility was demonstrated in the extrusion of fueled-tungsten tubing for the concentric-cylinder fuel element, but additional studies are required to develop the technique of extruding fueled tungsten in a honeycomb geometry.

(2) The hot-extrusion process resulted in fueled composites with extensive UO_2 elongation which is believed to be detrimental to the properties of the fueled tungsten.

Vapor-cementation. - Vapor-cementation was investigated under a contracted study (ref. 14) as a possible method of fabricating $W-UO_2$ cylinders and plates without deform-

ation of the UO_2 particles. The deposition process consisted of infiltrating (cementing) the interstices of packed W-coated UO_2 spheres (60 to 90 μm) by tungsten deposition from the hydrogen reduction of tungsten hexafluoride (WF_6). The coated spheres were contained in the desired cylindrical or rectangular geometry during cementation by suitable mold materials. Two cementation techniques, termed "free diffusion" and "forced flow", were investigated in the development of this process. In the free-diffusion technique, the reactants were allowed to diffuse into the voids between the packed spherical particles, while the forced-flow technique employed a pressure differential to force the reactants between the spheres.

Cementation of the spheres to form cylinders was accomplished by passing the reactant gases along the axes of the cylinders, and cemented densities of 85 percent were achieved. The resultant free standing cylinders were densified further by filling the exposed surface voids by free-diffusion cementation. This two-step approach was used to obtain cylinders with measured densities of about 95 percent of theoretical. A representative cylinder made by the tungsten-cementation process is shown in figure 13 along with the microstructure of a typical cemented composite after heat treatment at 1300° C for 1 hour in hydrogen. This heat treatment eliminated the deposition interfaces and resulted in equiaxed structures. As shown in figure 13(b), voids remained at some of the interstices between coated particles even though high measured densities were obtained. These voids are expected to be detrimental to the mechanical and physical properties of the cemented composites. Dimensionally, the cylinders were within tolerances and of uniform size. Extension of the cementation process to larger diameter cylinders (up to 2 in. (5.1 cm)) was not achieved readily. In addition to changes in processing parameters required by the scale-up in size, cracking in some of the cylinders was encountered as a result of thermal stresses generated between the cylinders and the molds.

Tungsten-UO_2 plates for subsequent evaluation were fabricated by the free-diffusion process. Densities of about 95 percent of theoretical were obtained, and deposition interfaces were eliminated by post-heat-treating for 1 hour at 1300° C in hydrogen. Results from in-house tests (ref. 15) conducted on these plates indicate that fuel losses were excessively high (greater than 20 percent after heating for 2 hr at 2500° C in hydrogen) and that the plates were extremely fragile and exhibited about half the tensile strength of roll-compacted material at temperatures up to 2500° C. However, these results may not be truly indicative of the properties attainable in vapor-cemented composites as there were indications of impurities (oxy-fluorides) in the WF_6 used in preparing these plates. One specimen prepared from higher purity material exhibited suprisingly good fuel retention characteristics under thermal cycling conditions. This improved behavior was attributed to the stable fine grain size of vapor-cemented composites.

Since the consolidation goals were not fully met in this study and since other consolidation methods appeared more promising, study of this consolidation method was discon-

tinued. However, this process may warrant further development in the future if nondistortion of the fuel particles is essential. This process also appears attractive for consolidation of porous UO_2 particles in applications where porous fuel is required.

The results of this initial investigation of the vapor-cementation process are summarized as follows:

(1) Tungsten-UO_2 cylinders and plates that have densities of about 95 percent of theoretical were fabricated by the vapor-cementation process; however, further development of this process is needed to accomplish more nearly complete infiltration between coated particles.

(2) Prior bond interfaces of cemented composites were eliminated by post heat treating at 1300° C for 1 hour in hydrogen.

Magnetic pulse forming. - Under another contracted study (ref. 16), the feasibility of using a magnetic pulse forming (Magneforming) process for fabricating thin wall, seamless, W-UO_2 cylinders was investigated. This forming process uses a high-energy-rate metal-forming technique that involves the rapid collapse of a magnetic field to generate radially compressive pressure that can be used to swage partially dense, preformed cylinders over a mandrel.

In this program, a powder-compaction die (which relied on differential thermal expansion of die materials to develop compaction pressures) was developed to hot press powders directly into the preformed cylinders. Several materials were evaluated for the die body and mandrel of this compaction die, and the best results were attained by using a graphite die body and an alumina mandrel. Compaction of unfueled tungsten powders in this die at 1800° C resulted in preformed cylinders with densities of up to 92 percent of theoretical.

Subsequent attempts were made to swage these preforms magnetically in a specially developed apparatus at temperatures to 1400° C and radial pressures of about 50 000 pounds per square inch (~ 350 MN/m^2). However, density increases of only about 5 percent were achieved. In addition, cracking of the cylinders usually occurred during removal from the forming apparatus. Because of these unresolved difficulties with unfueled tungsten cylinders, this fabrication study was terminated before any attempts were made to fabricate W-UO_2 cylinders.

Discussion and summary of consolidation techniques. - Although further development is required for most of the fabrication processes to optimize processing variables and overcome various difficulties, the feasibility of fabricating the three configurations studied was demonstrated for several consolidation processes.

Flat plates were produced by most of the consolidation processes studied. Roll-compaction was used most extensively during the program as a reference fabrication processes for consolidation of test specimens. Near the conclusion of the program, hot isostatic compaction was used extensively to produce test specimens to avoid the UO_2

particle elongation encountered in roll compaction. However, the quality of the isostatically compacted plates varied and generally was not as good as that of roll-compacted plates. Therefore, additional study of hot isostatic compaction of plates appears to be necessary before it can be used reliably as a reference fabrication process.

Cylinders were fabricated by forming of roll-compacted flat plates with subsequent welding of the longitudinal seam, and direct consolidation of seamless cylinders was accomplished by use of the vapor-cementation process. In addition, the processes that were used successfully to produce honeycomb grids should be usable for consolidating cylinders directly; however, this was not emphasized in the program because maximum effort was though to be needed for the fabrication of the more difficult honeycomb configuration.

The honeycomb configuration was produced by use of three different fabrication processes: hot isostatic compaction, hot pneumatic impaction, and green-state rolling and sintering. Representative grids produced by these methods (fig. 14) were all produced from W-coated UO_2 particles and had radial fuel-loading variations from about 10- to 30-volume-percent UO_2. Results on an in-house evaluation of these grids (ref. 17) confirmed that the fabrication feasibility of these processes was successfully demonstrated but also indicated several problem areas where further development is required (as previously noted in the separate discussions for these processes). Although all three processes appear usable for fabricating honeycomb-type fuel elements with further development, the hot isostatic compaction and hot pneumatic impaction processes are thought to offer more potential than the green-state rolling and sintering process primarily because the former processes appear capable of attaining better dimensional control and process reproducibility. Methods of cladding the channels, however, must be developed for these processes before they can be used for fuel element fabrication.

Cladding Techniques

Early in the program, it became evident that the loss of UO_2 from fuel elements was excessively high when the elements were heated above about 1900° C. As discussed in the section FUEL RETENTION STUDIES (and in ref. 5), this loss is primarily a result of the high vaporization rate of UO_2 at these temperatures. The loss of UO_2 is more severe when UO_2 particles are interconnected within the composites and to the surface. One obvious solution to the problem was to clad the composites with a thin layer of unfueled tungsten.

Various techniques for applying a tungsten clad to the composites were investigated to determine which cladding methods best meet the following requirements:

(1) High-strength, pore-free, high-density tungsten metallurgically bonded to the fueled substrate

(2) Complete encapsulation

(3) Uniform thickness

(4) High purity

The cladding also should be capable of being applied to both simple and complex shapes, and no damaging side reactions with the dispersed fuel should occur. Several of the cladding techniques which were developed did not result in complete encapsulation of the composites, but they did produce effective claddings which permitted the laboratory testing of both cladding and substrate materials. All the claddings were evaluated initially on thin, rectangular W-UO$_2$ composites in which the fueled substrate was produced by the powder-sintering and hot-rolling technique described previously. One of the cladding methods (vapor deposition) also was extended to cladding of roll-compacted cylinders and contoured tensile specimens and to hot isostatically compacted plates. Unfortunately, termination of the program prevented any attempts to clad the channels of fabricated honeycomb grids. The various cladding methods studied are summarized in the following paragraphs.

Powder-metallurgy methods. - In the initial cladding studies conducted at Lewis (ref. 18), a powder metallurgy technique was used to clad flat-plate composites on the two major exposed surfaces (edges were left unclad). In this technique, clad composites were fabricated in a manner very similar to the sintering and hot-rolling process extensively used for plate fabrication. In the earlier technique, a layer of unfueled tungsten powder was loaded manually into the bottom of the die. Then a weighed amount of the W-UO$_2$ mixture was added, and finally another layer of unfueled tungsten was applied. The resulting sandwich then was consolidated by cold pressing, sintering, and hot rolling. The cladding was dense and well bonded to the core; however, the thickness and uniformity of the cladding was difficult to control because of the manual loading of the powders in the die. Despite this difficulty, the process was important in providing laboratory test specimens early in the program.

In an extension of this process, cladding of entire fuel cores was achieved by a slight modification of the powder-pressing procedure. With this modified process, W-UO$_2$ cores were completely encapsulated by using a picture-frame technique. This process consists of the following steps: After the first layer of unfueled tungsten powder was placed in the die cavity, a second die with a smaller opening was placed over the original die cavity. The second die was filled with a weighed amount of the W-UO$_2$ powder mixture and then pressed to form a shape-retaining W-UO$_2$ briquette. After removal of the second die, the unfueled tungsten powder was added between the W-UO$_2$ briquette and the edge of the die cavity. Finally, the top surface was covered with unfueled tungsten powder. The composite then was pressed, sintered, and hot rolled. Only a few samples were fabricated by this technique, but enough data were obtained to confirm that complete

encapsulation of the W-UO$_2$ composite was very effective in retaining the fuel at elevated temperatures.

Hot-roll-foil cladding. - Hot rolling also was used at Lewis to bond thin (0.003 in. (0.076 mm) starting thickness) tungsten foil to the major surfaces of the fuel plates (ref. 1). In this cladding process, the sintered core was surface ground to provide clean, smooth surfaces for bonding. Then, the tungsten foil cladding was folded around the core and spot brazed to one end of the core with tantalum. The assembly was hot rolled at 1950° C until a total reduction of 40 to 50 percent was achieved. The quality of the cladding and the core-clad bond was generally excellent, as shown in figure 15. Final cladding thickness was established mainly by the thickness of the starting foil and the amount of reduction. Variation of the cladding thickness did not exceed ±0.0005 inch (0.013 mm). The quality and uniformity of plates surface clad by this method were consistent, and many hundreds of plates were produced by using a variety of fuel types and fuel loadings. Because of this uniformity, claddings applied by this method (termed "face cladding" in subsequent sections of the report) were used as a reference for evaluation of all other cladding methods.

The roll-bonding process was also combined with the picture-frame technique described previously to produce fuel plates that were clad on all surfaces. The sintered W-UO$_2$ cores, which were clad on the edges by the powder-metallurgy picture-frame technique, were clad on the major faces by hot roll bonding tungsten foil to these faces.

A considerable number of these all-clad specimens were produced during the program to evaluate the effect of various additives on the stability of the UO$_2$ fuel (as discussed in the section FUEL RETENTION STUDIES). The major drawback associated with this cladding process is that it is only applicable to configurations that can be flat rolled (e.g., plates).

Gas-pressure-bonded foil cladding. - Fuel plates also were clad on all surfaces with 0.001-inch-thick (0.025 mm) tungsten foil by gas-pressure bonding under a contracted study described in reference 19. In this process, the sintered and rolled fueled core was wrapped with tungsten foil, sealed in an evacuated molybdenum can, and hot isostatically pressed at 1600° C and 15 000 pounds per square inch (~100 MN/m^2). Although these conditions generally resulted in good bonding, results from more recent studies indicate that higher temperatures and pressures yield better results. Thus, any additional gas-pressure-bonding - cladding studies should be performed at 1650° C and 30 000 pounds per square inch (~200 MN/m^2). Results of fuel-loss studies on plates clad by this method have indicated that this type of cladding is extremely effective in retaining fuel (i.e., less than 0.5-percent-UO$_2$ loss from a W - 20-volume-percent-UO$_2$ composite when tested at 2500° C for 2 hr in hydrogen). Figure 16 shows clad and unclad composites after testing at 2500° C.

Although this method of cladding is quite effective in retaining fuel at high temperatures, further study was not pursued because this method is difficult to use in cladding complex shapes such as the honeycomb configuration.

Plasma spraying. - Plasma spraying of tungsten was developed as a method of separately cladding the edges of face-clad fueled composites and as a method of repairing local defective areas in the cladding. The feasibility of achieving a metallurgically bonded plasma-sprayed cladding was demonstrated with simple hand-operated equipment at Lewis (ref. 20). This process involved spraying tungsten powder through a plasma torch operating with a hydrogen-nitrogen gas mixture in a nitrogen-filled glove box. Prior to cladding, the substrate plate was heated in excess of 2000° C with the plasma torch in order to achieve clean surfaces to attain metallurgical bonding with the plasma-sprayed cladding. Multiple passes were used in order to ensure full coverage.

Additional development of this cladding process was performed in a contracted study in order to obtain process reliability and to optimize the spraying parameters (ref. 21). Although considerable progress was made in this study, full control and reliability were not completely achieved: the clad thickness variation could not be controlled within the desired dimensional tolerances (± 0.0005 in. (0.013 mm)). However, face-clad composites which were edge clad by plasma spraying showed very low fuel losses at elevated temperatures (i. e., less than 0.5-percent UO_2 loss from W - 20-volume-percent-UO_2 composites tested at 2500° C for 2 hr in hydrogen).

This method of cladding also is limited to simple configurations and thus is not considered as a good method of cladding fuel elements. However, it does appear attractive as an auxiliary cladding process to repair local defects which might occur in clad fuel elements during machining, handling, or inspection processes.

Vapor deposition. - Vapor deposition of tungsten appears to offer the most promise as a fuel element cladding method since it is felt that both simple and complex shapes can be clad by this method. Two successful methods for vapor deposition of claddings on simple configurations were developed under contracted studies. One method utilized hydrogen reduction of WF_6 (ref. 22), and the other used the hydrogen reduction of tungsten hexachloride (WCl_6, ref. 23). Several other vapor-deposition methods were studied but were unsuccessful because of such factors as side reactions with the UO_2 fuel, contamination, or slow deposition rates. The unsuccessful methods which were investigated included the thermal decomposition of tungsten hexabromide, thermal decomposition of tungsten carbonyl, and hydrogen reduction of tungsten iodide.

Development of the successful vapor-deposition processes utilizing WF_6 or WCl_6 initially involved study of the process parameters, substrate preparation methods, and substrate holding jigs necessary to clad W-UO_2 plates. The resultant specimens were clad with one of three cladding thicknesses in the range of 0.0005 to 0.005 inch (0.013 to 0.127 mm). The claddings were applied at 650° C for the fluoride process and at 950° C

for the chloride process. After methods were successfully developed for cladding the flat plates, thin-walled cylinders and contoured tensile specimens also were clad by both processes.

Results of an in-house evaluation (ref. 24) of the W - 20-volume-percent-UO_2 samples clad by these processes indicated that both processes met all the major cladding goals. Figures 17 and 18 show cross sections of specimens clad with about 0.002-inch-thick (0.05 mm) tungsten before and after testing at 2500° C for 2 hours in flowing hydrogen. As evident in these figures, both types of claddings were very effective in retaining UO_2 during the high-temperature test. All three cladding thicknesses investigated were effective in retaining fuel, but the effectiveness generally increased with increasing thickness: the fuel loss resulting from the high-temperature test decreased from about 0.3-percent-UO_2 loss with the nominal 0.001-inch-thick (0.025 mm) claddings to about 0.1-percent-UO_2 loss with the nominal 0.005-inch-thick (0.127 mm) claddings.

One potential problem area associated with the fluoride-type claddings was encountered in metallographic examination of the specimens tested at 2500° C. In several of these specimens, microporosity was evident in the grain boundaries of the tungsten cladding (as shown in fig. 19). This porosity is believed to be caused by residual fluoride contaminants in the coatings that volatilize at high temperatures. Attempts were made to eliminate this problem (e.g., by use of higher deposition temperatures) but were not completely successful in that pore-free coatings were not consistently produced. Although this porosity did not seem to reduce the fuel retention effectiveness of the fluoride-type claddings, it represents a potential problem area under more severe test conditions and thus warrants further investigation. Since this porosity problem was not encountered with the chloride-type claddings, this method of cladding (at the current state of development) is preferred for applying tungsten claddings to W-UO_2 composites.

Discussion and summary of cladding techniques. - The results of these cladding studies showed that vaporization losses of UO_2 at elevated temperatures can be reduced to low levels by using external, unfueled, tungsten claddings that have a thickness of about 0.001 inch (0.025 mm) or more. These studies showed that complete encapsulation of W - 20-volume-percent-UO_2 composite reduced the fuel loss in a 2-hour test at 2500° C in hydrogen to a very low level (less than 0.1 percent). Several methods were used successfully for cladding W-UO_2 composites, but most of the methods are not easily adaptable to complex configurations. Vapor deposition from the hydrogen reduction of either WF_6 or WCl_6 is felt to be the most promising cladding technique of those investigated. Additional development work, however, is required to demonstrate the feasibility of applying uniform, vapor deposited claddings on the more complex configurations (such as the honeycombs).

Methods of applying a cladding as an integral part of fuel-element consolidation processes also appear attractive, particularly for cladding internal channels of configurations

like the honeycomb grid. Although extensive study of such methods was not made in this program, a cursory study of one method was conducted as part of the study of pneumatic impaction of honeycomb grids (ref. 8). In this study, the molybdenum mandrels were precoated with tungsten by vapor-deposition or flame-spraying techniques. During impaction, the mandrel coating bonded to the tungsten matrix of the composite core to produce a tungsten cladding on all the channels. The results of this study were attractive enough to warrant future study of this mandrel precoating technique as a method of cladding the channels of complex fuel element configurations.

Welding Techniques

A need for suitable welding techniques for $W-UO_2$ composites was recognized early in the fuel-element development studies as more complex fuel-element geometries were evolving. Joining techniques were thought to be needed either for attaching support devices or for seam welding of cylinders formed from flat plates. Initial attempts to fusion-weld these composites by using either gas - tungsten-arc or electron-beam-welding processes were unsuccessful primarily because the high vapor pressure of UO_2 caused porosity in the weld zone. These exploratory studies indicated that successfully welded joints in $W-UO_2$ composites might be difficult to attain. Therefore, six independent welding techniques were studied concurrently to determine their potential use for $W-UO_2$ composites.

The goals established for these studies are as follows:

(1) The joint must be fully sound, that is, it must be free of pores, cracks, and voids.

(2) The joint should be usable over a range of temperature between ambient and 2750° C and should be capable of operating for at least 10 hours at the maximum operating temperature, with intermittent cycling to ambient temperature.

(3) Unfueled zones produced by the welding process should be as small as possible.

(4) The joint region should be at least as strong as the $W-UO_2$ composite at operating temperatures.

(5) All foreign materials added to the joint must be compatible with tungsten, UO_2, and hydrogen, and preferably should have low nuclear cross section.

(6) The welding conditions must prevent the volatilization of UO_2 from the composite during processing.

(7) The welding atmosphere must not oxidize, carburize, or otherwise contaminate the composite.

In each of the six welding processes studied, initial emphasis was placed on developing methods of producing butt joints in thin (0.02 in. (0.51 mm)) W - 20-volume-percent-UO_2 coupons produced by roll cladding $W-UO_2$ powder mixtures. If welding of these butt

joints was successfully accomplished, effort then was directed toward producing joints in plates, cylinders, and T-sections, as illustrated in figure 20. Representative samples of these joints subsequently were submitted to Lewis for evaluation. The results of the six processes studied are summarized in the following sections. More detailed evaluation of these welding methods is reported in reference 25.

Gas-pressure bonding. - Joining $W-UO_2$ composites by a gas-pressure-bonding process was investigated in a contracted study (ref. 26). In this process, the composite plates were butted together inside an evacuated, deformable, molybdenum container and placed in an autoclave using processing techniques similar to those described for hot isostatic compaction. A pressure of 30 000 pounds per square inch ($\sim$200 MN/m^2) and a temperature of 1650° C for 3 hours were employed to achieve the bond. The molybdenum container then was removed by dissolution in a nitric acid solution.

Surface preparation, prebonding heat treatments, pressure-bonding parameters, and postbonding heat treatments were characterized in this study. A postbonding anneal at about 2000° C for 2 hours in vacuum improved the quality of the joints in that increased amounts of grain growth across the interface were promoted. Bonding of all joint configurations required was successfully accomplished, as shown by the examples in figure 21. The microstructure of a cross section of a typical gas-pressure-bonded joint is shown in figure 22. The joints generally were of excellent quality. Grain growth took place across the bond line, and a good cladding-to-cladding bond was achieved.

Dye-penetrant and metallographic examinations of the samples indicated small bond-line defects in only one of eighteen coupons in six of the twelve plates in two of six T-joints, and three of seven cylinders. Additional development work would probably increase the percentage of sound joints. The results of 2500° C tensile tests on the defect-free plates indicated that the joints were at least as strong as the composite base material. The joints produced by this method best met the goals established for these studies, and it was the only method that was used successfully to join all the required configurations.

Gas - tungsten-arc brazing. - The development of suitable alloys for brazing $W-UO_2$ composites by using a gas - tungsten-arc torch heat source was investigated in another contracted program (ref. 27). The brazing was done in an evacuated and backfilled welding chamber with a fully automatic carriage. Eighteen alloys, which have melting points above 2750° C, low nuclear cross sections, and minimum tendency to form hydrides, were evaluated. Buttons of these alloys were prepared by arc-melting in high-purity argon using a nonconsumable tungsten electrode and were subsequently crushed to a coarse powder. The alloys were evaluated on the basis of melting point, wettability, and the ability to produce sound butt joints with a minimum of base-metal dissolution.

On the basis of the results obtained, three alloys were selected for use in preparing the final evaluation samples: tungsten - 25 percent osmium, tungsten - 50 percent molyb-

denum - 3 percent rhenium, and molybdenum - 5 percent osmium. Joints were produced with each of these alloys by passing the welding torch over the butted joint regions which were filled with granules of the desired baze alloy. The resultant joints were resistant to hydrogen attack at 2750° C and had remelt temperatures in excess of 2750° C. All the required joints except the T-section configuration were successfully brazed in this manner. The T-section proved to be too difficult a configuration to braze at the current state of development. Further development of the brazing parameters and form of the braze alloy is needed before joining of the T-section can be considered.

Dye-penetrant inspection and metallographic examination of the brazed coupons indicated some microcracking in the joints produced by all the final three alloys used. This microcracking, which is thought to be the result of fixturing restraint during brazing, did not affect the high-temperature strengths of the brazed joints since tensile testing at 2500° C caused fracture in the base material away from the joints.

Of the final three alloys investigated, the results of the evaluation tests indicated that joints produced with the W - 25-percent-Os alloy best met the goals of this study. The microstructure of a typical joint produced with this alloy is shown in figure 23. The good quality of this joint demonstrates that brazing must be considered as a promising method of joining W-UO_2 composites, although further development of the process is required.

Magnetic-force welding. - Magnetic-force welding employs what is essentially a modified resistance welding machine. It differs from conventional welding processes in the manner in which the welding force is applied. Conventional machines use either pneumatic or hydraulic force systems, whereas magnetic-force welding machines use an electromagnet coupled to a movable electrode to supply the welding force. Precise synchronization can be achieved between the heat buildup at the joint and the weld force. The entire welding operation takes place in a fraction of a second.

The feasibility of using this process to join W-UO_2 composites was investigated in another contracted study (ref. 28). In this study, special tooling was developed and welding parameters were established to butt weld the composites. Welds were successfully produced in W - 20-volume-percent-UO_2 plates and cylinders. Because of time limitations on the study, no attempt was made to join T-sections. A microstructure of the best of these joints is shown in figure 24. This figure shows relatively good bonding with little evidence of the bond interface. The small degree of upset apparent in the weld joint indicates that the fixtures used to restrain the amount of upset in the weld zone were effective.

Further evaluation of these samples indicated a major unresolved problem associated with this process, namely, the presence of cracks transverse to the joint and oriented in a plane perpendicular to the surfaces of the plate. These cracks were found across every joint examined, even though high-temperature tensile testing produced failures in the

base material. Apparently the effect of these microcracks was limited since the tensile load was applied parallel to the cracks. The cracking problem could be the result of thermal stresses in the tungsten matrix due to rapid heating and cooling while under the rigid restraint of the weld tooling.

If the cracking problem can be resolved, magnetic-force welding offers good potential for very rapidly producing a solid-state weld with good strength at 2500° C. Rapid production would be particularly important if a considerable number of joints were required in producing reactor fuel elements.

Vacuum-hot-press diffusion bonding. - The feasibility of diffusion-bonding $W-UO_2$ composites was investigated in a contracted study (ref. 29) by using a mechanical means of applying pressure to resistance-heated joints in a vacuum chamber. Bonding temperatures were investigated over a temperature range of 1600° to 2200° C. The effects of postbonding thermal treatments of 1800° to 2500° C were also evaluated. The butt-joined coupons submitted to Lewis were well bonded with grain growth occurring across the bond lines, as shown in figure 25. The joint design shown in the sketch in this figure was necessary in order to produce a component of force normal to all mating surfaces during bonding. An insert of $W-UO_2$ machined with two of these stepped surfaces was used for the required cylinders in order to provide proper surface preparation and alinement of the joint. T-sections were prepared by bonding the upright member into a recess machined in the base member.

Evaluation of the samples submitted at the conclusion of this study indicated that the joints in the flat plates were of satisfactory quality, but the cylindrical and T-joints were of very poor quality. Metallographic examination revealed that only a small percentage of the joint areas in the cylinders and T-sections were bonded. The cylinders were out-of-round and contaminated with tantalum carbide from the bonding fixtures. However, tensile tests at 2500° C on the larger diffusion bonded plates indicated that the joints possessed strengths comparable to that of the base $W-UO_2$ material. These data also indicated that the samples bonded at 2000° C and subsequently heat treated at 2500° C for 2 hours in vacuum resulted in the highest strength.

Although the feasibility of using the vacuum-hot-pressure diffusion-bonding technique to join $W-UO_2$ plates was established, the generally satisfactory results, which were obtained on butt joints in flat plates, were not reproduced in the cylindrical or T-configurations. Since cylinders, in particular, were of primary interest in these studies, this joining process is not considered applicable to the specific needs of the program.

Vapor-deposition welding. - Welding $W-UO_2$ composites was attempted in another contracted study[1] using the hydrogen reduction of WCl_6 to deposit tungsten in the joints. This process is attractive since welding could be accomplished at the relatively low tem-

---

[1]Unpublished research by Sylvania Electric Products, Inc., Chemical and Metallurgical Division under NASA Contract NAS3-5206.

perature of 1000° C. The edges of the plates to be joined were ground to form a single V butt joint with an included angle of 90°. The joint then was inductively heated to 1000° C, and hydrogen and WCl_6 gases reacted at the hot surface of the plate to produce a buildup of tungsten in the V-groove. Recrystallization and grain growth across the centerline of the joint was achieved with a postdeposition heat treatment at 1950° C for 1 hour.

In-house evaluation of five small coupons joined by this welding process indicated that all contained serious joint defects. The most common defect was the presence of centerline voids in the V-joint resulting from the intersection of columnar grains growing out from the joint surfaces. Since the feasibility of welding $W-UO_2$ composites was not demonstrated for this process and since other welding processes appeared more capable of meeting the welding goals, this study was terminated before attempts were made to produce joints in larger plates, cylinders, or T-sections.

Special electron-beam-welding technique. - Since early attempts to fusion weld the $W-UO_2$ composites by using gas - tungsten-arc and electron-beam-welding processes failed because of gross porosity in the fusion zone, a special two-step electron-beam-welding technique was investigated at Lewis (ref. 25). The edges of the fuel plate were first clad with tungsten by the plasma-spray process described in reference 20. This clad edge was then machined so that a square butt joint would be produced when mating edges were butted together. The objective of the second step was to electron beam weld the tungsten cladding without allowing the beam to impinge on the $W-UO_2$ composite.

Although joints were produced in $W-UO_2$ composites with this process, porosity was evident in the plasma-sprayed tungsten. Another disadvantage of this process is that an unfueled zone, approximately 0.03 inch wide (0.76 mm), would be necessary for each joint. Because of these problems and the more encouraging results attained with the other processes, work on this process was terminated early in the study.

Discussion and summary of welding techniques. - Of the six welding techniques studied, the gas-pressure-bonding process is considered to have best met the goals established for joining $W-UO_2$ composites. This process was the only one that was successfully used to produce all the required configurations. In addition, joints produced by the gas-pressure-bonding process, unlike those resulting from the other welding methods, had no unfueled zone and no upset or excess material at the joint.

One possible drawback of gas-pressure bonding could be the high cost involved in producing numerous joints possibly required in fuel elements because of the special processing steps and equipment required. Therefore, alternate methods of welding may be desired. The two methods that appear most attractive as alternates are the gas - tungsten-arc-brazing and the magnetic-force-welding processes. Both of these processes required considerably more development for joining $W-UO_2$ composites, but the feasibility of producing joints was demonstrated. Also, both processes appear to be economically attractive.

The other three welding techniques studied do not appear attractive for use in producing joints in W-UO$_2$ fuel elements. The vacuum-hot-press bonding process does not appear to have any advantage over gas-pressure bonding, and the vacuum-hot-press bonding process has serious potential drawbacks associated with the complex joint configurations required and contamination from the die materials. Feasibility for welding W-UO$_2$ composites was not fully demonstrated for the other two processes, vapor-deposition welding and electron-beam welding of tungsten-clad coupon edges, and these methods necessarily result in relatively large unfueled zones at the joint.

Inspection Techniques

In order to ensure the high reliability required in the TWMR fuel elements, inspection methods are needed to measure the following fuel-element parameters nondestructively:

(1) Fuel loading

(2) Fuel core and cladding integrity

(3) Core-to-clad bond quality

(4) Cladding thickness

(5) Dimensional tolerances

Because very few inspection techniques were available for W-UO$_2$ composites (particularly for a complex configuration like the honeycomb grid), a contracted study (ref. 30) was conducted with the purpose of modifying existing testing techniques and developing new ones, if necessary.

The prime objectives of this study were as follows:

(1) To evaluate the feasibility of using various inspection methods and to determine the most promising methods

(2) To develop the most promising methods for use in W-UO$_2$ fuel-element configurations

(3) To evaluate experimentally the effectiveness of the developed methods by use of other nondestructive and destructive tests on W-UO$_2$ samples

(4) To construct prototype systems for those nondestructive test methods whose applicability had been demonstrated

Initial studies were conducted on the simplest geometry: flat plates. The more suitable test methods then were adapted to the more complex honeycomb-grid geometry. Because of the increased emphasis on the honeycomb-grid geometry, no work was performed on the testing of cylindrical fuel-element configurations. It is thought, however, that the test methods developed for the honeycombs could be adapted readily to the cylindrical geometry.

Three general testing methods proved to be satisfactory for one or more of the fuel-element parameters previously cited. These methods include ultrasonic testing, electromagnetic (eddy current) testing, and nuclear testing. In addition to those methods, special visual or mechanical techniques were used to measure dimensional tolerances. None of the test techniques, however, were developed to their ultimate capability because of the termination of the TWMR program.

Ultrasonic testing. - The feasibility of using ultrasonic testing was demonstrated for the determination of fuel loading, clad-to-core bond quality, and core and cladding integrity. A mechanical scanning system was developed for inspection of flat plates, and miniaturized probes were built for inspection of honeycomb webs. Water was used to transfer energy between the ultrasonic crystals and the honeycomb webs.

A through-transmission ultrasonic test technique was extensively investigated for measuring UO_2 fuel loading in flat plates. This test utilizes a wide-band ultrasonic system to determine the resonant frequency of the W-UO_2 plate. This frequency was thought to be primarily a function of the fuel loading of the plate. Unfortunately, in many cases the data obtained from this test did not agree with either chemical analysis or with the results obtained from other testing techniques. This difference was probably a result of the fact that the resonant frequency of the fuel plate was not only a function of fuel loading but also a function of plate thickness, density, grain size, and UO_2 particle size and shape. Because of the large number of fuel element variables affecting the ultrasonic fuel loading test, this process is not too promising at its current state of development. This test method might be used, however, as a process control method, since it is sensitive to variables such as density and particle shape.

Through-transmission ultrasonics techniques also were employed for detecting clad-to-core bond defects. One problem with this method was that it was impossible to tell the difference between a tight mechanical bond and a metallurgical bond in which there is grain growth across the interface. Additional work must be done to resolve this problem area.

Internal defects, such as cracks and voids, were detected in W-UO_2 cermet plates by an ultrasonic pulse-echo technique using a focused transducer. The test system utilized a scanning mechanism that was interchangeable with that used in the fuel-loading test. However, efforts still are needed to improve the sensitivity of this defect test since the surface condition of the plate greatly affects the test response.

Because of the complex geometry, it was not possible to use the ultrasonic pulse-echo technique to detect flaws in the honeycomb grid, but a through-transmission method was developed. Initial work employed two transducers in adjacent flow channels with the ultrasonic beam passing through the thickness of the webs. Another technique was developed in which the ultrasonic energy was sent across the width of the web rather than across the thickness. This system resulted in increased sensitivity to small transverse

cracks which were typical of the majority of the flaws observed.

Electromagnetic testing. - Electromagnetic (eddy current) testing proved feasible for the detection of fuel loading and plate-thickness variation on flat $W-UO_2$ plates and for the determination of fuel loading, integrity, and channel dimensions for the honeycomb configuration.

A through-transmission eddy-current system was developed to determine the fuel loading of flat plates by measuring the bulk resistivity of the cermets. Unfortunately, the resistivity of the samples was found to be a function of not only the fuel loading but also the plate density. In addition, the thickness of the plates also affected the results of the test. For example, a change of 1 percent in the density of the plate caused a change of about 2.3 percent in the indicated fuel loading, and a change of 0.001 inch (0.025 mm) in thickness resulted in a 1-percent change in indicated fuel loading. This test system, however, is relatively insensitive to UO_2 particle elongation, and it probably one of the more promising of the fuel-loading tests.

Although eddy-current techniques were used to measure the fuel loading and channel dimensions of honeycomb grids, most of the effort on this technique was devoted primarily to the detection of flaws and cracks within the honeycomb. In this technique, an oscillator energized a single coil probe which was mounted on the end of a shaft and inserted into the flow channels of the honeycomb grid. The eddy currents induced by this probe flowed around the channel walls and were most sensitive to cracks oriented at right angles to the current flow. Test results correlated very well with the ultrasonic crack inspection data; however, interpretation was hindered by the lack of defect standards.

Nuclear testing. - A beta-gamma activity measuring technique was developed for the determination of the fuel loading of flat plates and honeycombs. The measurement error on flat plates known to contain 10- or 20-volume-percent fuel loadings was ±0.70-volume-percent UO_2 at a 95-percent confidence level. The advantage of this method is that it is relatively insensitive to changes in the density or overall thickness of the plate. Excellent test results were obtained when the cladding thickness was held constant since the system was sensitive to changes in cladding thickness. In the case of honeycombs, the probe responded to activity from all six sides of each channel and thus measured the average fuel loading. The test results obtained with this method agreed quite well with the chemical analysis, as shown in figure 26, for a variably loaded honeycomb.

Autoradiography, which uses radiation from the $W-UO_2$ composite to expose x-ray film, also was used to determine fuel-loading and cladding variation. A densitometer technique was developed to determine fuel loading from autoradiographs accurately. This method was time consuming and difficult to adapt to complex geometries; however, it was used as a check on other testing methods.

Dimensional measurements. - An optical technique was developed for qualitatively determining the warp, maximum web thickness, and flow-channel alinement of honey-

comb grids. In this technique, the test sample was alined in a parallel light beam so that the light rays would travel axially through the flow channels, as shown in figure 27(a). Any deviation from parallel was observed as a broadening of the shadow. Similarly, increases in web thickness broadened the shadow, and if the flow channels were parallel, maximum web thickness was determined from the width of the shadow. Shadowgraphs of representative honeycomb grids with poor or good dimensional control are shown in figures 27(b) and (c), respectively.

A mechanical web-thickness gage was developed to measure web-thickness variations in honeycomb grids. The unit employed spring-loaded fingers (connected to a dial indicator) that moved up and down the flow channels and was capable of measurements accurate to ±0.0005 inch (±0.013 mm) (fig. 28).

Discussion and summary of inspection techniques. - Several methods appear promising for nondestructive inspection of W-UO$_2$ fuel elements, but considerably more development of these processes is needed for them to be used quantitatively. Inspection is complicated by the fact that many of the test systems responded to more than one fuel element variable, and thus the effects of all these variables must be known. The relative performance of the various test methods is summarized in table I (from ref. 30).

Several of the methods investigated to determine the fuel loading of W-UO$_2$ composites were quite sensitive to variables such as the thickness and density of the composite and the size and shape of the UO$_2$ particles. When all these variables were closely controlled (as in the case of test standards), good agreement on indicated fuel loadings was achieved among the various test methods, as shown in figure 29. Cross correlation of test results on other samples, however, was not so promising. Of the methods investigated for the determination of fuel loading, only the nuclear testing techniques were relatively unaffected by other fuel element variables.

The determination of fuel-core and cladding integrity appeared to be a less difficult problem than the determination of fuel loading. Eddy current and ultrasonic methods could be used to detect cracks in the W-UO$_2$ composites. The eddy-current technique was used only on the honeycomb grids, while the ultrasonic method was applicable to both plates and honeycomb grids. Both systems were sensitive to the surface condition of the samples, and more work is required to minimize this sensitivity. In addition, the ultimate resolution of the two systems is still unknown because of the lack of suitable test standards.

The detection of clad-to-core bond defects was investigated by the through-transmission ultrasonic technique. This method responded well to actual separation of the core and cladding, but it could not differentiate between a good mechanical bond and a metallurgical bond.

Only a limited effort was directed toward measuring the fuel element cladding thickness. The nuclear techniques easily detected variations in cladding thickness, but for

these techniques to provide usable information, the fuel loading must be held constant. The eddy-current test also appeared sensitive to cladding thickness, but considerably more work is required on this test technique before it is applicable.

Two techniques, one optical and the other mechanical, were developed to check the dimensional tolerances of the honeycomb grids. Because of the excellent results obtained with these methods, prototypes of these systems were constructed and supplied to Lewis.

It is apparent from the results of this study of nondestructive testing techniques that more work is required to evaluate the various test systems fully. In addition, it is probable that no one test system will meet all the goals of the program; therefore, a combination of test systems will be required to ensure high fuel element quality.

FUEL RETENTION STUDIES

One of the principal requirements of the $W-UO_2$ fuel elements in the tungsten water-moderated nuclear rocket reactor concept is that the fissionable material be retained under the reactor operating conditions. The target of the work conducted in this feasibility study was that there should be less than 1 weight percent of the fuel lost during operation for 10 hours at temperatures up to at least 2500° C in a turbulent flow of hydrogen at pressures ranging from 15 to 600 pounds per square inch (0.1 to 4.1 MN/m^2) or in a vacuum. In addition, it should be possible to thermal cycle the composites from ambient to maximum temperatures at least 25 times for reactor testing and operation.

An extensive investigation was made of the modes of fuel loss and of methods for limiting fuel loss. The important results and the present status of this work are described in this section of the report.

Modes of Fuel Loss

Surface vaporization loss. - A large amount of fuel is volatilized from unclad $W-UO_2$ composites which are held at temperatures above about 1900° C. This fuel loss can be reduced by cladding the composite with a thin layer (0.001 in. (0.025 mm) or greater thickness) of tungsten. Figure 30 shows the difference in fuel loss between unclad and face-clad[2] $W-UO_2$ plate-type specimens containing 20-volume-percent UO_2 after being heated at 2500° C in flowing hydrogen for the indicated periods of time. For example, the curves show that after 6 hours of heating the unclad composites lost about 25 percent

---

[2] A face-clad specimen, usually a coupon nominally 1.4 by 1 by 0.02 inch (3.6 by 2.5 by 0.05 cm) was clad with tungsten on the major faces by foil roll cladding with the edges remaining exposed.

of their fuel, wheras the face-clad composites lost only about 2 percent. Metallographic examination of the heat-treated composites showed depletion of UO_2 on all unclad surfaces, as shown in figure 16(a); however, no such loss was observed through clad surfaces.

The high vapor pressure of UO_2, about 3 millimeters (400 N/m^2) at 2500° C, is responsible for the observed loss of UO_2 particles exposed at the surfaces of unclad $W-UO_2$ composites. Factors which, if present, can cause increased loss of fuel by volatilization are interconnection of the UO_2 particles, microscopic pores and cracks in the tungsten matrix and cladding, and impurities which can react or vaporize at high temperatures to cause defects in the fuel element (e. g., carbon or fluorine compounds).

Fuel migration and loss induced by thermal cycling. - Tungsten-clad specimens, which retained fuel for many hours of continuous heating at 2500° C, suffered catastrophic fuel loss and structural deterioration when repeatedly cycled from ambient temperature to 2500° C in flowing hydrogen (see ref. 5). The catastrophic fuel loss is demonstrated in figure 31 which compares the fuel losses from face-clad specimens heat treated for up to 10 hours at 2500° C, continuously or with intermittent cooling. In 10 hours, the continuously heated specimens lost only 2 percent of their fuel (mostly from the unclad edges), whereas the cycled specimens lost 43 percent of their fuel.

The shape of the fuel-loss curves obtained by thermal cycling of face-clad composites can be explained as follows:

(1) The initial rise in the curve during the first cycle was caused by volatilization of exposed UO_2 at the unclad edges.

(2) The subsequent region of essentially constant slope was the result of a slow decomposition of the fuel followed by migration of the decomposition products through the grain boundaries of the tungsten matrix and cladding and to volatilization of these products at the surface.

(3) The final sharp rise, indicating failure, resulted from rapid volatilization of exposed UO_2 due to extensive embrittlement and cracking of the tungsten matrix and cladding and complete invasion of the grain boundaries by migrating UO_2.

An example of a typical microstructure which resulted from the thermal cycling of a $W-UO_2$ composite is shown in figure 32. The third phase, located between the W and UO_2 particles and in the grain boundaries of this unetched structure, is a uranium-rich phase that precipitates in the low-temperature part of the thermal cycles.

The mechanism by which fuel migration is initiated and enhanced under thermal-cycling conditions depends on the facts that UO_2 becomes oxygen deficient at temperatures above about 1400° C in dry, oxygen-free hydrogen and that, on cooling, the substoichiometric UO_2 disproportionates to free U and UO_2 (see refs. 31 to 33 for expanded discussions). The resultant uranium metal (melting point of about 1130° C) can readily migrate along grain boundaries in the tungsten matrix, can rapidly form uranium hydride

(UH$_3$) at about 225° C with a large increase in volume, and/or can reoxidize to UO$_2$ with a large increase in volume. These reactions, involving volume changes, can cause separation of the tungsten grains and create avenues for subsequent migration of UO$_2$ to the surfaces of the composites. This mechanism is based on metallographic, electron-microprobe, mass-spectrometric (to detect species which evolve from composites in a vacuum at elevated temperature), and analytical chemistry studies.

Control of Surface Vaporization Losses

Two approaches were taken to reduce losses due to vaporization of exposed UO$_2$ (ref. 34):

(1) Cladding all exterior surfaces of the composite with a thin ($\geq$0.001 in. (0.025 mm) thick) coating of tungsten

(2) Eliminating interconnection of UO$_2$ particles by coating the particles with an even thinner (~0.0002 in. (0.005 mm) thick) layer of tungsten before consolidation

The effectiveness of these approaches is indicated in figure 33, which shows the results of heating clad and unclad W - 20-volume-percent-UO$_2$ composites which were fabricated from W-coated UO$_2$ particles or from powder mixtures of W and UO$_2$. Composites with a complete external cladding show little fuel loss with or without the use of coated particles. However, use of coated particles in unclad specimens leads to improved fuel retention. The combined use of a full cladding and W-coated UO$_2$ particles is an attractive approach to control vaporization loss since greater reliability should be attained through applying both processes.

Control of Fuel Migration and Fuel Loss Induced by Thermal Cycling

Several methods for reducing the rate of fuel loss from W-UO$_2$ cermets under thermal cycling conditions were investigated (refs. 5 and 31). These methods include

(1) The use of fine UO$_2$ powder instead of coarse UO$_2$, that is, powder having an average particle diameter of about 1 micron as opposed to an average diameter of about 50 microns

(2) The addition of a submicron dispersion of thorium dioxide (ThO$_2$) to the tungsten matrix

(3) The addition of metal oxides in solid solution with the UO$_2$ to serve as stabilizers

(4) Complete cladding of the composite with tungsten which, in addition to its effect in controlling losses due to volatilization, acts to suppress the decomposition of UO$_2$

A brief discussion of each of these methods is given in the following paragraphs.

Fine uranium dioxide particles. - A dispersion of UO_2 as micron-size (i. e. , about 1 μm in diam) particles throughout the tungsten matrix was tried as a way of refining the tungsten grain size in the hope that this would lead to improved fuel retention. The experimental results, plotted in figure 34, confirm that fuel retention was significantly improved. Unfortunately, the high-temperature tensile strength of sintered and rolled composites containing micron-size UO_2 is much less than that of composites containing 50-micron UO_2 (see section, PROPERTY EVALUATION). This decrease in strength may be assoicated with the increased probability of interconnection of fuel particles and/ or with the greater difficulty in fabricating the composites leading to the introduction of microscopic cracks in the specimens. Therefore, methods would have to be developed to separate the UO_2 particles or otherwise increase the strength of these composites before this type of material could be considered for reactor use.

Matrix dispersions. - Because fine dispersions of ThO_2 are known to give grain refinement in tungsten, composites were prepared containing about 2 volume percent of fine ThO_2 particles (about 0.6 μm) in the tungsten matrix and either 50-micron or 1-micron particles of UO_2. These composites showed improved fuel retention (fig. 34). The addition of fine ThO_2 also led to greater high-temperature tensile strength (see section PROPERTY EVALUATION) than with specimens that were compacted from mixtures of tungsten and 50-micron UO_2 powders. The improvement in properties could not be attributed to grain refinement of the tungsten (as shown in ref. 31) of the tungsten matrix, but it must be the result of some undetermined factor, such as the increased interface area. In cases where composites are fabricated from particles of UO_2 vapor coated with tungsten, techniques for introducing a fine dispersion of ThO_2 in the tungsten coating have not been worked out. Because of the benefits to be gained with these matrix additions, possibly in combination with other methods for improving thermal cycling stability, future fuel element requirements may justify development of processes to disperse fine oxides (e. g. , ThO_2 or other refractory oxides) in the tungsten coatings on fuel particles.

Fuel stabilizers. - Other test results indicated that stabilizing additions to the UO_2 were highly effective in preventing fuel loss; therefore, more recent studies (refs. 33 and 35) concentrated on this method of reducing fuel losses. These studies were conducted on composites that contained the highest fuel loading that might be considered for the TWMR, 35-volume-percent UO_2, as this UO_2 content represents the most difficult case for fuel retention (see fig. 35). Figure 36 summarizes the results of screening tests on face-clad composites containing a variety of metal oxides tested as stabilizers. Each oxide was added in solid solution to UO_2 at the 10-mole-percent concentration level, and then the solid solution was incorporated with tungsten in face-clad composites. The composites then were thermally cycled to 2500° in flowing hydrogen, and fuel-loss data were obtained. On the basis of these data, yttrium oxide (Y_2O_3) and cerium oxide (CeO_2)

were selected for further evaluation as stabilizing additives to UO_2 in fully clad specimens because these oxides were representative of two of the best groups and both yttrium and cerium are suitable for thermal reactor use because of their low thermal neutron cross sections.

Curves of fuel loss during thermal cycling to 2500° C (in purified hydrogen at 0.1 MN/m^2 pressure) for fully clad specimens are shown in figure 37. These specimens contained 35-volume-percent UO_2 stabilized with 10-mole-percent Y_2O_3 or with 10-mole-percent Ce_2O_3 (added as 18-mole-percent CeO_2 since CeO_2 can be reduced to Ce_2O_3 at high temperatures in hydrogen). These plots indicate little difference in behavior for the two types of composites; however, Ce_2O_3 appears to be a more effective additive than Y_2O_3 judging by metallographic examination (see fig. 38) of these composites after 25 cycles and after 60 cycles to 2500° C. These photomicrographs show less migration of fuel in the cermet containing Ce_2O_3-stabilized UO_2. After twenty-five 10-minute cycles to 2500° C, however, fully-clad composites with either additive met the goal of less than 1 weight percent of fuel loss.

Studies were conducted to determine the effect of the concentration of a stabilizing additive in the UO_2 on fuel migration and loss. The additive concentration is important since it is desired to have sufficient chemical stability without unduly sacrificing composite strength by adding to the ceramic loading (see section, PROPERTY EVALUATION). The effects of 2.5-, 5-, and 10-mole-percent Ce_2O_3 on the fuel-loss rate from $W-UO_2$ composites are shown in figure 39. Although cermets containing 2.5-mole-percent Ce_2O_3 appear to meet the goals of less than 1-percent loss after 25 cycles, composites with the highest additive concentration tested (i. e., 10-mole-percent Ce_2O_3) gave the best results and thus should improve the reliability of the cermets. Further work is required to determine the optimum amount of additive to achieve low fuel loss and sufficient mechanical strength.

Some postulated mechanisms by which oxide additives stabilize UO_2 are discussed in detail in references 32 and 33. Both Y_2O_3 and Ce_2O_3 are thought to lower the partial molar free energy of oxygen in the ceramic phase without the possibility of forming free metal on cooling such as is the case with unstabilized, oxygen-deficient UO_2. The evidence at hand indicates that Ce_2O_3 is a somewhat more effective stabilizer than Y_2O_3. But the reason for this has not been determined. The fact that cerium has a fairly stable +4 oxidation state as well as a +3 oxidation state may be a clue to its behavior.

To help gain a better understanding of these results, two supporting studies were conducted. The effect of additives to UO_2 on the location of the phase boundary separating the solid solutions of U and UO_2 (i. e., UO_{2-x}) and the adjoining two-phase region consisting of U and UO_{2-x} was investigated by a thermal analysis technique in a contracted study (ref. 36). The results indicate that ThO_2, calcium oxide (CaO), Y_2O_3, or CeO_2 additives have no significant effect on the position of the solvus curve representing

the separation of U from UO_{2-x}. It was concluded from this work that since the additives do not increase the solubility of uranium in UO_2, their effect must be to stabilize the UO_2 against reduction.

In another study,[3] the gases evolved under thermal cycling conditions from $W-UO_2$ composites of various compositions were analyzed by using a mass spectrometer. The results confirmed those from thermal-cycling fuel-loss tests. For example, no U-bearing species were detected from composites stabilized with cerium oxide additives up to the maximum number of cycles tested (198 cycles to 2600° C); whereas, U-bearing species were observed in the mass spectrum of gases evolved from composites containing fuel with no additives, with CaO, or with Y_2O_3 after 1, 28, and 46 cycles, respectively.

This study also indicated that electrodischarge machining of $W-UO_2$ cermets in an oil bath results in the addition of carbon impurities which can be detrimental to the high-temperature stability of the fuel. Therefore, this type of machining should be avoided in the preparation of fuel elements.

The effect of controlled variations in oxygen-to-metal ratio of stabilized fuels has not been adequately studied in this program. This should be done (particularly the variation of the partial molar free energy of oxygen as a function of the oxygen-to-metal ratio in solid solutions) because quantitative data on the effect of the oxygen-to-metal ratio on fuel loss should lead to a better understanding of the mechanism of UO_2 stabilization.

Surface claddings. - In addition to preventing volatilization of UO_2, an external tungsten cladding on a $W-UO_2$ composite stabilizes the UO_2 against decomposition by retaining reaction products. This is believed to account for the large difference in thermal cycling behavior between face-clad and fully clad specimens (fig. 40) and, also, for the large effect of cladding integrity and cladding thickness on fuel loss during thermal cycling. Results from one series of thermal cyclic tests (ref. 24) indicate that thicker tungsten cladding (0.004 to 0.005 in. (0.10 to 0.13 mm)) also had an important effect in suppressing fuel loss (see fig. 41); however, migration of UO_2 in the $W-UO_2$ core was not prevented with the thicker claddings.

The role of the tungsten cladding in controlling fuel loss was clarified by high-temperature measurements of the rate of permeation of oxygen and hydrogen through tungsten membranes. This study was made under a NASA-supported contract (ref. 37). It is of special interest that the rate at which the oxygen-to-uranium ratio decreases in the UO_2 in a composite of known composition, dimensions, and cladding thickness, can be calculated from oxygen permeation data and oxygen partial pressure data (as discussed in ref. 35). The lifetime of a composite should decrease in direct proportion with increasing oxygen permeation rate.

---

[3]Unpublished work by Avco Corp., Research and Technology Laboratories under NASA Contract NAS3-6212.

Effect of Test Conditions on Fuel Loss

The rate of fuel loss from W-UO_2 composites depends on many test and materials variables. In view of the dramatic effect of thermal cycling on the fuel loss, fairly extensive studies were made of the influence of the following test variables: (1) the maximum temperature during each cycle, (2) the hold time at the maximum temperature during each cycle, (3) the heating and cooling rates at the beginning and end of each cycle, (4) the atmosphere in which the specimens are cycled, (5) the pressure of hydrogen where hydrogen is the cycling atmosphere, and (6) the flow rate of hydrogen. This work was conducted at Lewis (refs. 31 and 35) and under a NASA-supported contract (refs. 38 and 39). The majority of these studies was done on hot-roll-compacted powder-metallurgy W-UO_2 coupons that were clad on the faces with roll-bonded tungsten foil and on the edges with sintered, compacted tungsten powder. The effects of the test variables are summarized in the following paragraphs.

Maximum temperature. - To determine how well a composite will withstand high-temperature excursions such as in "hot spots" which might be generated in an actual operating reactor, the effect of cycling temperatures above 2500° C was studied. Figure 42 shows fuel loss curves for composites stabilized with 10-mole-percent Ce_2O_3 tested at either 2500° or 2600° C. Clearly the effect of an increase in maximum cycling temperature is to decrease the cyclic life of fueled composites. Actual measured values indicate a loss of about 1.5 weight percent from Ce_2O_3 stabilized composites after 25 cycles to 2600° C compared with less than 1 weight percent after 25 cycles to 2500° C. Qualitatively, the results were as expected since an increase in temperature results in higher rates of fuel decomposition, migration, and vaporization.

Hold time. - Increased time at temperature during each cycle also caused a greater loss of fuel for a fixed number of cycles, as indicated in figure 43. For long hold times (120 min) the total operating time goal of 10 hours to 1-percent fuel loss was met, but the number of cycles was small. On the other hand, for short operating cycles (2 min), the total operating time to 1-percent loss was less than 10 hours but more than 25 cycles were completed. Thus, reactor operating cycles, particularly during ground testing, should be carefully selected.

Heating and cooling rates. - Comparison of heating and cooling rates of 15 seconds and 10 minutes between ambient temperature and 2500° C (see fig. 44) showed a slightly greater fuel loss for the 10-minute interval. However, the loss rates were not greatly different, and it appears that the rates of heating and cooling do not play a significant role in determining fuel element life.

Test atmosphere. - Although fuel is lost on cycling specimens in either a vacuum of about 3×10^{-5} torr (4×10^{-3} N/m²), or in an inert gas like helium, the rate of loss was much greater in hydrogen, as indicated in figure 45. This high rate of loss is probably

a result of both the lower oxygen partial pressure in hydrogen at high temperatures affecting the degree of UO_2 decomposition and of UH_3 formation at low temperatures in an atmosphere of hydrogen. The lower oxygen partial pressure effect is the most important because damage is sustained regardless of the presence or absence of the hydriding effect when free uranium is present.

Hydrogen pressure. - Thermal cycling tests on fully clad composites containing stabilized UO_2 were performed under a contracted study (refs. 35 and 39). The results (see fig. 46) indicate that a hydrogen pressure increase did not cause any significant increase in fuel loss during twenty-five 10-minute thermal cycles to 2500° C. On further cycling and, especially, on raising the test temperature to 2600° C or increasing the hold time per cycle, some of the test specimens developed blisters and/or fractures in 600-pound-per-square-inch (4.1 MN/m^2) hydrogen, but not in 15-pound-per-square-inch (0.1 MN/m^2) hydrogen. These effects of high-pressure hydrogen should be investigated further.

Hydrogen flow rate. - Fuel losses from specimens cycled in hydrogen flowing at 0 and 35 standard cubic feet per hour (0 and 1 m^3/hr, enough to replace the gas in the cycling furnace about 20 times in 1 min) were compared. The losses were much less under zero flow conditions, probably due to accumulation of reaction products that suppressed further decomposition of the UO_2. The effect of higher hydrogen flow rates such as would be encountered in an actual rocket reactor were tested only cursorily on unclad specimens at Lewis. These tests indicated that fuel loss was not significantly increased by a change from laminar to turbulent flow. Testing of fully clad specimens by thermal cycling in a high-pressure, high-flow-rate, hydrogen atmosphere was not done, but it is expected that the fuel losses would not be significantly increased under these conditions.

Discussion and Summary of Fuel Retention Studies

Much progress was made in the discovery, selection, and development of methods for controlling fuel loss and migration in $W-UO_2$ composites at high temperatures. As a result of this progress, the principal emphasis was finally placed on a combination of the following methods: the use of a tungsten cladding over all external surfaces of each fuel element to minimize fuel volatilization; the use of W-coated particles of UO_2 in fabrication to prevent UO_2 particle interconnection and consequently to minimize fuel migration and volatilization; and the use of an oxide stabilizer, added in solid solution to the UO_2, to suppress fuel decomposition and migration. Composite specimens fabricated by isostatic compaction of coated particles containing stabilized UO_2 (10-mole-percent Y_2O_3 or Ce_2O_3 stabilizer) and clad by vapor deposition from WCl_6 were thoroughly tested (see ref. 39). The results qualitatively confirm the findings from powder-metallurgy speci-

mens. However, the inconsistent quality of the coated-particle specimens hindered quantitative comparisons. Thus, more work is required to realize the full potential of this combination of methods for fuel retention. Specifically, the best conditions for consistently achieving good quality coated particles, fully dense composites, and defect-free claddings must be determined.

The available evidence shows that a 0.001-inch (0.025 mm) cladding is sufficient to meet the goals set for fuel retention where ceria- or yttria-stabilized UO_2 is used. Where possible, from neutronic considerations, thicker claddings would improve fuel retention and/or mechanical strength.

Either Y_2O_3 or Ce_2O_3 fuel additives, at a concentration of 10 mole percent in UO_2, is sufficient to restrict fuel loss to less than 1 percent after twenty-five 10 minute cycles to 2500° C in flowing hydrogen at 15 to 600 pounds per square inch (0.1 to 4.1 MN/m^2). A decision as to which additive is best cannot be made on the basis of the data at hand although Ce_2O_3 appears to delay fuel migration somewhat longer than Y_2O_3.

The oxygen-to-metal ratio in the fuel was not known or controlled during preparation of composite specimens, except that the conditions of sintering were such that no uranium metal was produced. Although the fuel loss results were quite low on the composites tested, the possibility of improving these, of ensuring close reproducibility of results, and of distinguishing between the effectiveness of Ce_2O_3 and Y_2O_3 as additives by adjusting and controlling the oxygen-to-metal ratio in fuels should be investigated.

PROPERTY EVALUATION

To form a basis for the conceptual design studies of the TWMR, selected mechanical and physical properties of $W-UO_2$ composites were evaluated over the temperature range of interest to the TWMR (to 2750° C). The properties determined included high-temperature tensile strength, creep-rupture life, modulus of elasticity, bend-transition temperature, thermal expansivity, and thermal conductivity.

Initially, all these properties were determined for the sintered and rolled $W-UO_2$ composites that were considered as the reference materials for this program, and the resultant data are presented in the first part of this section. As changes were made in the starting material and fabrication processes, additional tests were conducted to determine the influence of these changes on the high-temperature properties of the composites. The results of these tests are summarized in a subsequent part of this section.

For the following series of tests, plate-type specimens were produced from mixtures of W (about 1 μm) and UO_2 (about 50 μm) powders by the sintering and rolling process described previously. Approximately 0.002-inch-thick (0.05 mm) claddings were applied to the major faces of these samples by roll cladding. The properties were determined in both in-house and contracted studies primarily for composites containing 10-, 20-, 30-, or 40-volume-percent UO_2.

High-temperature tensile strength. - High-temperature tensile tests were conducted in vacuum (10^{-5} torr, 10^{-3} N/m^2) at temperatures in the range of 1650° to 2760° C. The test equipment and procedures used are described in references 40 and 41.

The initial tensile testing was conducted on composites containing 20-volume-percent UO_2, the average reactor core loading for the TWMR. The ultimate tensile strength of this material from 1930° to 2760° C at a nominal strain rate of 0.030 inch per inch per minute (0.030 cm/cm/min) is shown in figure 47. For comparison, the strength of un-fueled tungsten (produced by the same fabrication method) is included in the figure. Comparison of the curves indicates that the UO_2 apparently enhanced the strength of the composite over the entire temperature range studied.

Since fuel elements in the TWMR will operate primarily in a hydrogen atmosphere, similar tensile tests were conducted on W - 20-volume-percent-UO_2 composites in a static hydrogen atmosphere (3 psig (124 kN/m^2)) to determine if the test atmosphere affected the strength of the composites. The results from these hydrogen atmosphere tests were similar to those from the vacuum tests just described. Since the test atmosphere appeared to have no appreciable effect on the tensile strength of these composites, all other high-temperature tests were conducted in vacuum for testing convenience.

To determine the effect of fuel loading on the strength of these rolled composites, a series of tests was run in which the fuel loading of similarly fabricated composites was varied from 10- to 50-volume-percent UO_2 in 10-volume-percent increments. The resultant data, plotted in figure 48, indicate that UO_2 additions of up to 30 volume percent did not adversely affect the strength of these composites at 2500° C. However, at fuel loadings greater than 30 percent, the strength decreased with increasing fuel loadings. This strength decrease at high fuel loadings was an important factor in establishing the maximum fuel content in the TWMR fuel elements at about 35-volume-percent UO_2. The data shown in figure 48(b) indicate that the ductility of all the composites tested was greater than 10-percent reduction in area, which is considered adequate for reactor use.

Although tensile strengths as a function of temperature were not obtained for composites other than the W - 20-volume-percent-UO_2 composite, other composites with fuel loadings of interest for the TWMR (10- to 35-percent UO_2) probably would exhibit temper-

ature dependency characteristics similar to those of W - 20-percent UO_2 composites (fig. 47).

High-temperature creep-rupture strength. - In order to determine the load-carrying capability of the reference composites, short-time creep-rupture tests were conducted at Lewis. The loads used in these tests were selected to produce specimen rupture in less than 20 hours. The procedures and equipment used to conduct these tests are described in references 40 and 41. For testing convenience, all these tests were conducted in vacuum. Although the effects of hydrogen are not expected to be significant, the actual effects of hydrogen in these longer term tests were not determined.

The initial creep-rupture tests were performed on reference W - 20-volume-percent-UO_2 composites over the temperature range of 1650° to 2500° C. The resultant data are plotted in figure 49. These data indicate a temperature dependency similar to that observed in the tensile-test results.

To determine the effect of fuel loading on the creep-rupture properties of the reference material, creep-rupture tests were run at 2500° C on composites containing 10-, 30-, or 40-volume-percent UO_2. The resultant data from these tests are compared in figure 50 with those for W - 20-volume-percent-UO_2 composites and for unfueled tungsten produced by the same process. Contrary to the tensile results obtained with similar materials, the creep-rupture strengths of the W-UO_2 composites were consistently lower than that of the unfueled tungsten. However, the differences were small in comparison with the effects of temperature on W - 20-UO_2 composites (shown previously in fig. 49). There also were small differences in the 2500° C strengths of the composites of various fuel loadings, but the strengths of the composites did not fall in a consistent order. Because of some uncertainities associated with the reproducibility in quality of these composites (they were fabricated and tested at widely different times), the creep-rupture strengths of the four composites tested are thought to be not significantly different. Therefore, the temperature-dependent data shown in figure 50 for W - 20-volume-percent-UO_2 composites should be a good approximation of the creep-rupture properties of all W-UO_2 composites considered for TWMR fuel elements.

Modulus of elasticity. - Since the design of the TWMR requires a knowledge of Young's modulus of elasticity for the fuel element materials, tests were conducted under a contracted study (ref. 42) to determine this property over the temperature range from 1650° to 2750° C. A static method of modulus determination based on tensile loading of the test specimen was used in this investigation. This method was used because the resulting data were considered to be more applicable to the materials used in the TWMR than would dynamic modulus data obtained by sonic methods. In addition, the static method yields the more conservative data of the two methods. This study included initial establishing of baseline modulus data for unalloyed, commercially produced tungsten at 1650° to 2750° C and subsequent testing at these temperatures of reference W-UO_2 com-

posites containing 10-, 20-, 30-, or 40-volume-percent UO_2.

A plot of modulus against test temperature (fig. 51) shows that the moduli of fueled materials differ only slightly from that of unfueled tungsten in the temperature range from 1650° to 1900° C; however, from 1900° to 2200° C, or about 70 to 80 percent of the absolute melting point of UO_2, the moduli of the fueled materials drop sharply to values below that of unfueled tungsten. Above 2200° C, the moduli of the fueled materials decrease with temperature at approximately the same rate as that of unfueled tungsten. This behavior suggests that at temperatures below about 1900° C, the modulus of the tungsten was not affected by the presence of the UO_2 dispersoids. In the intermediate temperature range, however, the UO_2 began to soften much faster than the tungsten and thereby rapidly reduced the moduli of the composites. At temperatures above about 2200° C, the UO_2 apparently was completely softened and the rate of decline with increasing temperature for the composite moduli again approached that of the tungsten matrix.

As observed in the creep-rupture data, no consistent order of the composite moduli was noted. However, the moduli of the composites were less than that of unfueled tungsten at temperatures above 1900° C. The modulus data shown for unfueled tungsten are higher than any other static moduli data for tungsten in the literature. The minimization of creep effects in the tests conducted in this study is believed to be the reason for the higher modulus values.

Bend-transition temperature. - Since fuel elements in the TWMR probably would not be permitted to operate at temperatures below the ductile-to-brittle transition temperature of the fuel elements, the effects of fuel loading on this transition temperature were determined in a bend test. In this test, reference $W-UO_2$ composites with fuel loadings varying from 0- to 40-volume-percent UO_2 were heated and bent to an angle of about 90° in a three-point-loaded bend tester over a radius six times the composite thickness. The lowest temperature at which each material bent without cracking was considered the ductile-to-brittle transition temperature for that material.

The results of these tests are shown in figure 53. These data indicate that the bend-transition temperature for unfueled recrystallized tungsten (produced by the same process) and of the W - 10-volume-percent-UO_2 composites were similar (approximately 255° C), but the bend-transition temperature increased rapidly as additional UO_2 was added to the composites. In fact, composites with fuel loadings of 30- to 40-percent UO_2 could not be bent at the maximum test temperature of the bend-test apparatus (about 650° C). This is another reason for keeping the UO_2 content of the fuel elements to as low a value as possible.

Thermal conductivity. - The thermal conductivity of reference composites containing 10-, 20-, 30-, or 40-volume-percent UO_2 was determined in a contracted study (ref. 43) over the temperature range from room temperature to 2430° C. The conductivity values were determined by measuring the thermal diffusivity, specific heat, and density of the

plate-type specimens and calculating the conductivity of the composites as the product of these three properties.

The thermal conductivity values resulting from this study are shown in figure 53. For comparison, literature values for W and UO_2 are included in the figure. As expected, the thermal conductivities of the composites decrease with increasing temperature and UO_2 content. However, the determined values were lower than those that can be calculated by using the "mixture rule" (a linear interpolation between the individual values of W and UO_2). Apparently the low conductivity of UO_2 had an appreciable effect on the overall conductivity of the composites.

Thermal expansivity. - Thermal expansion values for reference W-UO_2 composites also were measured in a contracted study (ref. 43). Lengthwise expansions of plate-type specimens were directly measured over the temperature range of room temperature to 2660^0 C for composites containing 10-, 20-, 30-, or 40-volume-percent UO_2.

The resulting thermal-expansion values for the composites are compared with literature values for W and UO_2 in figure 54. The expansion values for the composites are close to those of unfueled tungsten and are appreciably less than those obtained from the mixture rule. Apparently, the greater expansivity of the dispersed UO_2 particles (almost twice that of tungsten) did not have as great an effect on the overall expansivity of the composites, as would be predicted from the mixture rule.

The thermal expansion values shown in figure 54 were used to calculate the following coefficients of expansions for composites as a function of temperature:

Composite, vol. %	Coefficient of expansion, per degree centigrade
W - 10 UO_2	$(5.2193 \times 10^{-6}) - (2.3261 \times 10^{-10})T + (3.6791 \times 10^{-13})T^2$
W - 20 UO_2	$(7.0202 \times 10^{-6}) - (3.9045 \times 10^{-9})T + (1.9879 \times 10^{-12})T^2$
W - 30 UO_2	$(5.1100 \times 10^{-6}) + (7.0105 \times 10^{-10})T + (1.2963 \times 10^{-13})T^2$
W - 40 UO_2	$(7.0025 \times 10^{-6}) - (9.5560 \times 10^{-10})T + (8.4054 \times 10^{-13})T^2$

Factors Affecting Properties

As the program progressed and different materials and fabrication processes were investigated, the effect of these changes on the properties of composites became an important consideration. Therefore, selected high-temperature tests (primarily tensile and creep-rupture tests) were conducted on several modified composites to evaluate the

effect of the changes. All the properties determined for the reference material were not evaluated in these series of tests. Rather, the data obtained from limited testing of one or more properties were compared with those obtained for the reference material to determine the trend of the effect caused by the change in material or fabrication processes. These trends are briefly described in the following paragraphs and are discussed in more detail in reference 41.

Fuel particle size. - To determine the effect of changes in fuel particle size, W - 20-volume-percent-UO_2 composites containing various sizes of UO_2 particles were similarly fabricated by sintering and hot rolling and were tensile tested at 2500° C. Average UO_2 particle sizes in the range of about 1 to 125 microns were included in these tests. The results of these tests, shown in the upper curve of figure 55, indicate that composites produced from UO_2 particles of the size range of about 30 to 60 microns yielded the highest tensile strength values of those tested. This was the prime reason that UO_2 particles of about 50 microns were used in most of the studies described in this report.

To determine if a similar particle size effect occurred in composites produced from W-coated UO_2 particles, W - 35-volume-percent-UO_2 composites produced from various sized coated particles were consolidated by roll compaction and were tensile tested at 2500° C. Average particle sizes of about 10 to 100 microns were used in these tests. The averaged results of these tests are shown in the lower curves of figure 55. Comparison of the curves shown in this figure indicates a similar particle-size dependency at the larger particle sizes, but the composites produced from coated particles exhibited a strength increase with decreasing particle size. Based on these results, the strength decrease obtained with the composites produced from the smaller uncoated particles is thought to result from an interconnecting UO_2 network caused by the numerous small particles. This interconnecting network was prevented by use of precoated particles.

Further comparison of the data shown in figure 55 indicates that the maximum strength of the composites produced from coated particles is much less than that of the composites produced from powder mixtures. Part of this difference may be a result of the difference in fuel loading in the two types of composites. This lower strength, however, was observed consistently in testing composites (even of the same fuel loading) produced from coated particles regardless of the method used to consolidate them. The reason for the lower strength of composites produced from coated particles is not known, but the most probable reason is thought to be that the methods used to produce and consolidate coated particles are not as well developed and optimized as is that used to sinter and hot roll powder mixtures. Improvement in coated-particle-consolidation techniques might result in increased strength of the composites.

Fuel particle shape. - As discussed previously, in the section FABRICATION DEVELOPMENT, some of the particle-consolidation methods result in distortion of the initially spherical UO_2 particles in the W-UO_2 composites. To determine the effect of the UO_2 particle elongation on the strength of composites, W-UO_2 composites were consolidated by different methods (hot isostatic compaction, roll compaction, and extrusion) to produce varying degrees of fuel particle distortion. The average length-to-width ratios of the particles in the resulting composites ranged from about 1 to 200.

The results of high-temperature (1930° C) tensile tests on these composites are shown in figure 56. From this plot, it is apparent that fuel particle elongation (in the direction of the applied tensile load) and/or the associated effects of greater amounts of working caused an increase in the ultimate tensile strength of the composites. Although tests were not conducted on composites with the elongated particles oriented in another direction, it is thought that the greater strength of the composites with severely distorted fuel particles is anisotropic and that these composites were probably much weaker in the transverse direction. Therefore, even though higher strengths can be obtained with W-UO_2 composites containing distorted UO_2 particles, the expected undesirable anisotropy of these properties suggests that a minimum degree of fuel distortion in composites is desirable.

A theoretical analysis (ref. 12) of the thermal conductivity data shown in figure 53 supports the contention that particle distortion should be minimized. This analysis indicates that a nonspherical shape of dispersoids can appreciably affect the thermal conductivity of composites. This is thought to be the prime reason why the conductivity values determined for the reference material (length-to-width ratio of about 4) were less than those calculated from the mixture rule. Thus, less severe working processes might result in higher thermal conductivity values for W-UO_2 composites.

The effect of UO_2 particle shape was not encountered in the thermal expansivity of W-UO_2 composites. Expansion measurements (at temperatures above 2000° C) of the thickness increase of plate-type reference W - 20-percent-UO_2 composites yielded values similar to those previously discussed (fig. 54) for length expansions of the same composites. Apparently the thermal expansion of these composites was isotropic.

Cladding. - To determine the effect of thin (approximately 0.002 in. (0.05 mm)) surface claddings on the strengths of W-UO_2 composites, reference composites and roll-compacted coated particles were tensile tested in both the unclad and clad conditions. Results of numerous tests (made over a range of temperatures and fuel loadings) indicated similar strengths (ref. 41). Thus, the thin cladding used in these tests apparently did not affect the strength of the composite.

Results previously discussed in the section FUEL RETENTION STUDIES indicated that thicker claddings were helpful in reducing fuel losses under thermal cycling condi-

tions; therefore, the effect of thicker claddings on composite strength was evaluated. Since merely adding tungsten cladding to the surface of composites undesirably increases the fuel element weight and the amount of neutron absorption material, the tungsten used in cladding the specimens for this series of tests was in essence transposed from the composite core to the cladding by roll compacting thinner cores with higher fuel loadings and subsequently vapor depositing thicker tungsten claddings onto the cores. This technique resulted in a uniform specimen thickness (0.02 in. (0.05 mm)) and total fuel loading (35-percent UO_2), but a varying cladding thickness (0.001 to 0.005 in. (0.025 to 0.127 mm)) and core fuel loading (35- to 60-percent UO_2). The results of tensile tests at 2500° C on these roll-compacted composites indicated that the tensile strength of the composites did not vary appreciably with changes in cladding thickness. Apparently, the transfer of tungsten from the core to the cladding did not affect the strength of the composites.

Additives. - As discussed in the section FUEL RETENTION STUDIES, the use of certain oxide additives in either the matrix or fuel was helpful in reducing fuel losses under thermal cycling conditions. To determine the effect of these additives on the strength of composites, W - 20-volume-percent-UO_2 specimens incorporating either ThO_2 in the tungsten matrix or CaO in solid solution with the fuel were fabricated (by sintering and hot rolling powder mixtures) and were tensile tested over the temperature range of 1930° to 2700° C. The resultant strength data are plotted in figure 57. For comparison, the data for the reference W - 20-volume-percent-UO_2 composites are included in the figure.

The addition of 2-volume-percent ThO_2 to the matrix of the composites resulted in an appreciable strength increase over that of the reference material. For example, the thoriated material is about 25 percent stronger than the reference material at 2500° C. Tests on composites with 6-volume-percent-ThO_2 matrix additions yielded similar results. Thus, addition of ThO_2 (or possibly other high-temperature oxides) to the matrix of W-UO_2 composites appears to be an attractive method for increasing the strength of these composites if additional strength is needed in future fuel element designs. However, additions of this type complicate composite consolidation processes, particularly if W-coated particles are used.

The data for the composites that contained 10-mole-percent CaO in the UO_2 indicate that the strength of this material was similar to that of the reference material at the higher test temperatures. At the lower test temperatures, the composites containing CaO were slightly stronger than the reference material. Thus, small quantities of solid-solution additions to the fuel do not seem to affect the strength of the composites adversely, and may even result in strength increases.

This contention is supported by the 2500° C creep-rupture test results shown in

figure 58. These data indicate somewhat longer stress-rupture lives and lower creep rates for the W - 20-volume-percent-UO_2 composites with additives than for those of the reference material. Also shown in this figure are creep-rupture data for W - 35-volume-percent-UO_2 composites roll compacted from coated particles that contained 10-mole-percent Ce_2O_3 in UO_2. As previously observed with the tensile strengths of composites produced from coated particles, these composites are weaker than composites produced from powder mixtures. Although the fuel loadings of the composites were different, the strength differences are greater than would be anticipated from the effect of fuel loading (see fig. 50). The reason for these strength differences is not known, but possibly the strength differences are a result of small changes made in the processing variables used in coating the particles and consolidating the particles into composite specimens. Further improvement of these processes must be accomplished before selection of the best composites can be made.

Thermal cycling. - Since thermal cycling of W-UO_2 composites produces partial decomposition and migration of the fuel, the effect of this thermal treatment on the strength of various composites was investigated. For this study, composites were produced by roll compacting W-coated UO_2 particles and cladding all surfaces of the composites by vapor deposition. Composites containing unstabilized UO_2, and UO_2 with 10 mole percent of either Y_2O_3 or CeO_2 were used. These composites were thermally cycled from ambient temperature to 2500° C with 10 minutes at temperature per cycle at the maximum cycling temperature and subsequently were tensile tested at 2500° C.

The measured fuel loss and tensile data resulting from these tests are plotted in figure 59. As expected, the strength of the composites containing UO_2, or UO_2 stabilized with Y_2O_3, began to decrease at about the same number of cycles as the fuel loss began to increase. These effects are thought to be caused by the migration of the fuel through the tungsten matrix. The strength of the composites containing ceria-stabilized UO_2 held up well over the total number of cycles tested (100) even though the fuel losses for these composites were appreciable at 100 cycles. These data yield another piece of evidence to support the use of ceria, rather than yttria, as a fuel stabilizer.

The rise in strength for all three types of composites after the first few cycles was somewhat surprising. However, metallographic examination of the specimens indicated that thermal cycling produced subgrain structure and coalescence of the small pores that were present in these specimens. These structural changes could account for the increased strength.

In addition to the effects of thermal cycling on fuel decomposition and migration in W-UO_2 composites, the thermal cycling that would be required of TWMR fuel elements during preflight ground testing and in-flight operation might cause thermal fatigue of the structures. Because of this potential problem, the thermal fatigue resistance of W-UO_2 composites was indirectly evaluated in a contracted study (ref. 44). In this study,

samples consisting of solid cylindrical cores of various $W-UO_2$ composites encased by sleeves (0.02-in. (0.51 mm) thick) of either unfueled W or another $W-UO_2$ composite were cycled between room temperature and 2500° C in a helium atmosphere. The differential thermal expansion between the core and sleeve produced strain in the sleeve, and the resistance of the sleeves to the cyclic thermal strains was determined.

Results of the tests indicated no cracking of the tungsten sleeves on cores containing 10-, 20-, or 30-volume-percent Y_2O_3-stabilized UO_2 in 50 cycles (the maximum number in this study). In addition, a sleeve of W - 20-volume-percent UO_2 on a core of W - 30-volume-percent UO_2 did not fail after 50 cycles. Thus, it appears that the thermal fatigue life of W and $W-UO_2$ composites is sufficient to withstand the thermal cycling conditions that will be required in the TWMR.

Discussion and Summary of Properties

The property values determined for the reference composites indicate that both the mechanical and physical properties of $W-UO_2$ composites are adequate for nuclear-rocket fuel element applications. The mechanical properties of the composites of interest for the TWMR are close to those of unfueled tungsten, while the physical properties are close to those that can be calculated from the mixture rule.

The test results for other composites indicate that the properties can be improved somewhat by optimizing the fuel particle size and shape for the particular consolidation method used. Although the use of W-coated UO_2 particles improved the dispersion homogeniety and fuel retention characteristics of $W-UO_2$ composites, composites produced from coated particles consistently exhibited lower strength than those produced from powder mixtures. This strength difference possibly can be overcome by improvements in methods of producing and consolidating coated particles. If these improvements can be accomplished, small fuel particles might offer additional strength advantages in this type of composite.

The use of stabilizing additives in the fuel of $W-UO_2$ composites did not adversely affect the strength of the composites, and in some cases, it improved the mechanical properties. In addition, the use of ThO_2 in the tungsten matrix appears to be an attractive method of strengthening composites. Use of this method, however, will depend on development of specialized particle coating techniques if coated particles are to be used in producing fuel elements.

The strength of $W-UO_2$ composites does not appear to be adversely affected by the limited thermal cycling required in nuclear rockets, provided that an effective fuel stabilizer is used.

The property values reported in this section can be used as approximate values for

conceptual design studies. However, these values probably will change appreciably as the technology of fuel element fabrication advances. Thus, before final fuel element designs are made, the properties of W-UO$_2$ composites should be reevaluated by using samples of the materials and consolidation methods to be used in producing the fuel elements.

CONCLUSIONS AND RECOMMENDATIONS

The following general conclusions on fueled materials for the tungsten water-moderated reactor (TWMR) can be drawn from the work performed under this program:

1. Methods for fabricating tungsten - uranium-dioxide (W-UO$_2$) composites were sufficiently developed to demonstrate the feasibility of producing complex fuel element configurations for the TWMR. However, refinement of these methods is needed to improve the dimensional control and to ensure reproducible quality in fuel elements. Development of techniques for application of surface claddings to complex fuel element configurations also is required.

2. Methods were developed for controlling fuel losses from W-UO$_2$ composites to tolerable levels at temperatures to 2500° C. These methods include stabilizing the fuel with metal oxide additions, precoating of the UO$_2$ particles with W, and applying thin W claddings on all exposed surfaces of the composites.

3. The critical mechanical and physical properties of W-UO$_2$ composites appear to be sufficient for design of fuel elements, but changes in materials and fabrication techniques can appreciably affect these properties.

Based on the results obtained in this program, it is recommended that fuel elements for the TWMR should incorporate the following features:

1. Spherical UO$_2$ particles should contain metal oxide stabilizing additives (preferably cerium oxide) in solid solution with the fuel.

2. The stabilized fuel particles should be coated with the appropriate amount of tungsten prior to consolidation: this coating can be best applied by utilizing hydrogen reduction of tungsten hexachloride (WCl$_6$). Addition of thorium dioxide (ThO$_2$) in the tungsten coating should be used, if possible, to increase the strength and improve the fuel retention of the composites.

3. The W-coated, stabilized fuel particles should be consolidated (by processes such as hot isostatic compaction or pneumatic impaction) into a fully dense (>98 percent of theoretical density) composite of the desired configuration.

4. All surfaces of the dense composite should be clad with a thin (approximately 0.001 in. (0.025 mm) minimum) layer of unfueled tungsten, preferably by hydrogen reduction of WCl$_6$.

These recommended features will probably be changed somewhat as the technology for W-UO$_2$ composites expands. However, a fuel element that incorporates these features can be expected to lose less than 1 weight percent of its fuel and show no significant fuel migration after twenty-five 10-minute thermal cycles to 2500° C in flowing hydrogen and to have mechanical properties not greatly different from unfueled tungsten.

Lewis Research Center,
    National Aeronautics and Space Administration,
        Cleveland, Ohio, March 15, 1967,
           122-28-01-01-22.

APPENDIX A

MATERIALS

Considerable effort was directed toward controlling the quality of the starting materials required in all phases of the program. A prime requirement established for the powders was that of high purity. This requirement for high purity was necessary because all elements with high neutron capture cross sections must be maintained at extremely low levels. Second, and more important, the extremely high operating temperatures for this reactor require that elements or compounds which have low melting points (less than 2500° C), which have high vapor pressures at these temperatures, or which will react with W or UO_2 must be kept at low concentrations.

Although the effects of individual impurities are not known (and need to be studied in future work), reasonable assumptions can be made about several elements that could cause problems with the fuel. These include elements which can reduce UO_2 and add to the fuel-decomposition problem. In addition, these and other elements may form low-melting eutectics with the UO_2, W, or both and thereby result in undesired side effects. Elements particularly suspected in these respects are carbon, fluorine, and excess oxygen. Therefore, attempts were made to keep the amounts of these elements as low as possible in the W and UO_2 powder starting materials and throughout subsequent processing.

Tungsten Powder

The tungsten powder used in preparing most of the powder composites used in this program was commerically produced, had particles of irregular shape, and had an average particle size of less than 1 micron. This powder was used because it sintered well, even with large UO_2 particles dispersed in it. A typical analysis of this tungsten powder is shown in table II.

Uranium Dioxide Particles

The UO_2 particles incorporated in most of the powder blends discussed were spherical particles of about 50 microns in diameter. Spherical particles were used to ensure a smooth particle surface with no angular protrusions that could be chipped off during blending operations to produce fines in the powder blends. The size of these particles was initially optimized for the hot-rolling process on strength and fuel-loss considera-

tions, but changes in consolidation processes may require more study to find the best particle size. Another prime requirement of these particles was that they be high-fired (above 1700° C) in hydrogen to produce an oxygen-to-uranium ratio in the range of 2.00 to 2.03. Close control of stoichiometry was done to aid in the control of fuel decomposition and migration during elevated temperature testing of the composites. Addition of stabilizing additives to the UO_2 particles was accomplished in several ways, but the selection of a method usually was left to the discretion of the fuel supplier, provided that the attainment of solid solution was verified. However, the firing schedule described in reference 32 was used effectively at Lewis in preparing solid solutions of UO_2 with many different additives. This firing schedule included heating in a helium atmosphere to 1100° C, a 30-minute hold at 1100° C in hydrogen to reduce excess oxygen, and further heating in helium to 2200° C with a 6-hour hold at temperature.

To assist possible future investigators in this type of work, the general specifications used to procure fuel of this type are listed as follows:

Shape: spheroidal (the major to minor axis ratio shall be less than 2)

Size: 30 to 77 microns in diameter (-270/400 mesh)

Density: greater than 92 percent of theoretical

Heat treatment: high fired in hydrogen above 1700° C

Additives: must be in solid solution with UO_2 as verified by x-ray diffraction techniques (stipulate type and amount of additive in weight percent UO_2)

Purity: at least 99.95 percent UO_2 (less required amount of additive) no single metallic impurity shall exceed 200 ppm and carbon and total halides each shall not exceed 30 ppm

Oxygen to metal ratio: The oxygen to metal ratio for a solid solution of UO_2 and an oxide stabilizer shall be no less than that calculated for the mixed stoichiometric oxides and no more than 2.03. For UO_2 without an additive, the oxygen-to-uranium ratio shall be in the range of 2.00 to 2.03.

In addition to this commercially available fuel, ultra-high-purity UO_2 powder was produced under a NASA-sponsored program (described in ref. 21). This fuel, which had a total metallic impurity content (excluding W) of less than about 50 parts per million (ppm), was prepared to study the effects of impurities on the stoichiometry and compatibility of the fuel. A typical analysis of this fuel is compared with that of the more commonly used UO_2 in table II.

Tungsten Coating of Fuel Particles

Application of dense tungsten coatings onto the fuel particles received considerable

attention in order to develop a method that would not contaminate the high-purity particles (ref. 6). The coating method used by most vendors at the outset of this program was hydrogen reduction of WF_6. This fluoride-coating method produced a dense, uniform coating, but unfortunately, it also resulted in coatings with high residual fluorine contents (200 to 2000 ppm) which promoted the formation of pores in the coatings during high-temperature tests. The fluorine contamination of the particles is believed to be caused during deposition (at $\sim500^\circ$ C) by reactions of the fluoride reaction products with the UO_2 surface to form uranium tetrafluoride (UF_4) and with any oxide contaminants in the system to form tungsten oxyfluoride (WOF_4) or other oxyfluorides.

A wide variety of alternate coating methods (summarized in ref. 6) was studied by several organizations during the course of this program. These methods included both thermal decomposition and hydrogen reduction of tungsten iodide thermal decomposition of tungsten carbonyl, plasma coating of tungsten oxides and subsequent hydrogen reduction to tungsten, and electron beam vaporization of tungsten. All these processes indicated some promise of meeting the particle-coating goals, but considerably more development of each is required.

A process that was more successful in meeting the coating goals involved vapor deposition by hydrogen reduction of WCl_6. Because the probable reaction products (UCl_4) from this chloride coating process could be vaporized away from the particles at the higher deposition temperatures used $(\sim900^\circ$ C), the halide contamination problem encountered with the fluoride-coating process was overcome. The total halide contents of particles coated by the chloride process were usually less than 50 ppm, and no porosity was formed in the coatings during high-temperature tests. Therefore, this method of coating is the preferred particle-coating process. A typical analysis of a $W-UO_2$ composite produced by hot roll compaction of coated particles produced with the chloride process and subsequently clad by vapor deposition is shown in table II.

Because the chloride-coating process is more expensive than the fluoride process, the two processes were used in conjunction by some coating vendors. This duplex-coating process involved application of an initial, thin, protective layer (1 to 3 μm) of W on UO_2 by the chloride process and subsequent buildup of the coating to the required thickness by the fluoride process. Some batches of coated particles commercially produced by this process had less than 30 ppm of fluorine with no additional contamination from other impurities. However, other batches of particles coated by this process had much higher fluorine contents and exhibited coating porosity after high-temperature tests. Therefore, improved control of this coating process is necessary, particularly in minimizing oxide impurities which can lead to the formation of oxyfluorides in the coatings.

Submicron Dispersion of Uranium Dioxide in Tungsten

Since dispersions of fine UO_2 in W appeared to be somewhat helpful in reducing the detrimental effects of thermal cycling, a brief contracted study was conducted to produce a submicron dispersion of UO_2 in W by coprecipitation (ref. 45). The feasibility of producing the dispersion-type powders was established, but subsequent annealing of composites produced from these powders caused coalescence of the submicron UO_2 particles.

APPENDIX B

CHEMICAL ANALYTICAL METHODS

In the early stages of this research, reliable chemical analytical methods were not available for analyzing $W-UO_2$ composites; therefore, several contracted programs were supported to develop suitable methods. In particular, methods for determining the concentration of trace element impurities and for determining the oxygen-to-uranium or oxygen-to-metal atomic ratios in fabricated $W-UO_2$ composites were sought.

Trace Element Analysis

A contracted program to develop analytical methods for the determination of most trace elements in the high-purity $W-UO_2$ composites used in this program was conducted. Ten analytical procedures were developed as a result of this study, and these are reported in reference 46. Five of the procedures involved spectrographic techniques for determining metallic impurities while the other five procedures utilized other techniques to determine nonmetallic impurities. Most of these procedures were adapted from techniques previously used in analyzing high-purity uranium compounds. These 10 procedures permitted the determination of 68 elements (61 metallic and 7 nonmetallic) in $W-UO_2$ composites: 56 of these can be determined to levels in the range of 0.1 to 2 ppm.

Although these procedures were extensively used on a routine basis, laborious concentration procedures were necessary if a comprehensive analysis was required. In addition, 50 grams of material were required for duplicate determinations for all 68 elements, but this amount of material was rarely available in research-size samples. Thus, to reduce analytical costs and sample requirements, a further study of analytical methods also was conducted under a NASA contract (ref. 47). This study was aimed at extending a NASA-developed spectrographic method (ref. 48) for determining trace elements in refractory materials such as W and $W-UO_2$ composites. The analytical method developed in the contracted study utilizes a carrier distillation technique in an atmosphere of pure argon and requires a single determination for metallic impurities in a 250-milligram sample. Thus, it saves effort and material. In the contracted program, 15 elements were chosen for study to represent 50 to 60 elements. The results of the work reported in reference 47 and subsequent unpublished work indicate that 14 of the 15 elements could be determined at concentrations of 2 ppm or less in a single determination using only 0.5 gram of sample for duplicate determinations. Tantalum was the single element to which this method was not sufficiently sensitive under the conditions used presumably because of its refractory nature. Therefore, a separate procedure will probably be re-

quired for determination of tantalum and other refractory metals.

Fuel stoichiometry. - The determination of the stoichiometry of UO_2, particularly substoichiometric UO_2, in $W-UO_2$ composites posed a difficult problem for some time. However, a thermogravimetric method was developed for this purpose in another contracted study (ref. 49). In this method, which utilized standard laboratory furnaces and analytical balances, oxygen-to-uranium ratios were calculated from measured weight changes accompanying oxidation of samples and subsequent weight losses on hydrogen reduction of the sample. With this method it was possible to achieve adequate precision for both hypo- and hyper-stoichiometric materials by carefully controlling the conditions for oxidation and reduction.

This method also was shown to be applicable to $W-UO_2$ composites containing Y_2O_3, CeO_2, and probably ThO_2 additives. One requirement of the method is that the materials be of high purity; otherwise, changes in weight due to reduction or volatilization of impurity elements may cause systematic errors in the procedure. However, the high-purity materials used in this program satisfy the purity requirements of this method.

Discussion and summary of chemical analytical methods. - The methods used to analyze $W-UO_2$ composites (with or without metal oxide additives) chemically at Lewis and at other laboratories conducting research on these composites are summarized in reference 50. This reference includes (1) three techniques for measuring fuel stoichiometry (oxygen-to-uranium ratios); (2) a newly developed procedure for determining trace metals; (3) high-precision measurement of total oxygen; and (4) detailed analytical procedures for determining tungsten, uranium, sulfur, carbon, nitrogen, yttrium, cerium, and other rare earths.

The measurement of fuel stoichiometry has provided the greatest challenge to the analyst. The most applicable of the three methods reported in reference 50 for any given research program will be strongly dependent on the specific information desired and the physical and metallurgical state of the composite. For any future work in this area, a fruitful area of research should be the consolidation of all three techniques into a single apparatus designed to permit: gasometric additions of hydrogen, oxygen, and carbon monoxide; gas chromatographic detection of reaction products; and gravimetric monitoring of specimens.

In the determination of trace metals in $W-UO_2$ composites, the most useful procedures are based on chemical enrichment of the metallic impurities followed by standard emission-spectrographic techniques (ref. 46). The method described in reference 47, however, represents an attempt to eliminate the necessity of chemical enrichment and, at the same time, provide broader coverage in a single determination by using small amounts of material. Although this method was not sufficiently refined for use as a laboratory control method, the experimental results reported clearly demonstrate the advantages of the approach.

A continuing problem in trace-metal analysis, and one not limited to $W-UO_2$ materials, is the necessity of developing new elemental calibration curves for even small variations in cermet composition. Any further work in this area should include the development of a spectrographic procedure more universally applicable to the variation in composition likely to be encountered in research on $W-UO_2$ composites.

Analytical procedures for the elements not previously mentioned appear to be adequate for analysis of nuclear rocket fuel elements, with the possible exception of the halides (as discussed in ref. 6). The determination of fluorine, and possibly other halides, is of special importance because residual fluorides in $W-UO_2$ composites can lead to porosity at high temperatures. Therefore, to ensure good control of residual fluorides in coated particles and $W-UO_2$ composites, the pyrohydrolytic method of analysis currently used needs to be improved and validated with particular emphasis on resolving inconsistencies in determinations made at different laboratories.

REFERENCES

1. Watson, Gordon K.: Fabrication of Thin Tungsten-Uranium Dioxide Composite Plates. NASA TM X-1073, 1965.

2. Saunders, Neal T.; Watson, Gordon K.; and Buzzard, Robert J.: Investigation of Tungsten and Uranium Dioxide as a Nuclear Rocket Fuel Material. Proceedings of Nuclear Propulsion Conference, Monterey, Calif., Aug. 15-17, 1962.

3. Precht, W.; and Sundquist, L.: Investigation of Fuel Loss from Tungsten-Uranium Dioxide Bodies. Rep. No. MND-3178 (NASA CR-54329), Martin Co., Nov. 30, 1964.

4. Nelson, R. G.; Quinlan, F. B.; Brite, D. W.; and Sump, K. R.: Development of Tungsten-UO_2 Cermet Fuel Plates by Rolling or Pneumatic Impaction. Rep. No. BNWL-309 (NASA CR-54850), Battelle-Northwest, Sept. 1966.

5. Gedwill, Michael A.; Sikora, Paul F.; and Caves, Robert M.: Fuel-Retention Properties of Tungsten-Uranium Dioxide Composites. NASA TM X-1059, 1965.

6. Watson, Gordon K.; Caves, Robert M.; and Saunders, Neal T.: Preparation and Roll Compaction of Tungsten-Coated UO_2 Particles. NASA TM X-1448, 1967.

7. Goetsch, G. R.; Cover, P. W.; Gripshover, P. J.; Wilson, W. J.; and Boyer, C. B.: Fabrication of Tungsten-UO_2 Hexagonal-Celled Fuel Element Configurations. Battelle Memorial Inst. (NASA CR-54796), Oct. 30, 1965.

8. Drumheller, K.; and Sump, K. R.: Fabrication of Tungsten-Uranium Dioxide Honeycomb Fuel Element Structures. Rep. No. BNWL-253 (NASA CR-54838), Battelle-Northwest, Sept. 1965.

9. Johnson, D. D.; Pettman, R. E.; and Jackson, D. E.: Fabrication of Tungsten-UO_2 Composites by a Powder Metallurgy Process. Rep. No. 3M-8439 (NASA CR-54424), Minnesota Mining and Mfg. Co., May 20, 1965.

10. Foley, E. M.; Wagner, R. L.; and White, D. E.: Fabrication of Tungsten-Uranium Dioxide Honeycomb Structure. Rep. No. K-1648 (NASA CR-54483), Union Carbide Nucl. Co., Nov. 5, 1965.

11. Blankenship, Charles P.; and Gyorgak, Charles A.: Preliminary Investigation of Extruding Composite Tungsten-Uranium Dioxide Tubing. NASA TM X-1072, 1965.

12. Miller, John V.: Predicting Thermal Conductivity of Tungsten-Uranium Dioxide Dispersions. NASA TM X-1145, 1965.

13. Allison, G. S.: Extrusion of Tungsten-UO_2 Honeycomb Structures. Battelle-Northwest (NASA CR-54317), July 1965.

14. Nyce, A. C.; Burke, D. F.; and Vondra, B. L.: The Fabrication of Tungsten-Uranium Dioxide Composite Cylinders by the Tungsten Cementation Process. Rep. No. NUMEC-3728 (NASA CR-54315), Nuclear Materials and Equipment Corp., 1966.

15. Blankenship, Charles P.: Evaluation of Tungsten - Uranium Dioxide Composites Prepared by a Tungsten-Vapor-Cementation Process. NASA TM X-1447, 1967.

16. Abraham, L.; Katz, N. H.; and Supan, E. C.: Development of a Magneforming Process for the Fabrication of Thin-Wall Tungsten Cylinders. Rep. No. AI-65-12 (NASA CR-54316), Atomics International, Jan. 13, 1965.

17. Sikora, Paul F.; and Blankenship, Charles P.: Evaluation of Processes for Fabricating Tungsten - Uranium Dioxide Honeycomb Configurations. NASA TM X-1445, 1967.

18. McDonald, Glen E.; and Moss, Thomas A.: Fabrication and Retention of Uranium Dioxide in Tungsten-Uranium Dioxide Composites Containing 20 Volume Percent Dispersed Uranium Dioxide. NASA TM X-473, 1961.

19. Gripshover, P.: Fabrication of Core Structures. Paper presented at the Materials Information Meeting, Argonne National Lab., Illinois, 1964.

20. Grisaffe, Salvatore J.; and Caves, Robert M.: Fuel Retention Improvement at High Temperatures in Tungsten-Uranium Dioxide Dispersion Fuel Elements by Plasma-Spraying. NASA TM X-1028, 1964.

21. Cochran, W. L.; Knight, R. G.; and Stanley, F. S.: Tungsten-Uranium Dioxide Materials for NASA: Uranium Oxide Powders and Cladding and Joining of Tungsten Cermets by Plasma Spraying. Rep. No. K-1647 (NASA CR-54482), Union Carbide Nucl. Co., Oct. 11, 1965.

22. Hoppe, A. W.; and Lamartine, J. T.: Tungsten Cladding of Tungsten-Uranium Dioxide (W-UO$_2$) Composites by Deposition from Tungsten Hexafluoride (WF$_6$). Rep. No. WANL-PR(Z)-003 (NASA CR-54835), Westinghouse Electric Corporation, 1965.

23. MacInnis, M. B.; and Schulze, H. O.: Tungsten Cladding of Tungsten-Uranium Dioxide Composites by Chloride Vapor Deposition. Rep. No. SYL-6335-FRI (NASA CR-54728), Sylvania Electric Products, Inc., 1965.

24. Caves, Robert M.: Evaluation of Vapor-Deposited Claddings on Tungsten - Uranium Dioxide Composites. NASA TM X-1449, 1967.

25. Moore, Thomas J.; and Watson, Gordon K.: Evaluation of Welding Techniques for Tungsten - Uranium Dioxide Composites. NASA TM X-1405, 1967.

26. Peterson, J. H.; Meiners, K. E.; and Gripshover, P. J.: Joining of Tungsten-UO_2 Composites by Diffusion Bonding. Battelle Memorial Inst. (NASA CR-54791), Oct. 15, 1965.

27. Japka, J. E.; and Gordon, E.: Joining of Tungsten-Uranium Dioxide Composites by Gas Tungsten-Arc Brazing. Rep. No. UNC-5143 (NASA CR-54841), United Nuclear Corp., May 23, 1966.

28. Shaw, C. H.; and Boolen, R. F.: Magnetic Force Welding of Tungsten-Uranium Dioxide Composites. Rep. No. BNWL-286 (NASA CR-54839), Battelle-Northwest, Jan. 24, 1966.

29. Weinberg, A. F.; and Lindgren, J. R.: Joining of Tungsten-Uranium Dioxide Composites by Diffusion Bonding. Rep. No. GA-6602 (NASA CR-54842), General Dynamics Corp., Aug. 12, 1965.

30. Spanner, J. C.; and Brown, R. L., Jr.: Development of Nondestructive Testing Methods for NASA Tungsten Water-Moderated Reactor Fuels. Vol. 1, Rep. No. BNWL-383 (NASA CR-72139), and Vol. 2, Rep. No. BNWL-384 (NASA CR-72140), Battelle-Northwest, 1967.

31. Gedwill, Michael A.: An Investigation of Some Variables Affecting and Methods of Inhibiting Thermal-Cyclic Fuel Losses from Tungsten - Uranium Dioxide Composites. NASA TM X-1296, 1966.

32. Garfinkle, Marvin: Effect of Additives on Thermal Stability of Tungsten - Uranium Dioxide Composites. NASA TM X-1118, 1965.

33. Gluyas, Richard E.; and Gedwill, Michael A.: Stabilization of Tungsten - Uranium Dioxide Composites Under Thermal Cycling Conditions. NASA TM X-1295, 1966.

34. Saunders, Neal T.; Gedwill, Michael A.; and Gluyas, Richard E.: Retention of Fuel in Tungsten - Uranium Dioxide Fuel Elements. Paper presented at the AIAA Joint Propulsion Specialists Conference, Colorado Springs, June 14-18, 1965. (Also available as NASA TM X-52184.)

35. Takkunen, Philip D.; Gluyas, Richard E.; and Gedwill, Michael A.: Thermal Cyclic Behavior of Stabilized Tungsten - Uranium Dioxide Cermets Containing Metal Oxide Additives. NASA TM X-1446, 1967.

36. Langer, S.; Baldwin, N. L.; Burris, F. O., Jr.: Determination of Effects of Metal Oxide Additions on the Solubility of Uranium in UO_2. Rep. No. GA-6848 (NASA CR-54898), General Dynamics Corp., Nov. 30, 1965.

37. Aitken, E. A.; Conn, P. K.; Duderstadt, E. C.; and Fryxell, R. E.: Measurement of the Permeability of Tungsten to Hydrogen and to Oxygen. General Electric Co. (NASA CR-54918), May 1966.

38. Baker, R. J.; Daniel, J. L.; Lackey, W. J.; Lobsinger, R. J.; Scott, F. A.; Snajdr, E. A.; and Roake, W. E.: Basic Behavior and Fuel Retention Properties of Tungsten - Uranium Dioxide Cermets. Rep. No. BNWL-394 (NASA CR-54840), Battelle-Northwest, 1967.

39. Takkunen, Philip D.; and Baker, Robert J.: Thermal Cyclic Stability of Clad Cermets Prepared from Tungsten-Coated Uranium Dioxide Particles. NASA TM X-1450, 1967.

40. Buzzard, Robert J.; and Gill, Frank L.: High-Temperature Mechanical Properties of a Tungsten - Uranium Dioxide Composite. NASA TM X-1018, 1964.

41. Buzzard, Robert J.: Factors Affecting High-Temperature Strength of Tungsten - Uranium Dioxide Composites. NASA TM X-1444, 1967.

42. Zocher, R. W.: High Temperature Measurement of Young's Moduli for Tungsten and Tungsten - Uranium Dioxide Composites. Union Carbide Corp. (NASA CR-54847), Dec. 9, 1965.

43. Taylor, R. E.: Thermal Properties of Tungsten - Uranium Dioxide Mixtures. Rep. No. AI-64-153 (NASA CR-54141), Atomics International, Sept. 1, 1964.

44. Conway. J. B.; and Collins, J. F.: Determination of the Resistance of Tungsten - UO_2 Composites to Cyclic Thermal Strains. General Electric Co. (NASA CR-72047), Aug. 30, 1966.

45. Bowersock, R. V.; and Last, G. A.: Submicron Dispersion of UO_2 in Tungsten. Rep. No. BNWL-65 (NASA CR-54318), Battelle-Northwest, Aug. 1965.

46. Weber, C. W.; and Kwasnoski, T.: Determination of Impurities in Tungsten - Uranium Dioxide Mixtures. Rep. No. K-1621, Rev. (NASA CR-54275), Union Carbide Nucl. Co., Feb. 19, 1965.

47. Lee, T.; Farrar, R. B.; and Randolph, D. C. S.: Spectrographic Determination of Trace Impurities in Tungsten - Urania Mixtures Using D. C. Arc Excitation in Argon. Rep. No. K-1654 (NASA CR-54853), Union Carbide Nuclear Co., July 5, 1966.

48. Gordon, William A.: Use of Temperature Buffered Argon Arc in Spectrographic Trace Analysis. NASA TN D-2598, 1965.

49. Kallmann, S.; and Hobart, E. W.: The Determination of the Oxygen to Uranium Ratio in Tungsten-UO_2 Products. Ledoux and Company (NASA CR-72052), July 19, 1966.

50. Gordon, William A.; and Dupraw, William A., eds.: Chemical Analysis of Tungsten - Uranium Dioxide Materials. NASA TM X-1381, 1967.

TABLE I. - RELATIVE PERFORMANCE OF NONDESTRUCTIVE TESTING METHODS FOR TUNGSTEN - URANIUM DIOXIDE COMPOSITES

Parameter	Ultrasound	Eddy currents	Beta scan	Autoradiograph	Mechanical
Total fuel loading and fuel loading homogeneity	Reproducibility: ±2 vol. % UO_2 or better / Accuracy: approximately ±7 vol. % UO_2 (variable) / Scan rate: 2.5 cm/sec or more / Affected by particle elongation, grain size and shape / Recommended as a corrollary method and when testing speed is a primary factor	Reproducibility: ±1 vol. % UO_2 or better / Accuracy: approximately ±5 vol. % UO_2 (variable) / Scan rate: 2.5 cm/sec or more / Affected by plate thickness and density / Recommended for production testing on plates or grids	Reproducibility: ±0.5 vol. % UO_2 / Accuracy: ±0.7 vol. % UO_2 / Scan rate: 2.5 cm/min or less / Affected by cladding thickness / Most accurate method evaluated / Recommended for laboratory use on plates or grids	Comparable to beta scan, although slower	(a)
Fuel core and cladding integrity	Excellent crack detection capability / Hindered by rough surfaces and large grain size / More applicable to grid fuel than plates because x-ray is better on plates / Recommended for production testing of grid fuels	Moderate crack detection capability / Less resolution sensitivity than ultrasound and x-ray / High scan rate, 1 cm/sec / Testing done with same equipment as loading measurements / Recommended for production testing of grid fuels	(a)	Moderate detection capability for cracks in cladding of fuel plates	(a)
Cladding thickness	Boundary wave techniques may be applicable / Limited investigation only and the results were inconclusive	Low accuracy due to interaction with loading changes / Very high frequency required / Multiparameter approach could be promising but was not empirically evaluated	Tester output reduced with clad thickness / Accuracy degraded by fuel loading variations / Recommended for laboratory use only	Comparable to beta scan	(a)
Core-to-cladding bond	Excellent sensitivity to bonding defects / Realistic standards difficult to fabricate / Recommended for production usage on plates or grids	Eddy current bond test is theoretically possible; however, no experimental work conducted because ultrasonics provided an adequate test	(a)	(a)	(a)
Dimensional tolerance	Variations in acoustic properties reduced accuracies to well below that of mechanical gaging methods	Plate thickness and grid channel diameter measurements possible with fuel loading measurement equipment	(a)	(a)	Excellent grid warp, plate thickness and web thickness measurements obtainable using shadowgraph and other measuring methods / Recommended for production usage for both plates and grids

[a] Not applicable.

TABLE II. - TYPICAL CHEMICAL ANALYSIS OF MATERIALS USED

[< denotes less than the limit of detection indicated.]

Impurity element	Impurity content by weight, ppm				Impurity element	Impurity content by weight, ppm			
	Tungsten	Standard UO$_2$	High purity UO$_2$	Clad W-UO$_2$ composite		Tungsten	Standard UO$_2$	High purity UO$_2$	Clad W-UO$_2$ composite
Aluminum	3	160	5	1	Platinum metals	(b)	(b)	(b)	(b)
Antimony	(a)	<1	<15	<1					
Arsenic	<1	<30	<30	(a)	Potassium	70	<5	<5	10
Barium	<1	<10	<10	<3	Silicon	15	45	6	4
Beryllium	<1	<.1	<1	<.1	Silver	<1	.1	1	<1
Bismuth	(a)	<1	<1	<.5	Sodium	50	1	<1	2
Boron	2	<.1	<1	.5	Tantalum	(a)	<.5	(a)	<4
Cadmium	<1	<.1	<1	<1	Thallium	(a)	<2	<2	<1
Calcium	5	1	<1	2	Thorium	(a)	16	<1	(a)
Chromium	7	<1	3	<1	Tin	<1	<.5	<1	<1
Cobalt	<1	<5	<1	<10	Titanium	5	<.2	(a)	2
Copper	5	.2	3	<1	Tungsten	(a)	4	275	(a)
Germanium	(a)	<1	<1	<1	Zinc	<1	<2	<20	<10
Gold	(a)	<1	<1	------	Zirconium	<1	75	(a)	20
Hafnium	(a)	<1	(a)	<2	Carbon	18	25	28	15
Indium	(a)	<3	<3	<1	Fluorine	45	<1	<1	(a)
Iron	30	12	10	55	Halogens^c: Chlorine Bromine Iodine	5	43	6	65
Lanthanum and rare earths	(b)	(b)	(b)	(b)					
Lead	10	<3	<3	<1	Nitrogen	40	16	(a)	(a)
Lithium	<1	<1	<1	<1	Oxygen	3230	(a)	(a)	(a)
Magnesium	2	.1	7	2	Sulfur	<5	<1	(a)	<1
Manganese	<1	3	<1	1	Uranium	(a)	88.09%	(a)	(a)
Molybdenum	30	50	(a)	5	Oxygen to uranium atom ratio	(a)	2.001	2.000	(a)
Nickel	10	1	6	2					
Niobium	(a)	2	(a)	2					
Phosphorus	(a)	<50	<50	(a)					

^{a}Not determined.
^{b}Typically below the limits of detection where analyzed.
^{c}Calculated as chlorine.

(a) Concentric cylinder.　　　　　　　　(b) Honeycomb grid.
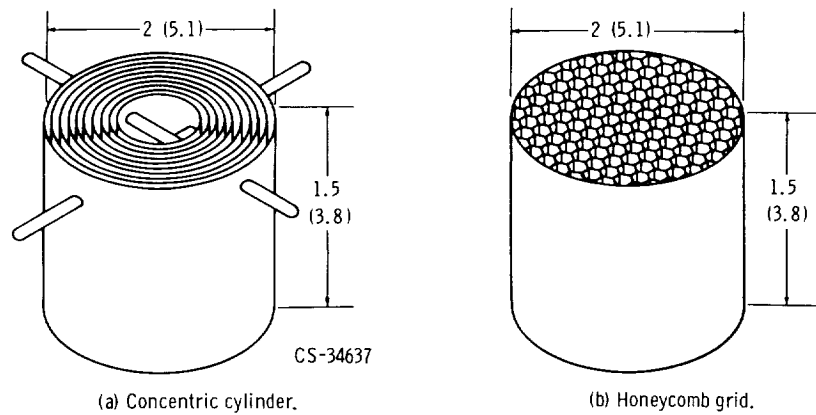
Figure 1. - Fuel element stage configuration. (All dimensions are in inches (cm).)
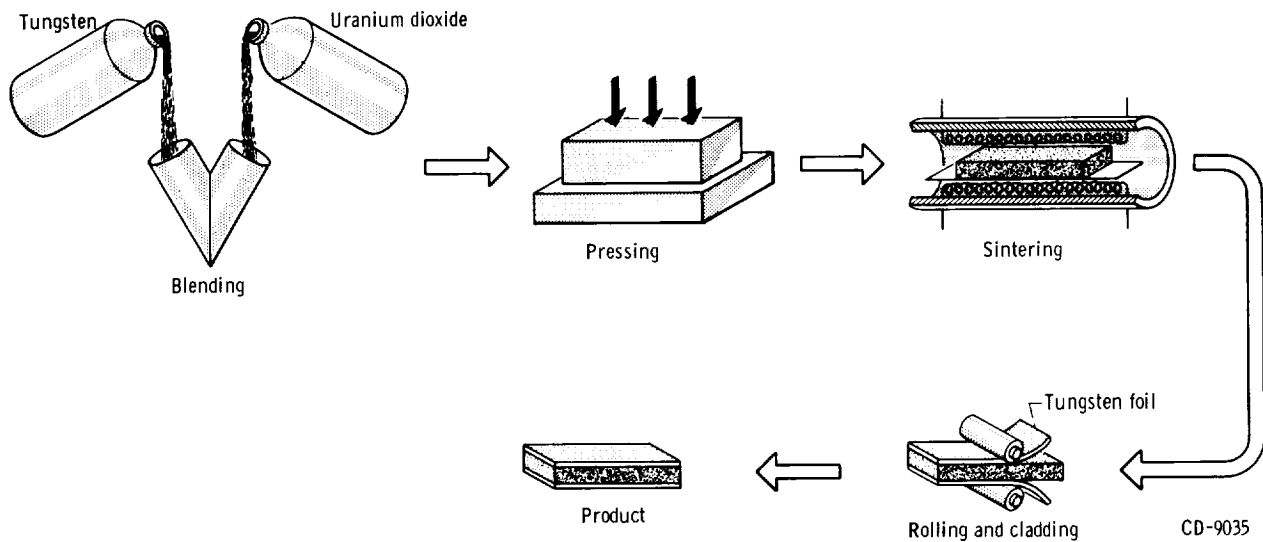
Figure 2. - Fabrication of W-UO_2 composites by roll compaction of powders.

(a) 10-Volume-percent UO_2.

(b) 20-Volume-percent UO_2.

(c) 30-Volume-percent UO_2.

(d) 40-Volume-percent UO_2.

C-67-952
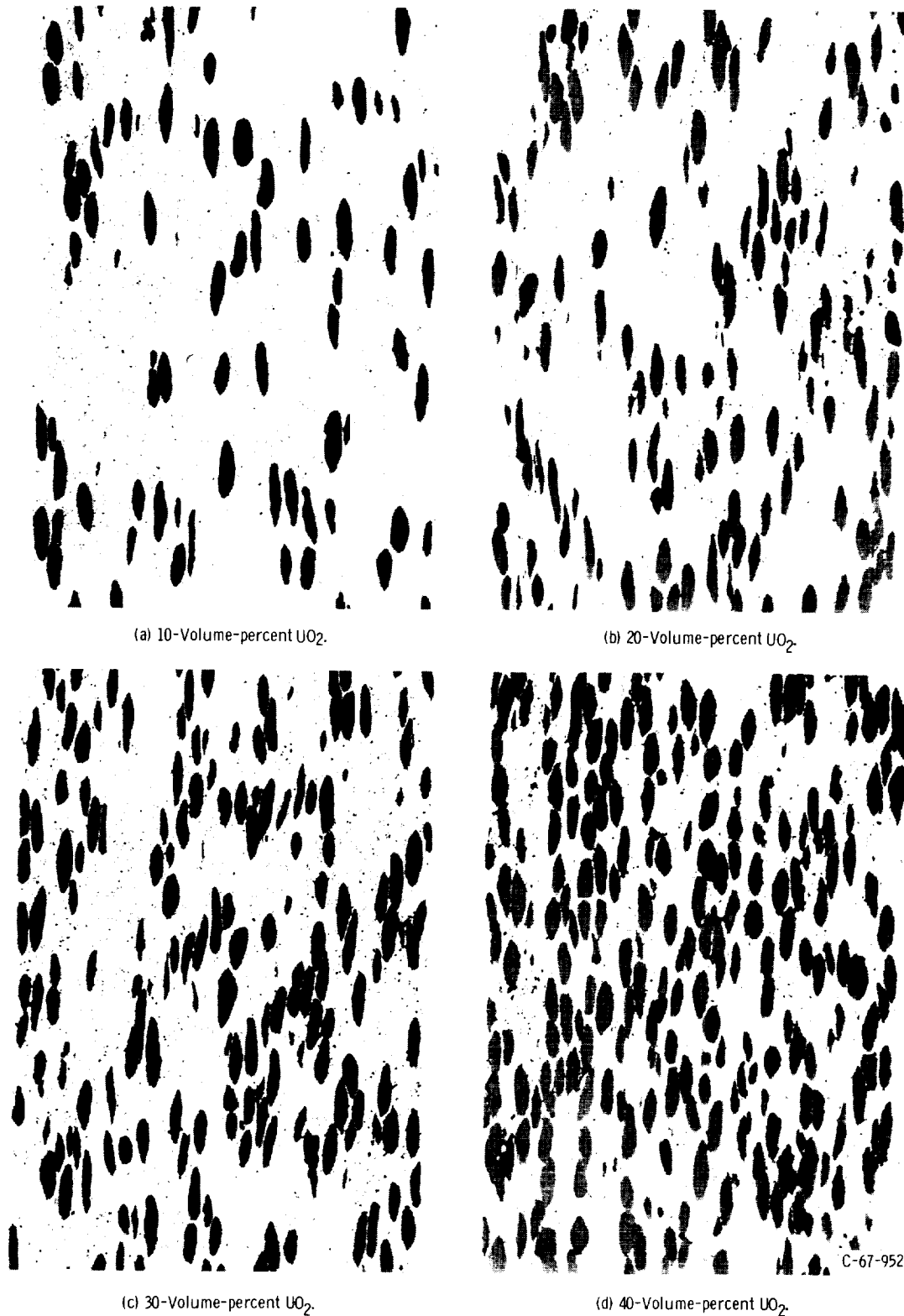
Figure 3. - Effect of fuel loading on microstructure of W-UO_2 composites with W-clad surfaces. (Black areas are result of particle pullout during metallographic preparation.) Unetched. X100.

(a) W-coated UO_2 particles prior to consolidation.
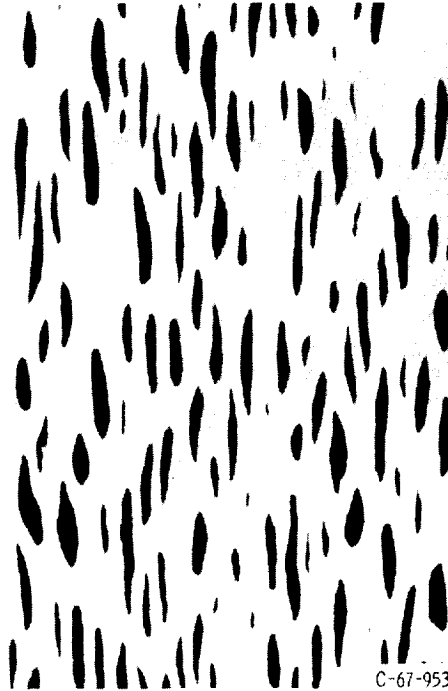
(b) Microstructure of plate consolidated from W-coated UO_2 particles by hot roll compaction.

C-67-953

Figure 4. - W-coated UO_2 particles and resulting roll-compacted W - 20-volume-percent-UO_2 plate. Unetched. X100.

C-66436
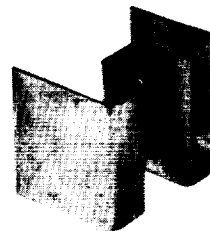
C-71991

Figure 5. - Shapes hot formed from flat W-UO_2 plates.

CD-8980
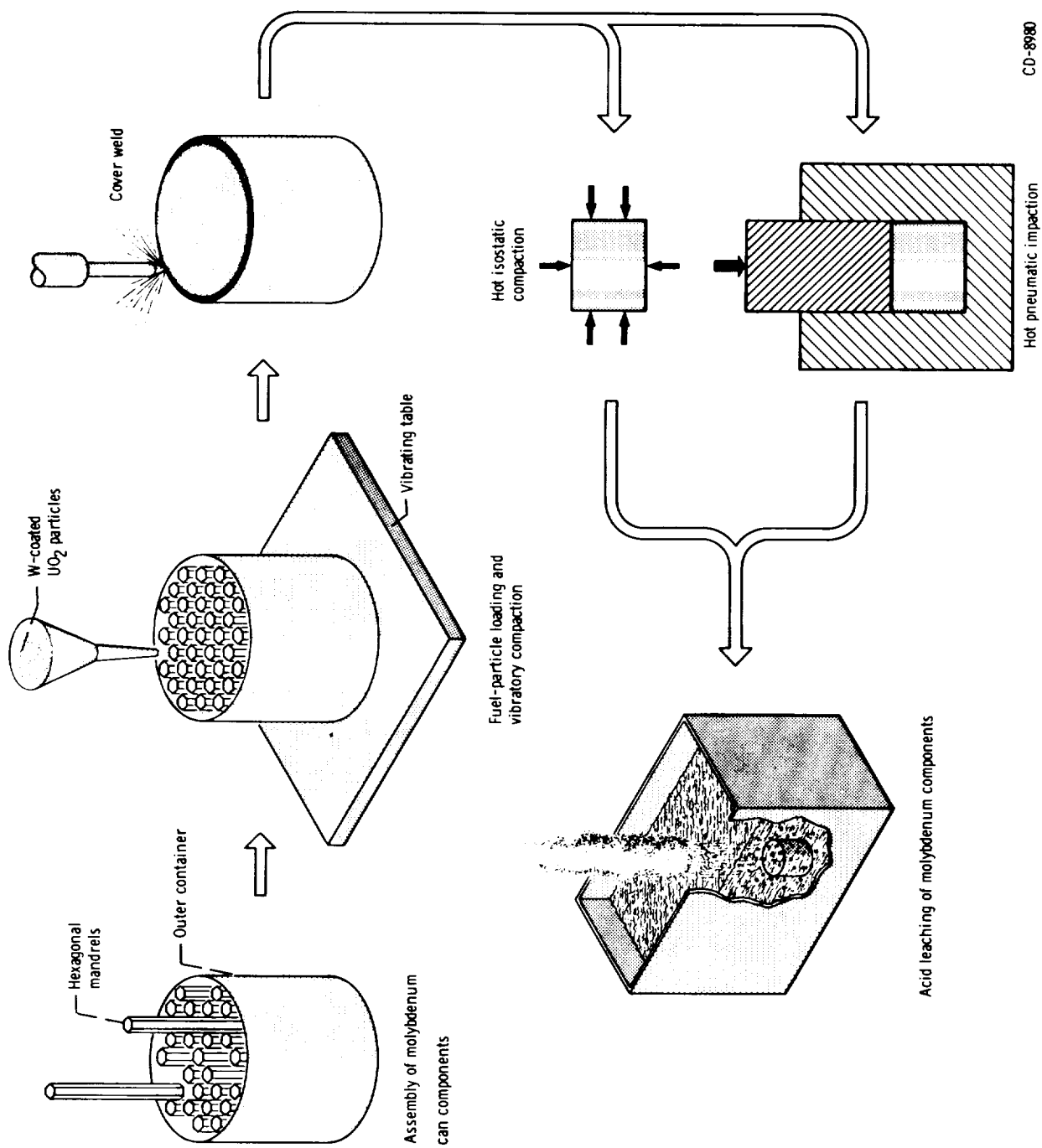
Figure 6. - Flow sheet for can loading and processing steps for hot isostatic compaction and hot pneumatic impaction.
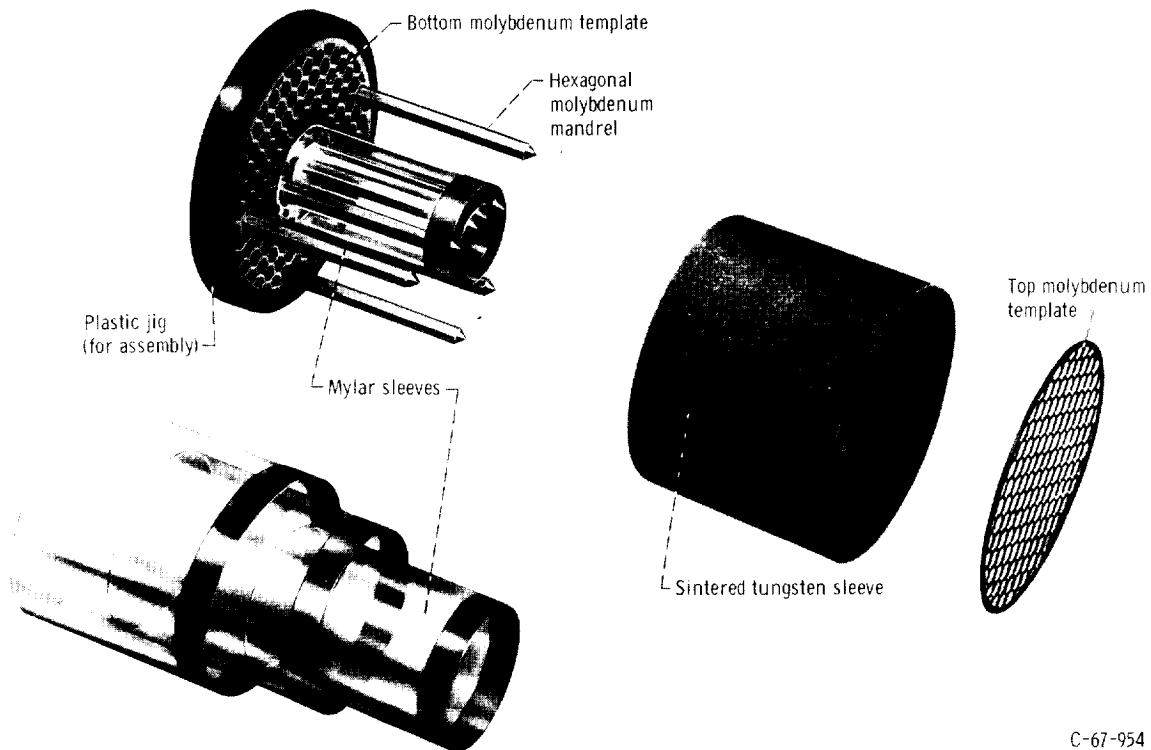
Figure 7. – Container components for hot isostatic compaction of honeycomb grids. (Courtesy Columbus Laboratories, Battelle Memorial Institute.)

C-67-954
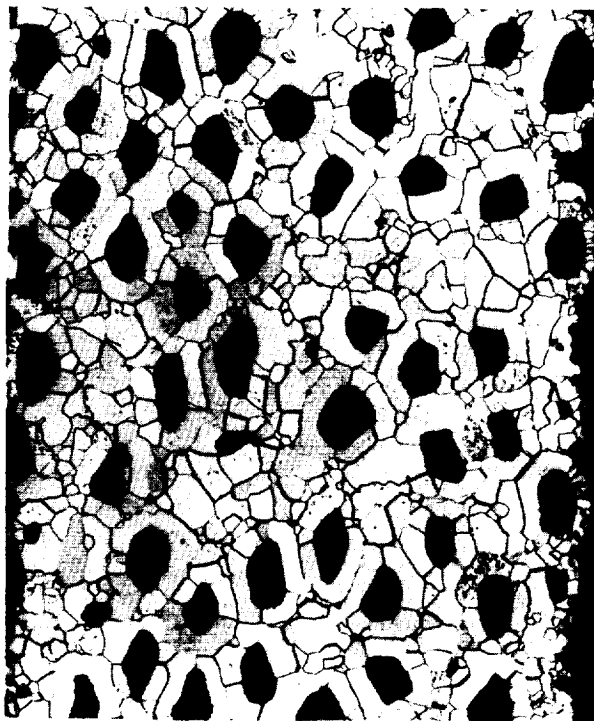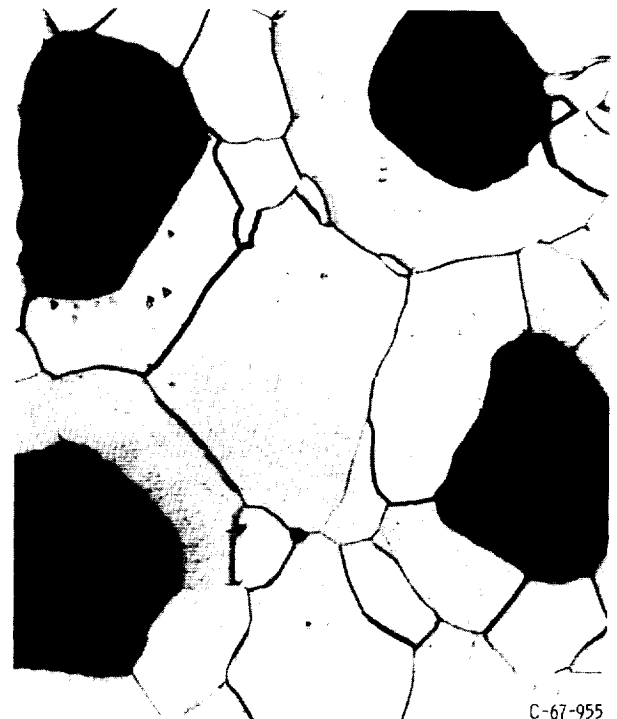
X150   X500

C-67-955

Figure 8. - Microstructures of W-UO₂ honeycomb web fabricated by hot isostatic compaction of W-coated UO₂ particles. (Dark areas in fuel particles are result of pullout during metallographic preparation.) Etchant, Murakami's reagent.
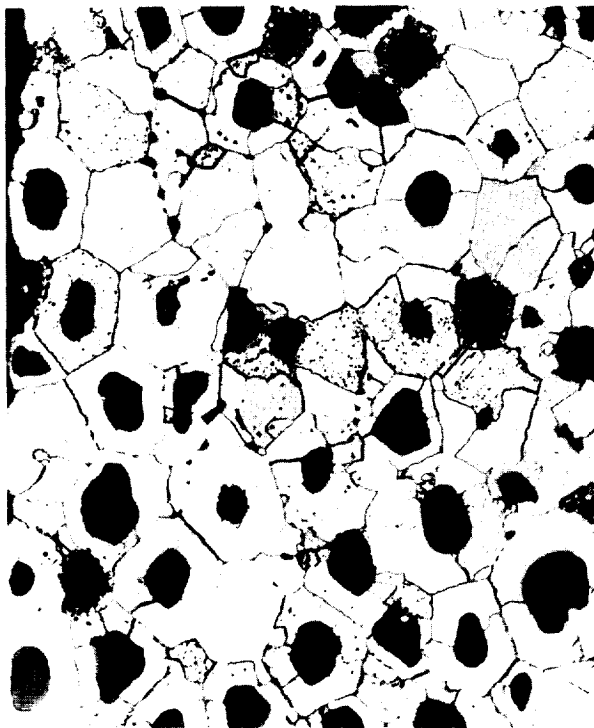
X150   X500

C-67-956

Figure 9. - Microstructures of W-UO₂ honeycomb web fabricated by hot closed-die impaction of W-coated UO₂ particles. Etchant, Murakami's reagent.
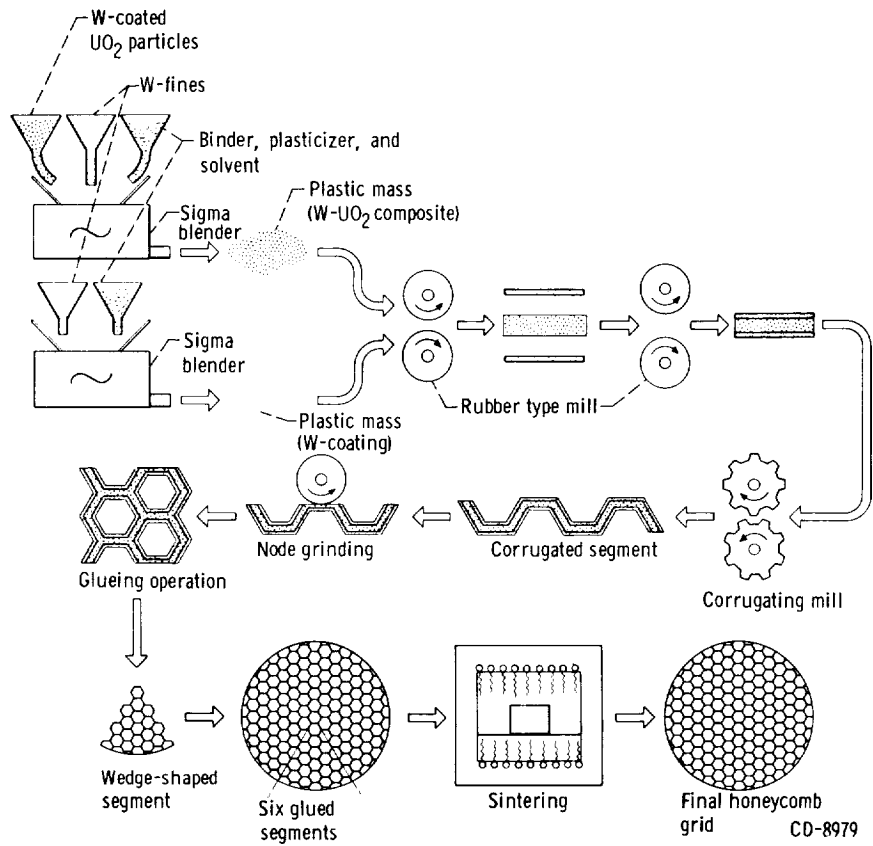
Figure 10. - Flow sheet for green state forming and sintering process.
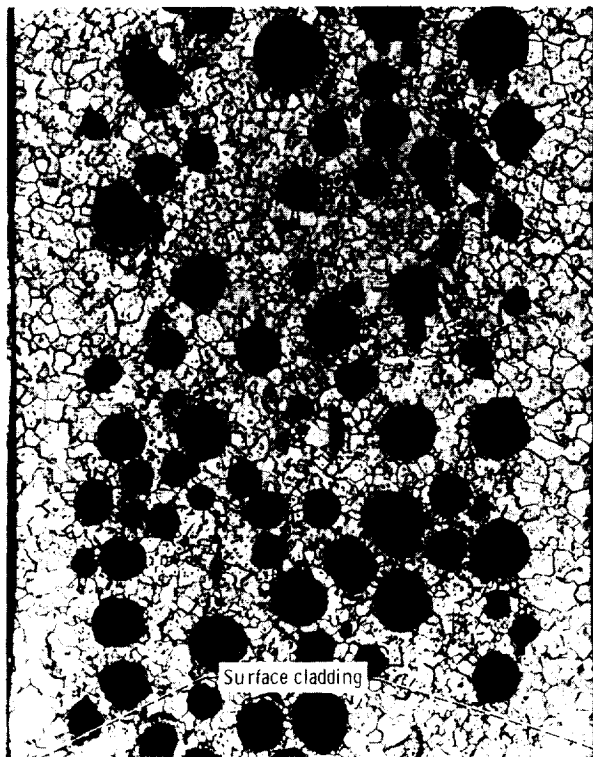
X150   X 500
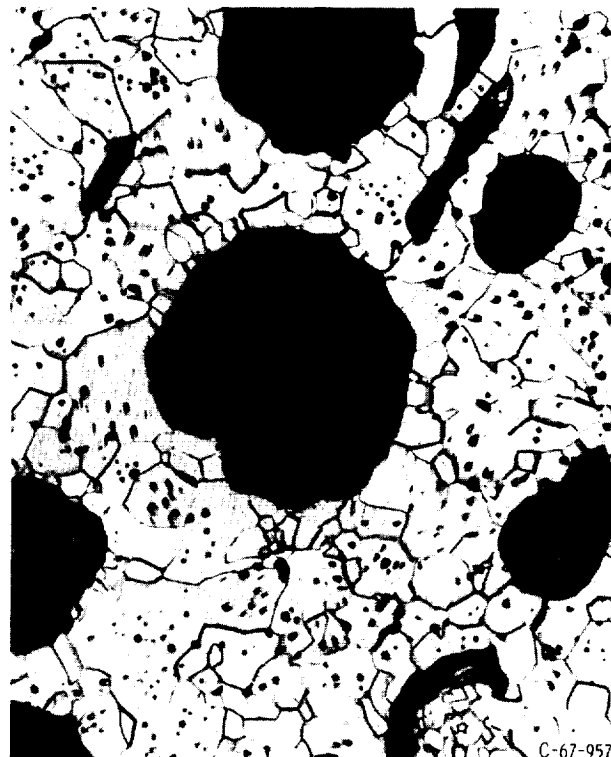
Figure 11. - Microstructure of W-UO_2 composite produced by green rolling and sintering technique. Etchant, Murakami's reagent.
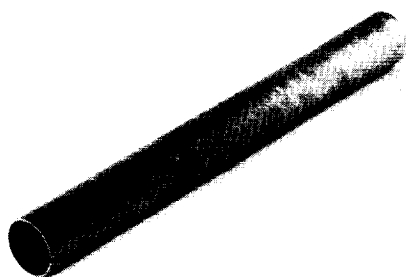
Figure 12. - W - 20-volume-percent-UO_2 tubing hot extruded at reduction ratio of 16 over a mandrel. Original magnification of photomicrograph, X250; etchant, Murakami's reagent.

70

(a) Vapor cemented cylinder. X2.

(b) Typical microstructure. Etchant, Murakami's reagent. X500.

Figure 13. - W - 20-volume-percent-UO$_2$ cylinder fabricated by vapor cementation and typical microstructure after heat treating at 1300° C for 1 hour in hydrogen.
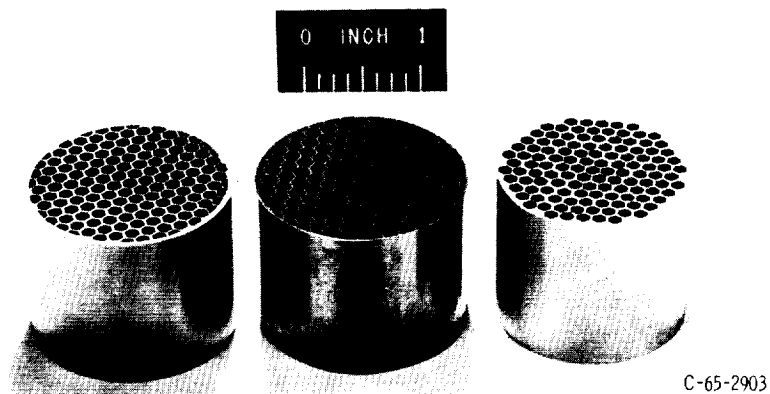
(a) Hot isostatic compaction. (b) Powder metallurgy forming and sintering. (c) Hot pneumatic impaction.

Figure 14. - W-UO$_2$ honeycomb structures fabricated by different processes.

Figure 15. - Photomicrograph of core-clad interface after hot rolling. Etchant, Murakami's reagent. X500.

Tungsten matrix
(background)⌐

⌐ Depleted UO$_2$
/ sites (black)

UO$_2$ particles
(grey) ⌐

(a) Unclad specimen.

Cladding

Core

C-67-960

(b) Clad specimen.
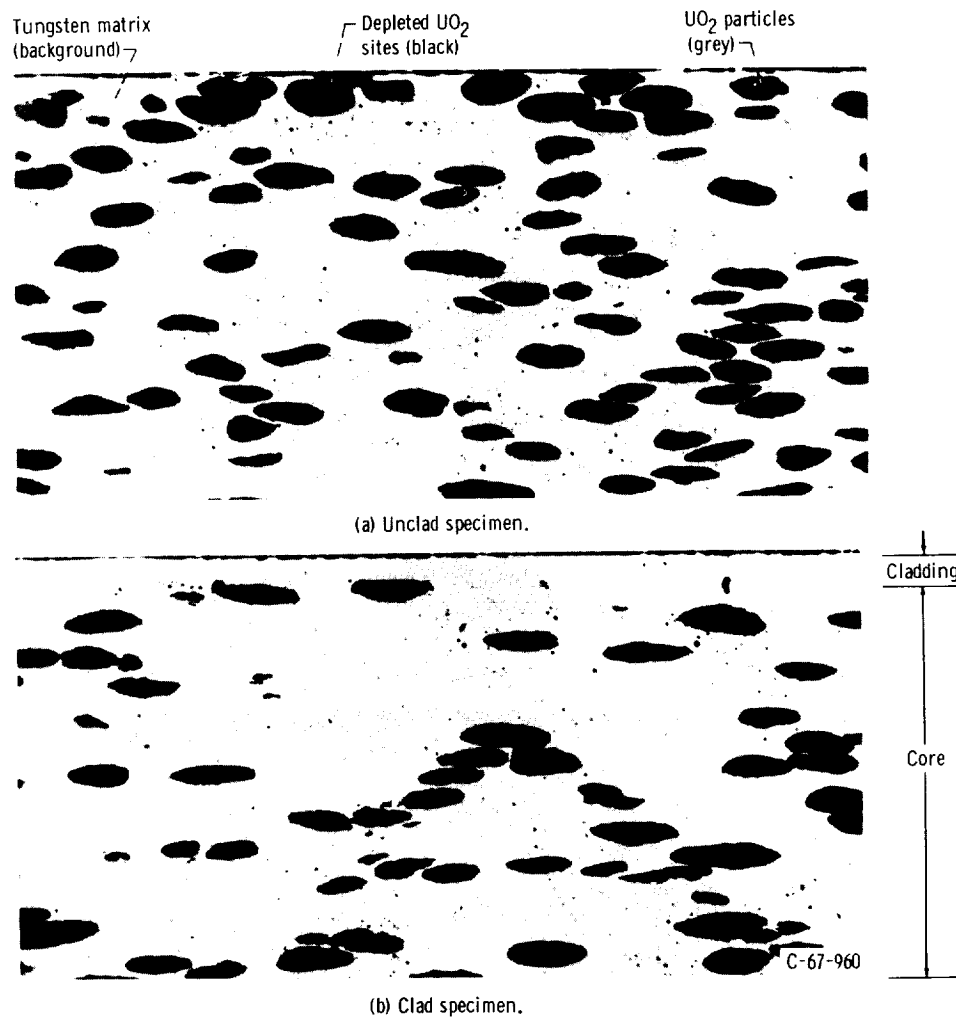
Figure 16. - Microstructure of W - 20-volume-percent-UO$_2$ composites unclad or clad (by gas-pressure bonding of W foil) after static heat treatment of 2500° C for 2 hours in hydrogen. X150.

(a) As clad.

(b) After heating to 2500° C in hydrogen for 2 hours.

C-67-961
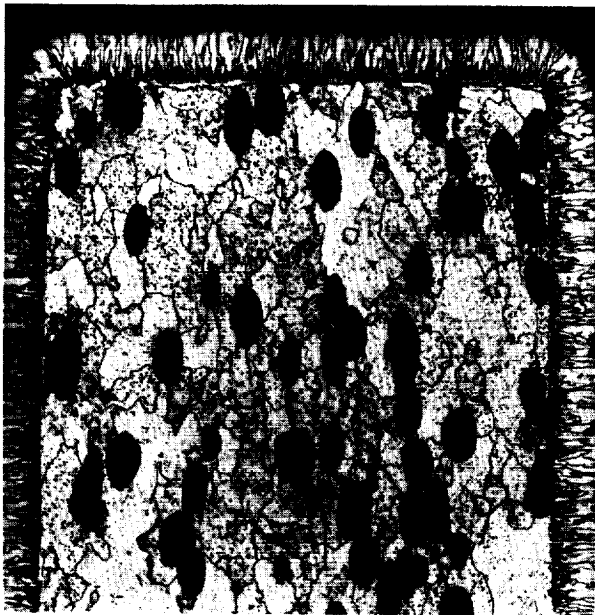
Figure 17. - Microstructures of W-UO$_2$ plates clad by vapor deposition from WF$_6$. Etchant, Murakami's reagent. X150.

(a) As clad.

(b) After heating to 2500° C in hydrogen for 2 hours.

C-67-962
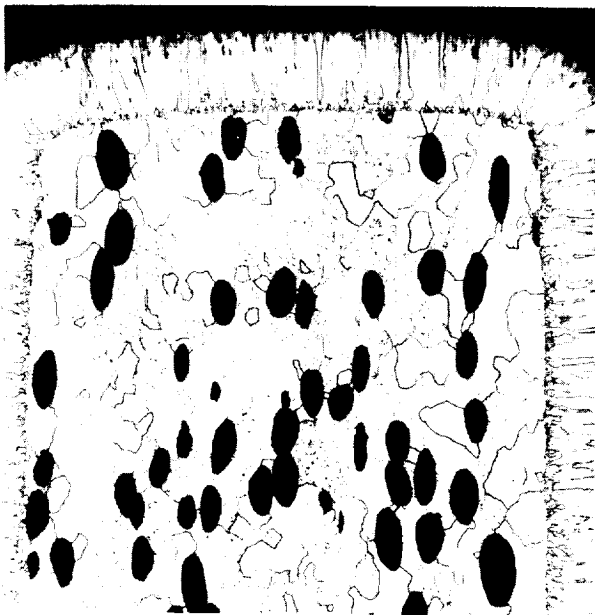
Figure 18. - Microstructures of W-UO$_2$ plates clad by vapor deposition from WCl$_6$. Etchant, Murakami's reagent. X150.

(a) Coupon.

(b) T-section.

(c) Plate.

(d) Cylinder.

CD-9054

Figure 20. - Joint configurations required for welding studies. (Materials 0.020-in.-thick (0.5 mm) W - 20-volume percent-UO_2 composites.) (All dimensions in inches (cm).)

C-67-963

Figure 19. - Microstructure of W - 20-volume-percent-UO_2 composite (clad by vapor deposition from WF_6) after testing at 2500° C for 2 hours in hydrogen. (Note cladding porosity that resulted from testing.) Etchant, Murakami's reagent. X150.
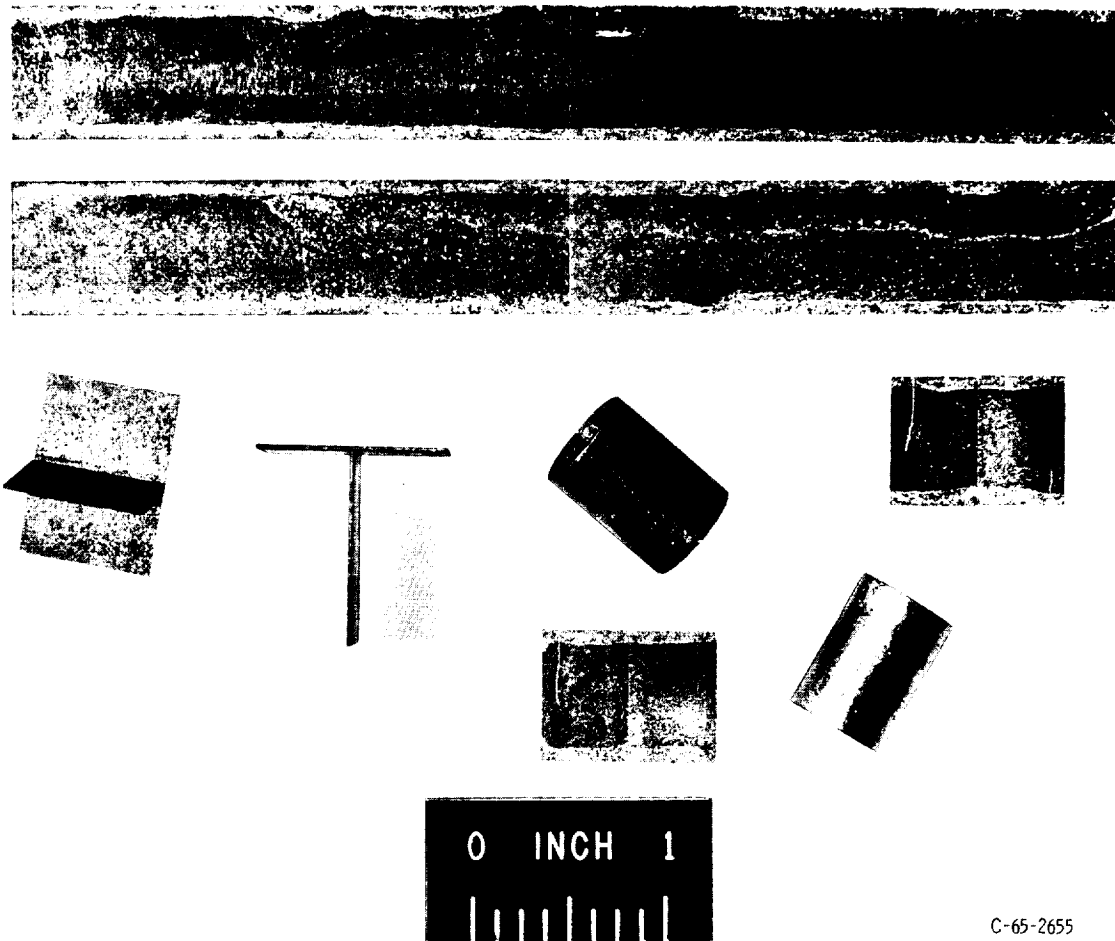
C-65-2655

Figure 21. - Typical joints in W - 20-volume-percent-UO_2 composites produced by gas-pressure bonding.
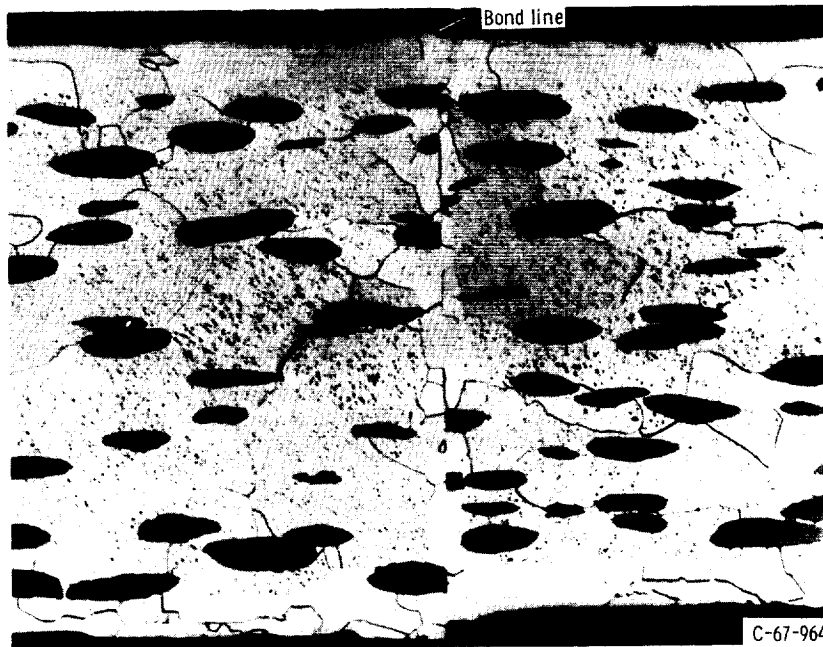
Figure 22. - Gas-pressure-bonded square butt joint (in heat-treated condition) of W - 20-volume-percent-UO_2 composite. Etchant, Murakami's reagent. X150.

Figure 23. - Butt joint produced with W - 20-volume-percent-UO_2 composite by gas - tungsten-arc brazing with W - 25-percent-Os braze alloy. Etchant, Murakami's reagent. X100.
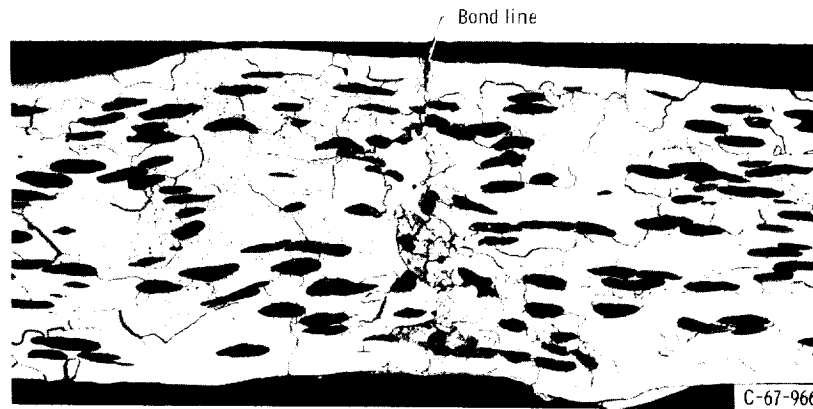
Figure 24. - Magnetic-force butt weld (in as-welded condition) in W - 20-volume-percent-UO_2 composite (Bond line is partially defined by deformed UO_2 particle that was extruded between composite during weld upset.) Etchant, Murakami's reagent. X75.

Joint design
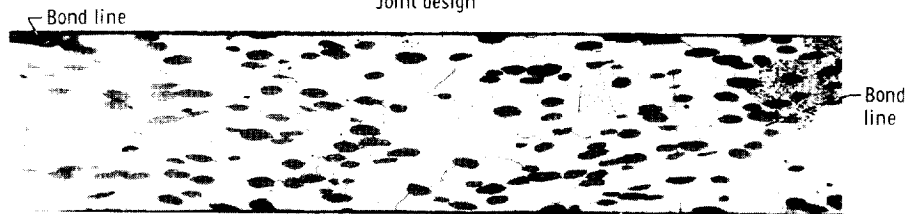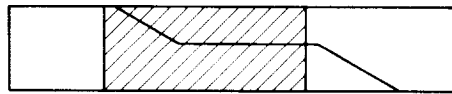
Etchant, Murakami's reagent; X50

Etchant, Murakami's reagent; X500

Figure 25. - Vacuum hot-press-diffusion bonded W - 20-volume-percent-UO_2 joint after annealing at 2500° C for 2 hours.

78
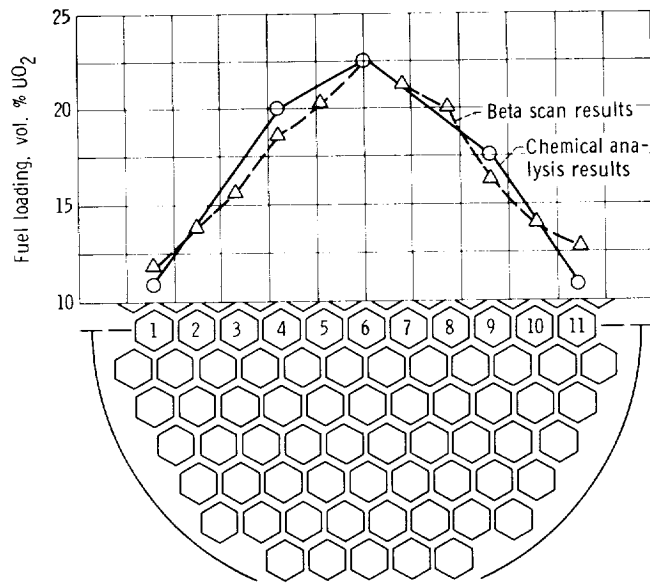
Figure 26. - Comparison of beta scan and x-ray fluorescence (wet chemical) analysis results for W-UO_2 honeycomb grid sample.
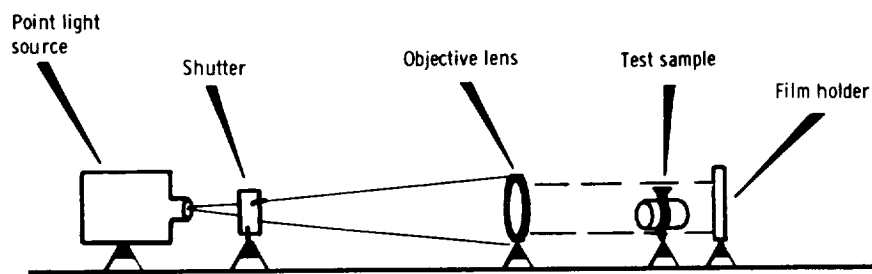
(a) Shadowgraph system.
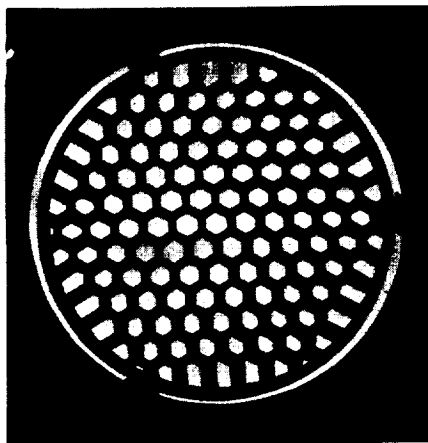
(b) Warped grid.
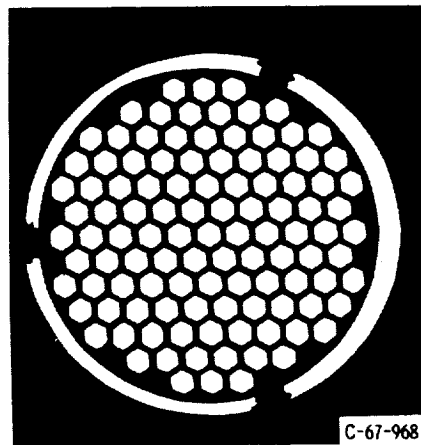
(c) Grid with good dimensional control.

Figure 27. - Parallel light shadowgraphic technique for measuring honeycomb grid warp, web thickness, and flow channel alinement. (Courtesy Pacific Northwest Laboratory, Battelle Memorial Institute.)
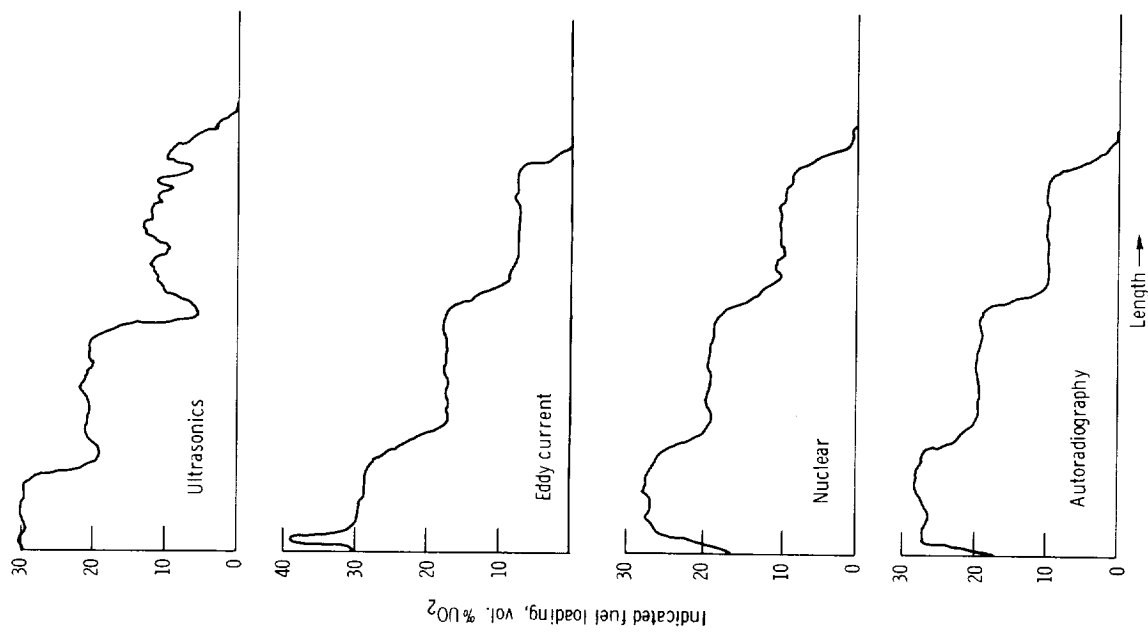
Figure 29. - Comparison of test records on W-clad, W-UO$_2$ plate incrementally loaded in nominal steps of 0-, 10-, 20-, and 30-volume-percent UO$_2$.
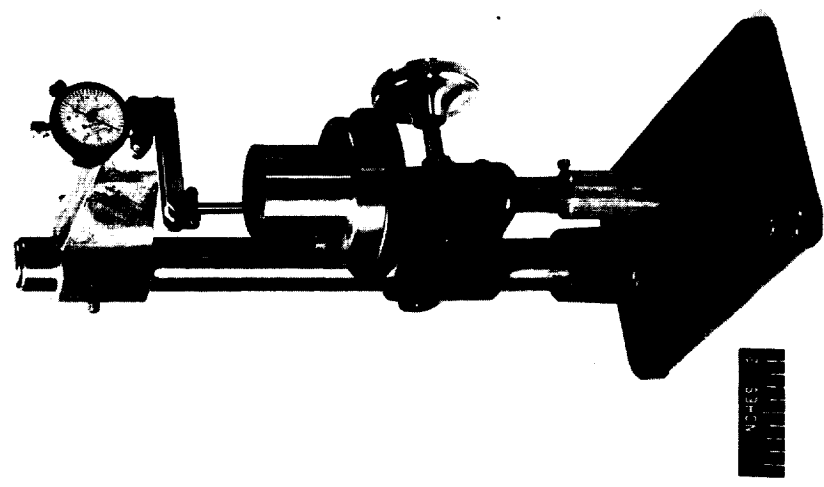
C-66-3147

Figure 28. - Mechanical gage for measuring thickness of webs in W-UO$_2$ honeycomb grids.
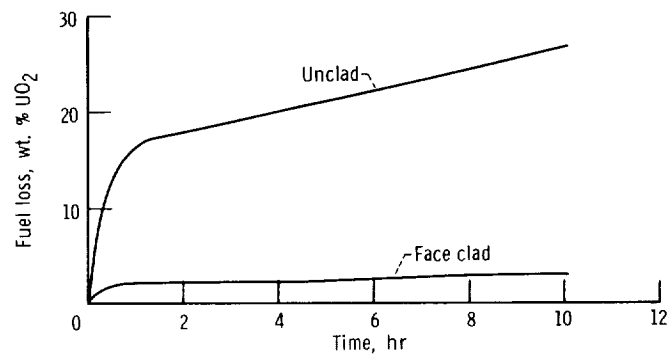
Figure 30. - Fuel loss as function of time at 2500° C in hydrogen for unclad and partially clad W - 20-volume-percent-UO_2 composites.
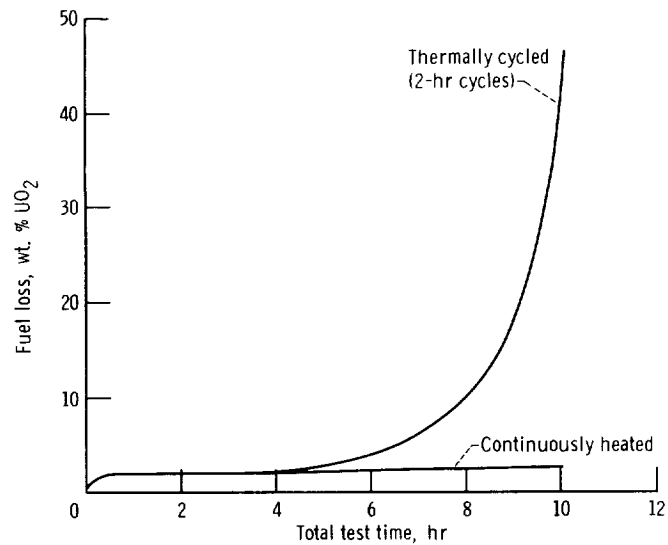
Figure 31. - Fuel loss as function of total test time at 2500° C in hydrogen for continuously heated and thermally cycled W - 20-volume-percent-UO_2 composites (face clad).
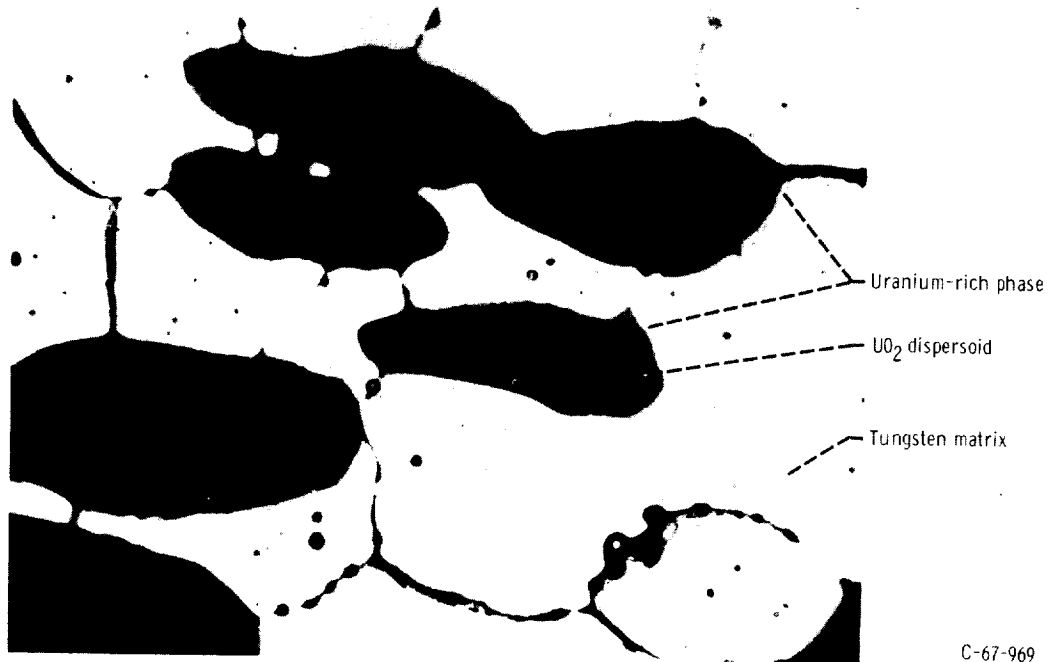
C-67-969

Figure 32. - Microstructure of thermally cycled W - 20-volume-percent-UO₂composite. Composite was heat treated for five 1-hour intervals at 2500° C in flowing hydrogen with cooling to ambient temperatures between intervals. Unetched.
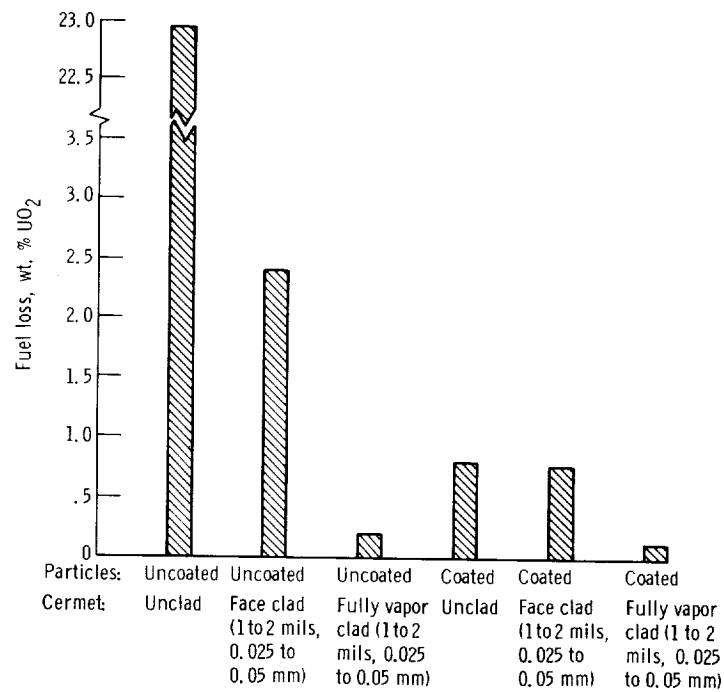
Figure 33. - Effect of W-coating of UO₂ particles and external W-cladding of W - 20-volume-percent-UO₂ composites on surface vaporization losses. Test conditions: 2 hours at 2500° C in flowing hydrogen.
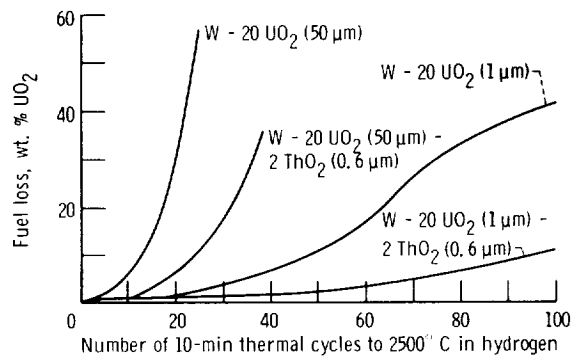
Figure 34. - Effect of UO_2 particle size and ThO_2 matrix additions on thermal cyclic fuel losses from face-clad W - 20-volume-percent UO_2 composites.
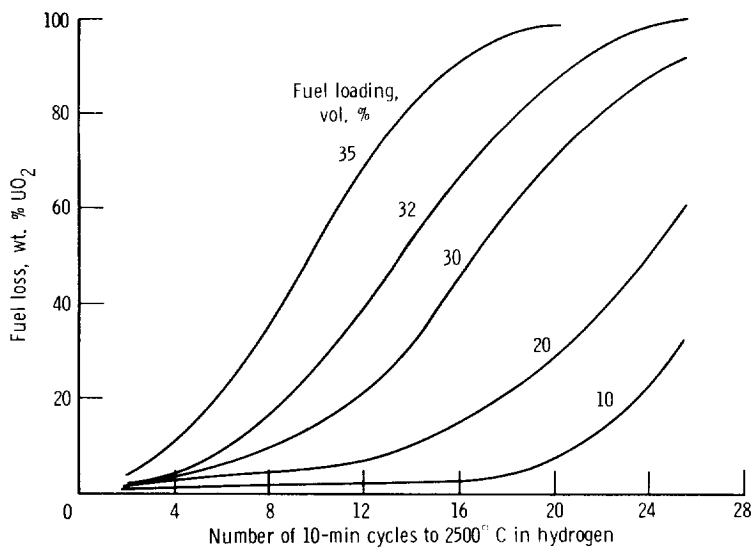
Figure 35. - Effect of UO_2 loading on fuel loss during thermal cycling of face-clad $W-UO_2$ from ambient temperature to 2500° C in flowing hydrogen.
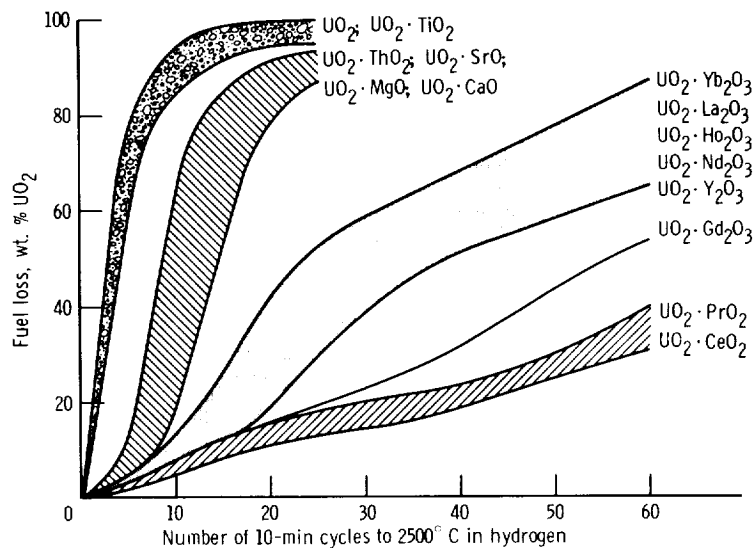
Figure 36. - Effect of 10-mole-percent oxide additives as stabilizers of UO_2 in face-clad W - 35-volume-percent-UO_2 composites cycled to 2500° C in flowing hydrogen.
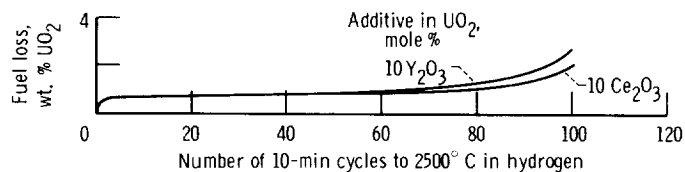
Figure 37. - Comparison of Ce_2O_3 and of Y_2O_3 as stabilizers of UO_2 in fully clad W - 35-volume-percent-UO_2 composites cycled to 2500° C in flowing hydrogen.

84
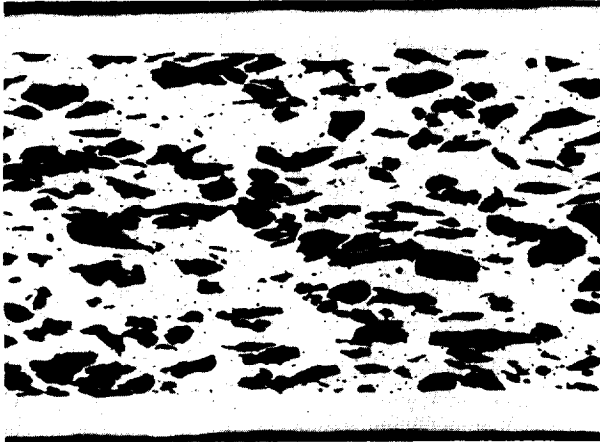
(a) 25 Cycles; Y_2O_3 stabilizer.

(b) 60 Cycles; Y_2O_3 stabilizer.

(c) 25 Cycles; Ce_2O_3 stabilizer.

(d) 60 Cycles; Ce_2O_3 stabilizer.

C-67-970

Figure 38. - Effect of thermal cycling on microstructure of stabilized W - 35-volume-percent-UO_2 composites containing 10 mole percent of indicated stabilizer in UO_2. Composites, all of which lost less than 1 percent of their fuel, were cycled either 25 or 60 times to 2500° C for 10 minutes per cycle in purified, flowing hydrogen at 15 pounds per square inch (0.10 MN/m^3) and 35 standard cubic feet per hour (10^{-4} m^3/hr). Unetched. X100.
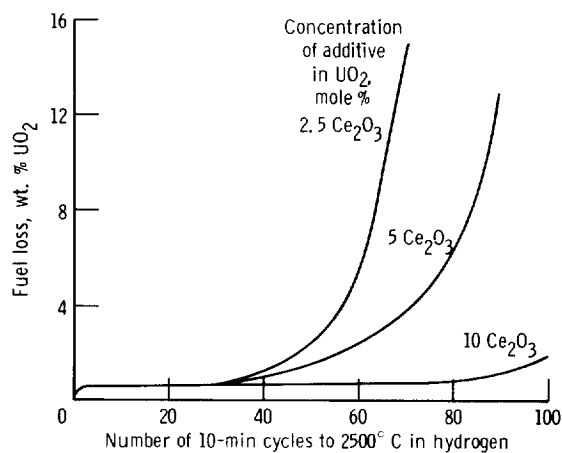
Figure 39. - Effect of concentration of Ce_2O_3 in UO_2 on fuel loss from fully clad W - 35-volume-percent UO_2 composites cycled to 2500° C in flowing hydrogen.
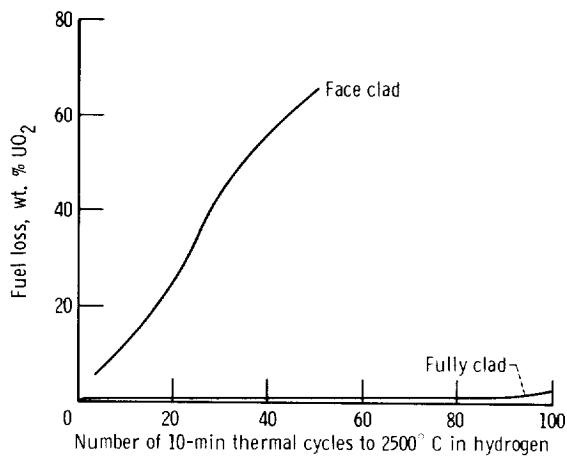
Figure 40. - Effect of cladding on fuel loss of W - 35-volume-percent-UO_2 cermets stabilized with 10-mole-percent Y_2O_3 dissolved in UO_2. (Clad thickness: faces, approximately 0.001 inch (0.025 mm); edges, approximately 0.2 inch (5 mm).)
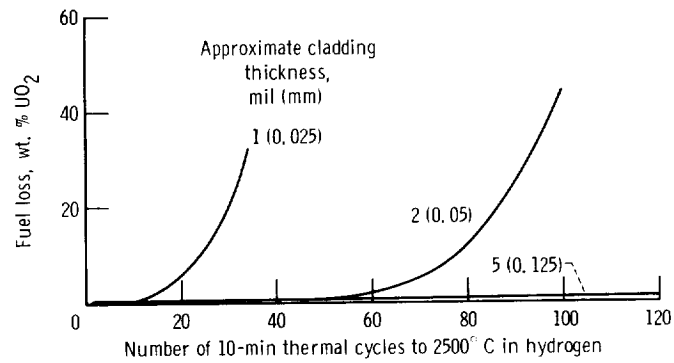
Figure 41. - Effect of tungsten cladding thickness on fuel loss rate from completely clad W - 20-volume-percent-composites stabilized with 2.5-mole-percent Y_2O_3.
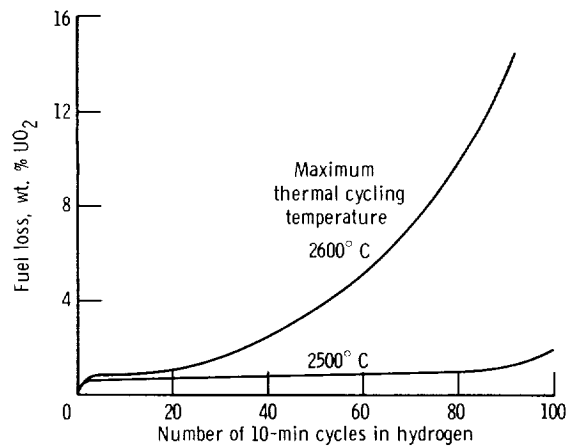
Figure 42. - Effect of maximum thermal cycling temperature on fuel loss from fully clad W - 35-volume-percent-UO_2 composites stabilized with 10-mole-percent Ce_2O_3 and cycled in flowing hydrogen.
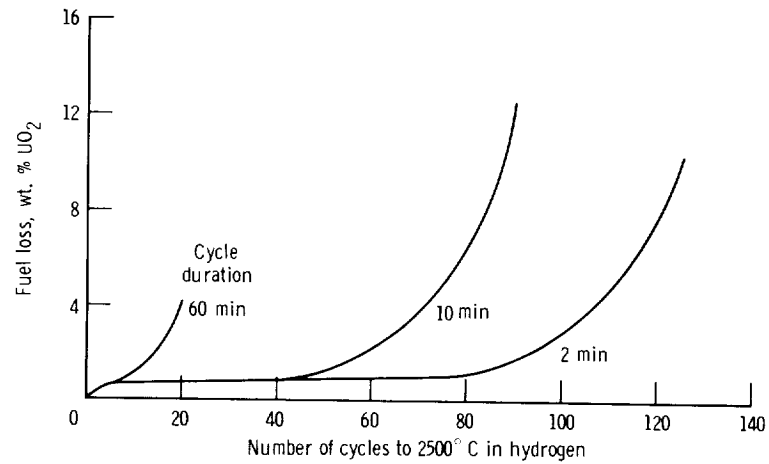
Figure 43. - Effect of hold time per cycle on fuel loss from fully clad W - 35-volume-percent-UO_2 composites stabilized with 5-mole-percent Ce_2O_3 and cycled to 2500° C in flowing hydrogen.
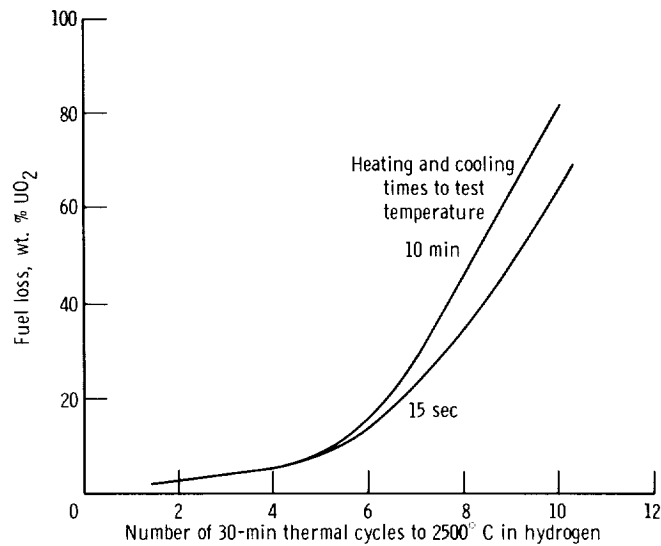
Figure 44. - Effect of heating and cooling rates on fuel loss from W - 20-volume-percent-UO_2 composites thermally cycled to 2500° C in hydrogen.
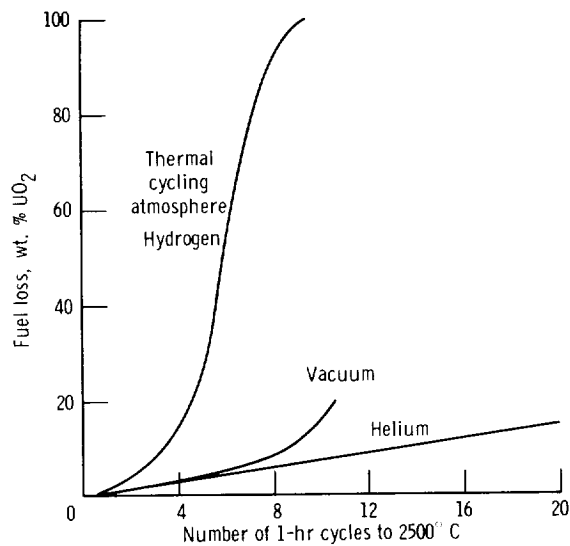
Figure 45. - Effect of test atmosphere in thermal cycling
face-clad W - 20-volume-percent UO_2 composites to
2500° C in hydrogen, vacuum, or helium.
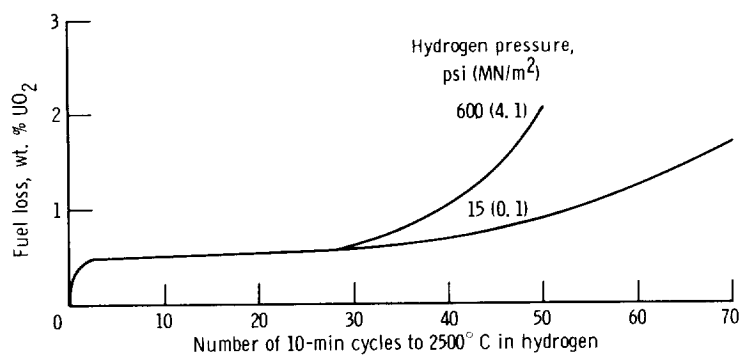
Figure 46. - Effect of hydrogen pressure on fuel loss from fully clad W - 35-
volume-percent UO_2 composites stabilized with 10-mole-percent Ce_2O_3.
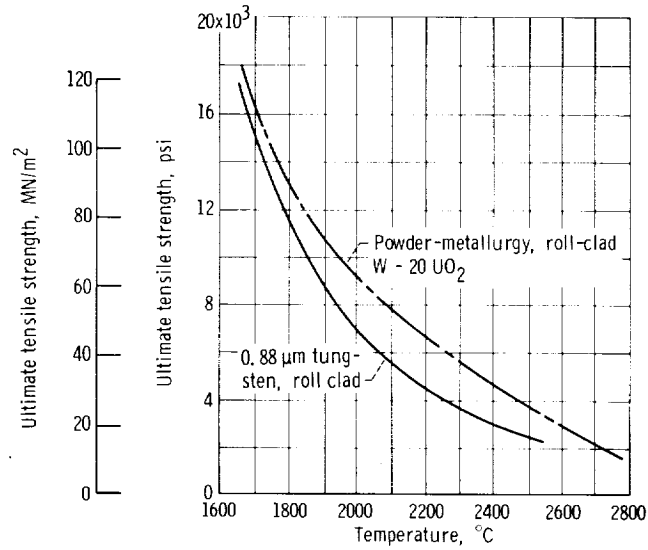
Figure 47. - Effect of temperature on tensile strength of W and W - 20-volume-percent UO_2 composites.
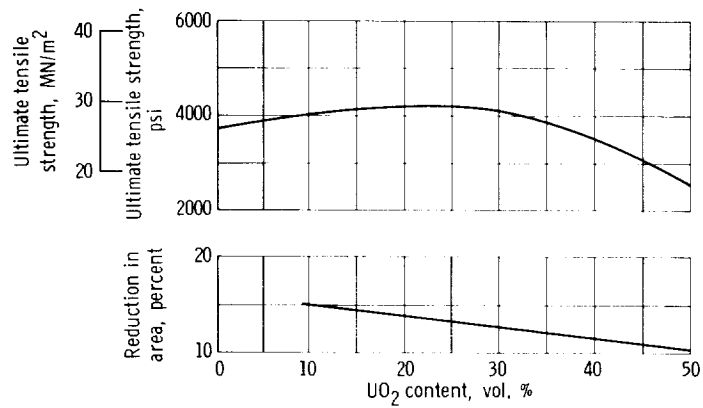
Figure 48. - Effect of fuel loading on 2500° C tensile properties of roll-clad W-UO_2 composites. Test temperature, 2500° C.
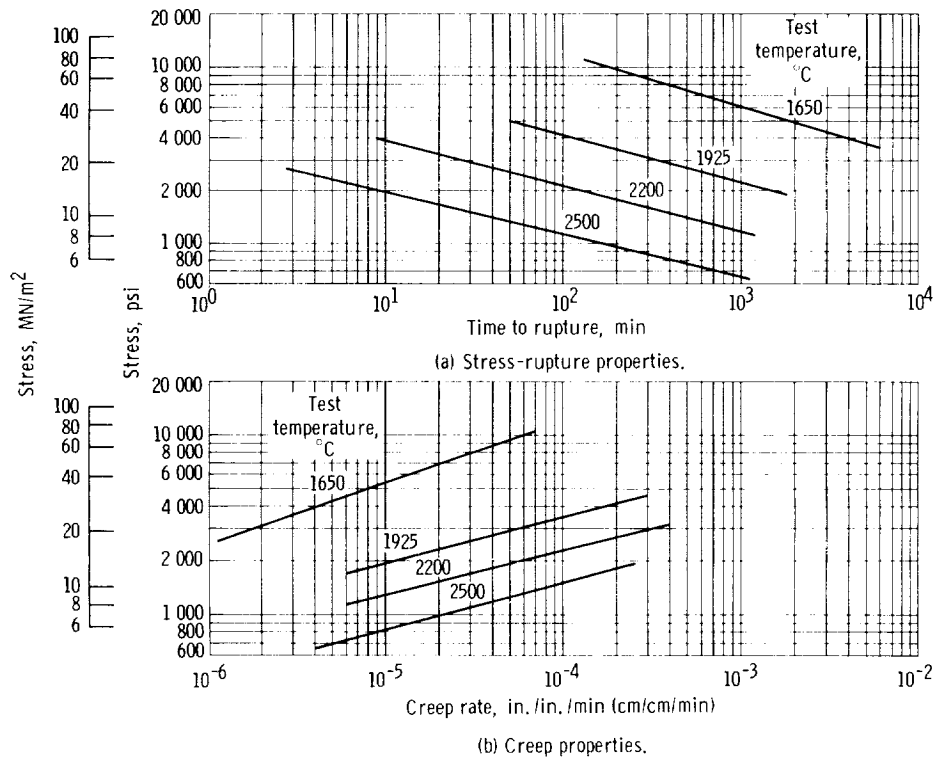
Figure 49. - Effect of temperature on creep-rupture properties of roll-clad W - 20-volume-percent-UO_2 composites.
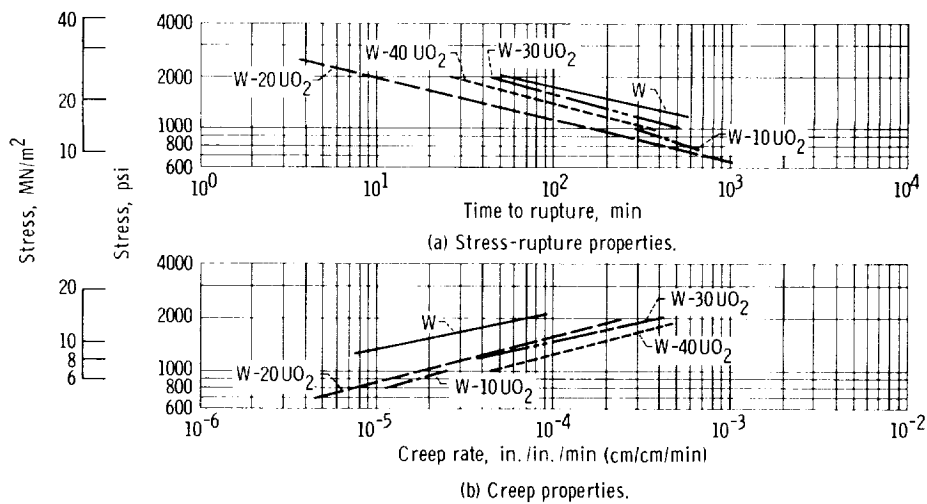
Figure 50. - Effect of fuel loading on 2500° C creep-rupture properties of roll-clad W-UO_2 composites. Test temperature, 2500° C.
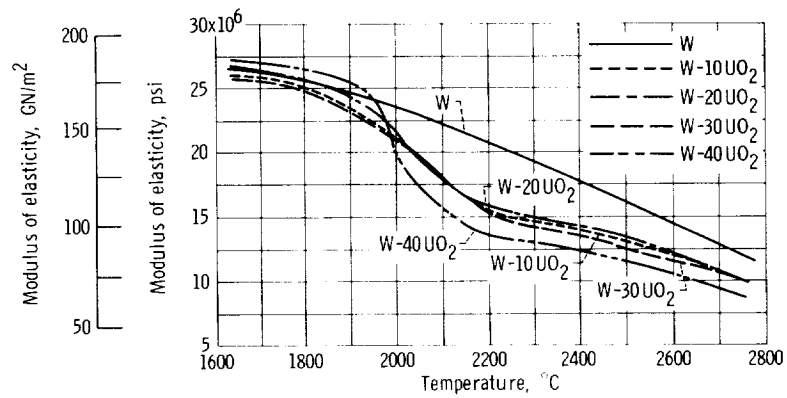
Figure 51. - Effect of temperature on static modulus of elasticity of roll-clad W-UO$_2$ composites.
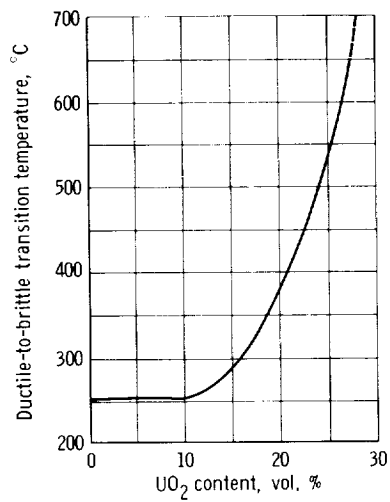
Figure 52. - Effect of fuel loading on ductile-to-brittle transition temperature of roll-clad W-UO$_2$ composites.
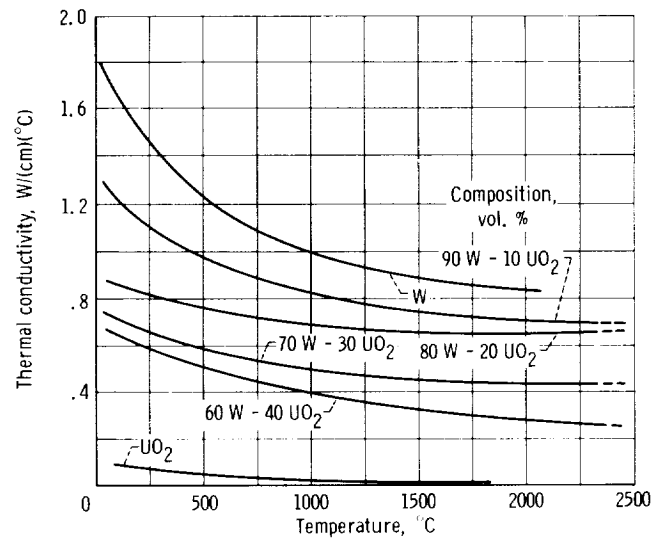
Figure 53. - Effect of temperature on thermal conductivity of reference W-UO₂ composites. (Data for W and UO₂ from RSIC-202, Thermal Properties of High Temperature Materials, June 1964.)
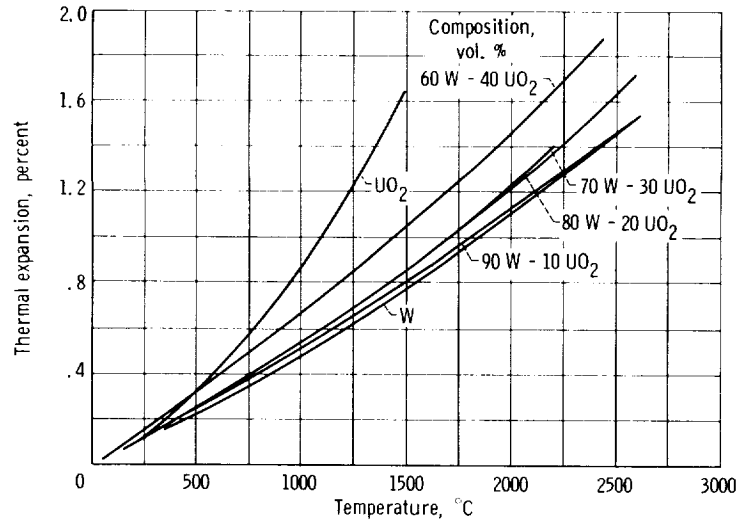

Figure 54. - Effect of temperature on thermal expansion of reference W-UO₂ composites. (Data for W and UO₂ from RSIC-202, Thermal Properties of High Temperature Materials, June 1964.)
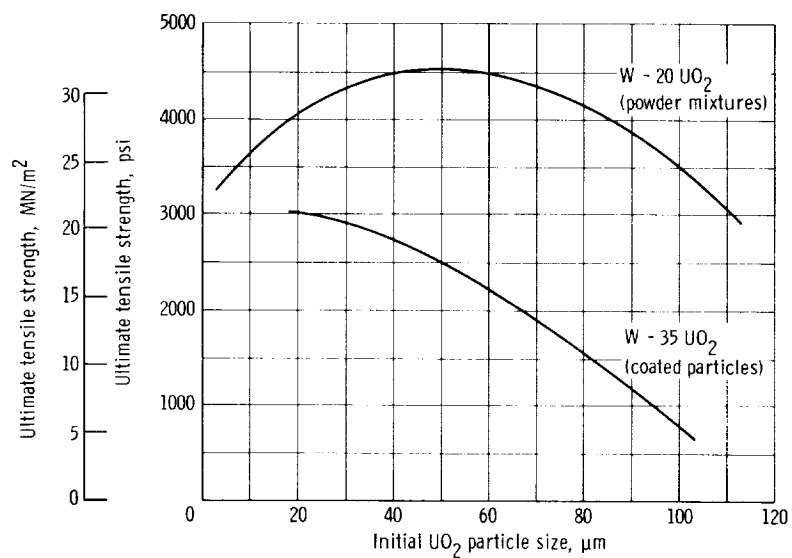
Figure 55. - Effect of UO_2 particle size on strength of roll compacted W-UO_2 composites. Test temperature, 2500 C.
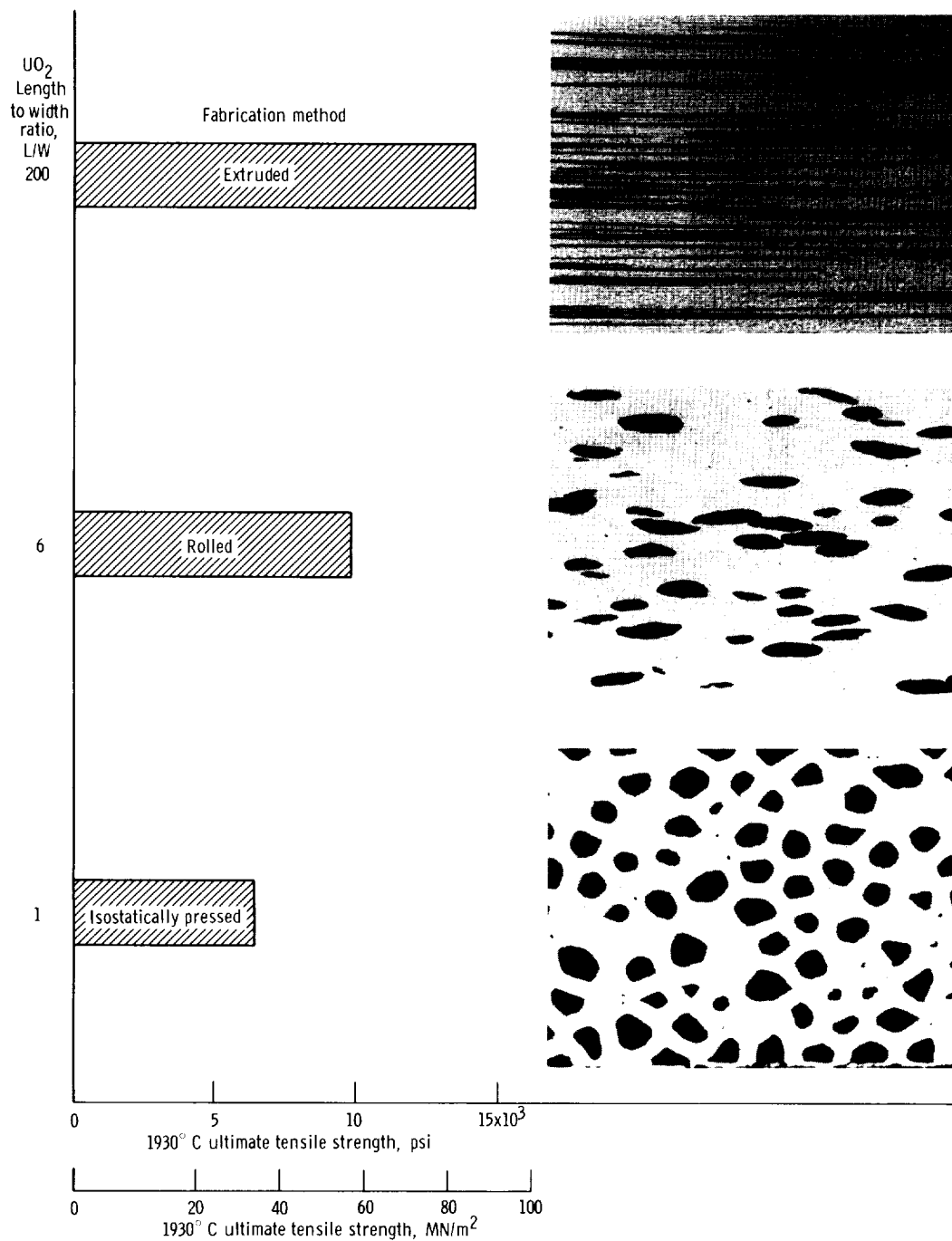
UO₂
Length
to width
ratio,
L/W
200

Fabrication method

Extruded

6

Rolled

1

Isostatically pressed

0   5   10   15x10³

1930° C ultimate tensile strength, psi

0   20   40   60   80   100

1930° C ultimate tensile strength, MN/m²

Figure 56. - Effect of UO₂ elongation on 1930° C tensile strength of W - 20-volume-percent-UO₂ composites. As-received unetched photomicrographs.
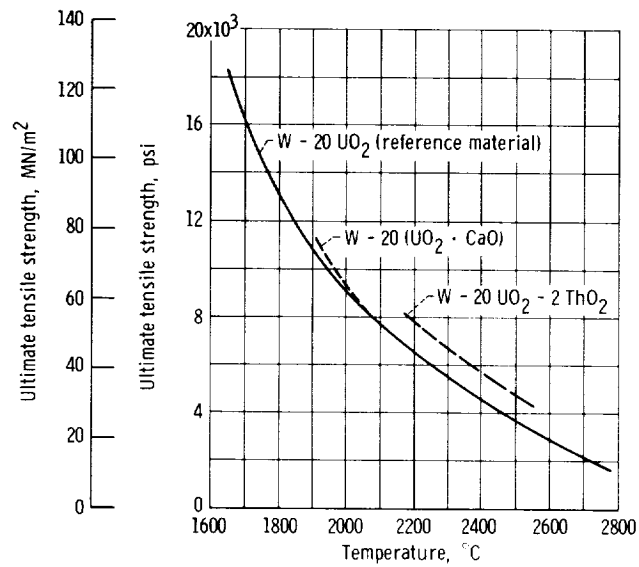
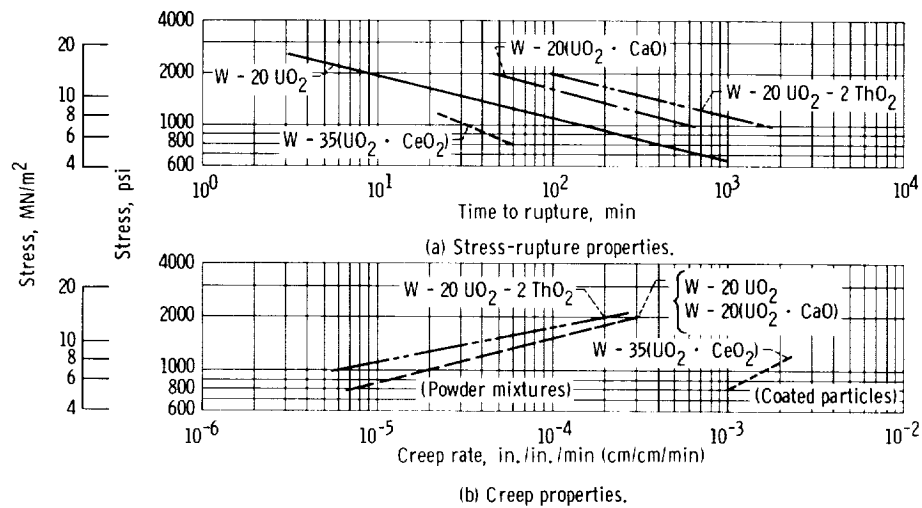Figure 57. - Effect of additives on tensile strength of W - 20-volume-percent UO$_2$ composites.

(a) Stress-rupture properties.

(b) Creep properties.

Figure 58. - Effect of additives on creep-rupture properties of W-UO$_2$ composites. Test temperature, 2500° C.
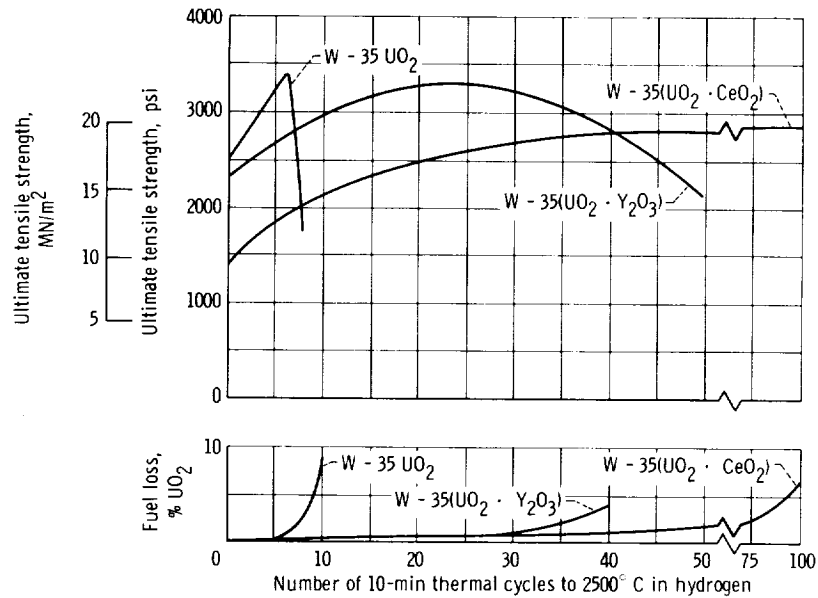
Figure 59. – Effect of thermal cycles on tensile strength and fuel loss of roll-compacted W - 35-volume-percent-UO_2 composites. Test temperature, 2500° C.

CONFIDENTIAL